

DETRITAL ZIRCON GEOCHRONOLOGY AND
PROVENANCE ANALYSIS OF THE DESMOINESIAN
(MIDDLE PENNSYLVANIAN) BARTLESVILLE AND
RED FORK SANDSTONES, CHEROKEE PLATFORM
AND ANADARKO BASIN, OKLAHOMA

By

ZACHERY T. TUNIN

Bachelor of Science in Geology

Oklahoma State University

Stillwater, Oklahoma

2018

Submitted to the Faculty of the
Graduate College of the
Oklahoma State University
in partial fulfillment of
the requirements for
the Degree of
MASTER OF SCIENCE
December, 2020

DETRITAL ZIRCON GEOCHRONOLOGY AND
PROVENANCE ANALYSIS OF THE DESMOINESIAN
(MIDDLE PENNSYLVANIAN) BARTLESVILLE AND
RED FORK SANDSTONES, CHEROKEE PLATFORM
AND ANADARKO BASIN, OKLAHOMA

Thesis Approved:

James O. Puckette

Thesis Adviser

Jack Pashin

James Knapp

ACKNOWLEDGEMENTS

I would like to dedicate this thesis to both my parents Tim and Shelley Tunin and my Savior Christ Jesus. The completion of this project would not have been possible without their never ending support and guidance. All credit be given to the Lord; it is not because of myself but He who works within me.

I also extend a sincere appreciation to the following individuals and entities for their support of this study; my committee members Dr. James Knapp and Dr. Jack Pashin, for their helpful suggestions and editing of the manuscript; Tim Munson who provided invaluable mentorship; my fellow graduate students, especially my colleagues John Clymer, Jessica Juenger, and Michael Rohrer, for there unending encouragement and emotional support; Unit Corporation for providing drill cuttings and financial support for analytical cost; Continental Resource Inc. for access to well logs, production data, and mapping software; the Arizona LaserChron Center for the use of their lab and analytical software; and Keith Edmonds the benefactor of this study, without who this study would not have been possible.

Most of all I would like to acknowledge my advisor Dr. Jim Puckette. Not only was his guidance invaluable but his confidence in my abilities was unmatched. There is also no doubt, that without his presence this study certainly wouldn't have been as exciting or interesting. Thank you for your incredible advisement over the past two years.

Name: ZACHERY T. TUNIN

Date of Degree: DECEMBER, 2020

Title of Study: DETRITAL ZIRCON GEOCHRONOLOGY AND PROVENANCE ANALYSIS OF THE DESMOINESIAN (MIDDLE PENNSYLVANIAN) BARTLESVILLE AND RED FORK SANDSTONES, CHEROKEE PLATFORM AND ANADARKO BASIN, OKLAHOMA

Major Field: GEOLOGY

Abstract: The Middle Pennsylvanian was a critical time in the evolution of the North American Craton. Tectonic events caused major changes in paleogeography, resulting in the emergence of new sediment sources that changed sediment dispersal patterns and initiated new and complex variations in detrital compositions of sediments. During the early Desmoinesian, the principal change in the Midcontinent Region was the introduction of lithics and, more specifically, metamorphics of unknown provenance to the northeast-southwest trending fluvial, deltaic sediment dispersal systems. This permitted the development of rock compositions and fabrics favorable for dissolution and reservoir genesis. These sandstones became the prolific oil- and gas-producing reservoirs of the Cherokee Group. This study reports 867 new concordant detrital zircon U-Pb ages and 120 new $\epsilon\text{Hf}(t)$ values from three early Desmoinesian, lower Cherokee, sandstone samples to determine sediment provenance. These samples include cuttings from the Red Fork Sandstone in the Anadarko basin and outcrops of the Taft Sandstone and Bartlesville Sandstone in northeastern Oklahoma.

Zircons in the analyzed sandstones are characterized by two major signatures: Type 1 and Type 2. Type 1 quartzarenites (Taft Sandstone) have a significant age cluster corresponding to the Yavapai-Mazatzal (1600-1800 Ma) province. In contrast, Type 2 sublith- to litharenites (Bartlesville and Red Fork sandstones) have major age clusters corresponding to the Appalachian Synorogenies (350-490 Ma) and the peri-Gondwanan (Neoproterozoic) terranes (530-760 Ma). Comparative analysis of published detrital zircon ages and $\epsilon\text{Hf}(t)$ signatures from Pennsylvanian aged sandstones and early Paleozoic strata and basement rocks across the North American Craton suggests the lower Cherokee sandstones reflect both local sourcing within the Midcontinent and sourcing by distal, extrabasinal, fluvial systems. Detrital zircon signatures from the Type 2 sandstones support the exhumation of exposed peri-Gondwanan basement material and the recycling of Cambrian-Ordovician sedimentary cover in the northern Appalachian region as the primary source of lithics (including metamorphic fragments) that emerged in early Desmoinesian sandstones on the Midcontinent. Signatures from Type 1, Taft, Sandstone indicate that quartz-rich detritus along the western flank of the Ozark Uplift was likely sourced from recycled late Mississippian strata and granitic basement exposed on the Ozark Uplift. Together, these compiled data support the extension of a NE-SW transcontinental sediment dispersal system with headwaters in present-day southeast New England to the southern Midcontinent in the Middle Pennsylvanian. This system was primarily sourced and influenced by the Alleghenian orogeny on the eastern Laurentian margin. Periodic filling of intracratonic basins also partially influenced the dispersal system. Local variation in detrital composition, including the absence of lithics in the Taft Sandstone, is attributed to local drainage networks that collected sediment from unroofed paleohighs.

TABLE OF CONTENTS

Chapter	Page
I. INTRODUCTION.....	1
II. REVIEW OF LITERATURE.....	4
2.1 Previous Studies.....	4
2.2 New Insights into Sediment Source and Dispersal	7
III. GEOLOGIC BACKGROUND	10
3.1 Pennsylvanian Paleogeography	10
3.2 Stratigraphy and Depositional Context.....	14
3.2.1 Bartlesville (Bluejacket) Sandstone	15
3.2.2 Red Fork (Taft) Sandstone.....	16
IV. POTENTIAL SEDIMENT SOURCES	18
4.1 Northern Provenance.....	19
4.2 Eastern Provenance.....	20
4.3 Western Provenance.....	23
4.4 Midcontinent Provenance.....	24
V. METHODOLOGY	26
5.1 Detrital Zircon Geochronology.....	26
5.1.1 Sample Collection and Preparation.....	27
5.1.2 U-Pb Age Analysis.....	30
5.1.3 Hafnium Isotopic Analysis	34
5.2 Sandstone Petrography.....	35

Chapter	Page
VI. RESULTS	37
6.1 Detrital Zircon Type Signatures	37
6.1.1 Type 1	39
6.1.2 Type 2	39
6.2 Multidimensional Scaling (MDS)	42
6.3 Hafnium Isotope (U-Pb- ϵ Hf(t)) Distribution	43
VII. DISCUSSION	49
6.1 Provenance Interpretation	49
7.1.1 Type 1 Provenance	49
7.1.2 Type 2 Provenance	52
6.2 Early Desmoinesian Sediment Delivery Pathways	54
VIII. CONCLUSIONS	59
REFERENCES	62
APPENDICES	70
APPENDIX A: ZIRCON IMAGES	70
APPENDIX B: DATA TABLES	77
APPENDIX C: PETROGRAPHIC IMAGES	82

LIST OF TABLES

Table	Page
1. Compositional characteristics of type signatures from this study and those from Kissock et al (2018).....	38
2. Age-pick calculations for sample TF-1.....	77
3. Age-pick calculations for sample RDFK-ST	78
4. Age-pick calculations for sample BV 1-4.....	79
5. U-Pb- ϵ Hf(t) date table for all samples analyzed in this study.....	80

LIST OF FIGURES

Figure	Page
1. Basement structure map of the Midcontinent (modified from Wang et al., 2019; Rascoe and Adler, 1983). Contours are in feet. Sample locations are indicated by colored stars.....	3
2. Compiled sandstone composition data (point counts) from the Red Fork and Bartlesville sandstones in surrounding areas on the Cherokee Platform and Anadarko Basin.	7
3. Paleogeographic reconstruction of the Middle-Late Pennsylvanian Laurentian Craton (modified from Algeo and Heckel, 2008).	12
4. Early Desmoinesian paleogeography of the Mid-Continent (modified from Rascoe and Adler, 1983).	13
5. a) Stratigraphic column of the Midcontinent Desmoinesian series illustrating surface and subsurface nomenclature.	15
6. Basement map of major North American geologic provinces (modified after Chapman and Laskowski, 2019).	19
7. U-Pb probability density plots of samples from selected provinces.....	22
8. U-Pb probability density plots of samples from the Illinois and Forest City basins.	25
9. Flowchart describing the workflow for this investigation (left to right) and the methods used.	27
10. Geologic map of northeast Oklahoma modified from Heran et al. (2003). Map shows the location of outcrop samples.....	29
11. Net sandstone isopach within the Lower Red Fork channel encountered by the 1HX Saratoga, No.1 Herring, and No.2 Switzer wells in South Thomas Field.	29

Figure	Page
12. a) Cathodoluminescence (CL) image of zircons from subsample BV 4.	33
13. Compiled point counts from samples analyzed in this study along with point counts from the No.1 Switzer and No.1 Hearing core.....	36
14. Relative age-probability (left) and relative frequency (right) plots of results from U-Pb analysis of detrital zircons.....	41
15. 3D and 2D MDS plots calculated using the coefficient of nondetermination and KS Test D value.	44
16. U-Pb- ϵ Hf(t) results from the Taft (TF-1) sandstone plotted as bivariate kernel density estimates.....	47
17. Combined U-Pb- ϵ Hf(t) results from the Red Fork (RDFK-ST) and Bluejacket (BV 1-4) sandstones plotted as bivariate kernel density estimates.	48
18. Middle-Late Pennsylvanian paleogeography reconstruction.	58
19. BSE image of mounted zircons from subsample BV 1.	70
20. CL image of mounted zircons from subsample BV 1	71
21. BSE image of mounted zircons from subsample BV 2	71
22. CL image of mounted zircon from subsample BV 2.....	72
23. BSE image of mounted zircons from subsample BV 3	72
24. CL image of mounted zircons from subsample BV 3	73
25. BSE image of mounted zircons from subsample BV 4	73
26. CL image of mounted zircons from subsample BV 4	74
27. BSE image of mounted zircons from sample TF-1	74
28. CL image of mounted zircons from sample TF-1	75
29. BSE image of mounted zircons from sample RDFK-ST.....	75
30. CL image of mounted zircons from sample RDFK-ST.....	76
31. Photomicrograph from the Bluejacket outcrop sample in plain polarized light (ppl).	82

Figure	Page
32. Photomicrograph of sample from Bluejacket Sandstone in cross polarized light (cpl).	83
33. Bluejacket outcrop photomicrographic (cpl).....	83
34. Bluejacket outcrop photomicrographic (cpl).....	84
35. Photomicrograph from the Taft outcrop sample (ppl).	84
36. Photomicrograph from Figure 35 in cross polarized light.	85

CHAPTER I

INTRODUCTION

During the Middle Pennsylvanian, it is widely understood that siliciclastic sedimentation was controlled by a complex interplay between source area tectonics, eustatic sea-level fluctuation, and climate. This resulted in spatial and temporal variability in sediment dispersal as well as complex mixing of source detritus in intracratonic and foreland basins throughout the North American Craton. This variability is readily apparent in the detrital composition of Desmoinesian age sandstones located on the Cherokee Platform and in the adjacent Arkoma and Anadarko basins of Oklahoma. Previous petrographic studies have allotted the compositional variability in these sandstones to changes in the abundance of metamorphic rock fragments and feldspars, which are necessary for secondary (dissolution) porosity development. While sediment provenance has still yet to be sufficiently studied, many have postulated that the major source area of these rocks included the central craton (including the northern Canadian Shield) (Dyman, 1989; Puckette, 1990, Anderson, 1992, Visher et al., 1971, etc.), and the Nemaha Uplift (Weirich, 1953; Dyman, 1989). Additionally, minor sourcing of grains is postulated to be derived from the Wichita Uplift (Anderson, 1992; Puckette, 1990) and Ouachita Uplift (Dyman, 1989) for sandstones in the southernmost Anadarko and Arkoma basins, and the Ozark Uplift (Johnson, 2008) in sandstones along the eastern flank of the Cherokee Platform. However, previous studies have yet to consider the tectonically active Appalachian margin as a potential sediment source.

This is problematic, since new evidence from recent compositional studies strengthens the hypothesis for a more distal easterly source of the Alleghenian Orogeny as playing a major role in sediment provenance during Pennsylvanian time.

Recently, detrital zircon U-Pb data from Pennsylvanian strata in the Grand Canyon and the intracratonic Forest City and Illinois basin were interpreted to reflect detritus shed from the Appalachian margin (Gehrels, 2011; Kissock et al., 2018). This connection would require the presence of a large northeast to southwest trending transcontinental fluvial system that facilitated the southern sediment transport across the North American Craton and into the rapidly subsiding Anadarko and Arkoma basins. This potential for a more distal northeasterly source of the Appalachian margin would greatly change our understanding of sediment dispersal systems for the Cherokee sandstone on the Cherokee Platform and in the adjacent Anadarko and Arkoma basins. Understanding this change, is critical in the continued effort to developing accurate sediment dispersal models necessary for correctly predicting the spatial and temporal variability in rock composition, and associated reservoir quality, observed in these sandstone reservoirs.

This study presents 867 new U-Pb ages, along with 120 new $\epsilon_{\text{Hf}}(t)$ measurements, from detrital zircons collected from the lower Cherokee Red Fork and Bartlesville sandstones outcropping on the Cherokee Platform and sandstone bodies in the Anadarko basin (Figure 1). These data integrated with recently published detrital zircon geochronology data and current paleogeographic models improve our understanding of sediment dispersal on and across the North American Midcontinent during Desmoinesian time. Furthermore, the utilization of these data to unmix sediment source proportions (relative contributions) permits the construction of a relationship between spatial variation in sediment dispersal patterns and detrital compositions. The development of this relationship advances the ability to accurately predict spatial changes in detrital compositions and inversely reconstruct sediment dispersal patterns from quantitative petrographic assessments.

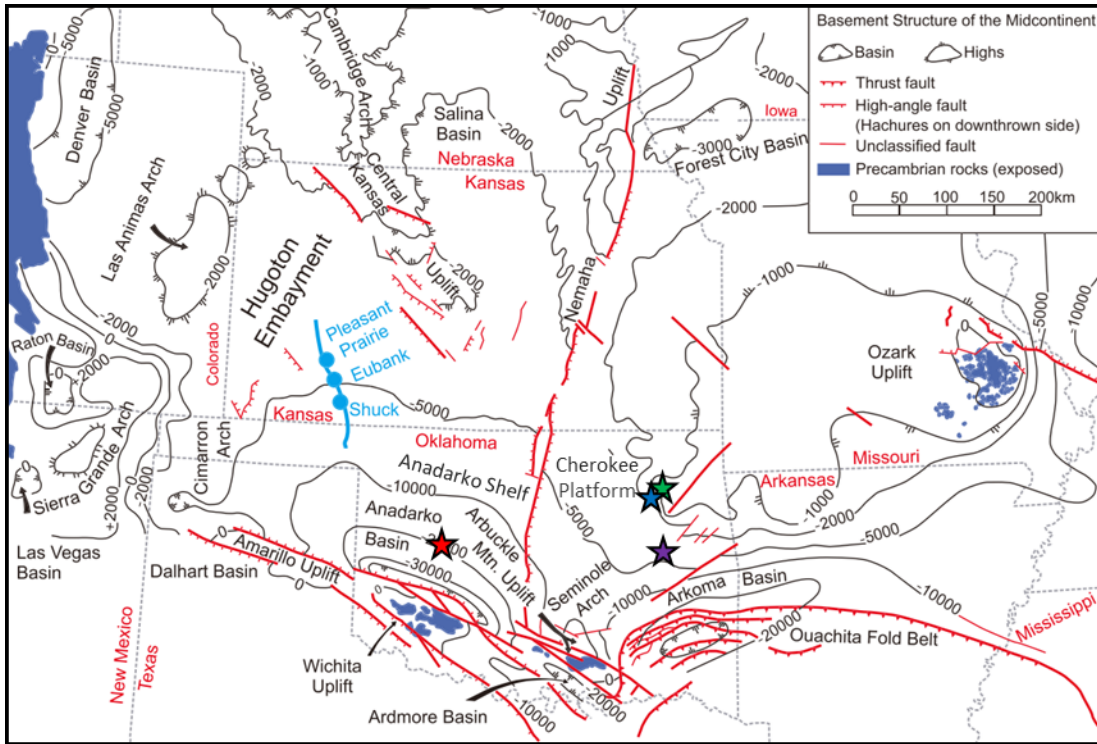


Figure 1. Basement structure map of the Midcontinent (modified from Wang et al., 2019; Rascoe and Adler, 1983). Contours are in feet. Sample locations are indicated by colored stars.

CHAPTER II

REVIEW OF LITERATURE

Previous investigations of Cherokee Group sandstones, particularly the Red Fork (Taft Sandstone in outcrop) and Bartlesville (Bluejacket Sandstone in outcrop), are numerous. These include a number of studies by past students within the Geology Department/School of Geology at Oklahoma State University whose studies looked at various aspects of these sandstone units, and utilized core, outcrop, and wireline logs to characterize these sandstones across their distribution in Oklahoma. Particularly, past research has focused on topics such as lithostratigraphy, petrology, diagenesis, and depositional environment in order to delineate reservoir trends. These interpretations, along with recent provenance studies of various middle Pennsylvanian sandstones, are synthesized with the addition of new geochronology data presented in this study. This is done in an attempt to establish both sediment provenance and determine its influence on reservoir development for the Red Fork and Bartlesville sandstones.

2.1 Previous Studies

While many past studies give detailed qualitative descriptions of the detrital constituents of the Bartlesville Sandstone, Mason (1982) and Kuykendall (1985) were two of the first to conduct quantitative petrologic assessments of the sandstone in northeast Oklahoma. Mason

(1982) investigated the sandstone along the Cushing Anticline in Creek County, Oklahoma and characterized the sandstone as predominantly subarkose to arkose in composition (**Figure 2a**), consisting predominantly of monocrystalline quartz and varying abundances of both plagioclase and microcline feldspar. Mason (1982) did not interpret sediment provenance, but rather followed the Visher et al. (1971) interpretation that sediment was likely sourced from the northeast as part of a large fluvial valley. Following his work, Kuykendall (1985) completed his own assessment of the Bartlesville Sandstone 30 miles to east in the Glenpool Field. Kuykendall (1982) found the sandstone to differ significantly from the sandstone on the Cushing Anticline. He characterized the sandstone as predominately sublitharenite to litharenite in composition consisting largely of monocrystalline quartz and metamorphic rock fragments and lesser amounts of feldspar. Metamorphic rock fragments were interpreted as foliated quartz-mica gneiss, quartzite, and phyllite. Despite the compositional variation, Kuykendall (1982) concluded that detritus was sourced from the same northeast trending fluvial system as Mason (1982) and Visher et al. (1971).

For the Red Fork Sandstone, quantitative petrographic studies include those done by Johnson (1984), Tate (1985), Robertson (1983), Balke (1984), Udayashankar (1985), and Anderson (1992) (**Figure 2**). Robertson (1983) and Balke (1984) studied the Red Fork Sandstone in north-central Oklahoma, east of the Nemaha Uplift on the Cherokee Platform. Both characterized the sandstone as litharenite to sublitharenite in composition consisting predominantly of monocrystalline quartzs and metamorphic rock fragments. Metamorphic rock fragments were interpreted as low grade mica schist, phyllite, and slate. Tate (1985) studied the sandstone farther to the south and found the sandstone to be compositional consistent with that noted by Robertson (1983) and Balke (1984). All three studies proposed the source of detritus to lie directly to the north of the study area.

West of the Nemaha Uplift, Johnson (1984) and Udayashankar (1985) investigated the Red Fork Sandstone in the western Oklahoma in the present day Anadarko basin above a proposed shelf hinge line. Both found the sandstone to be compositionally similar to that of the studies conducted in north-central and south-central Oklahoma, again, consisting predominantly of monocrystalline quartz and low grade metamorphic rock fragments. Sediment was interpreted to be sourced from the same system as the lith-sublitharenite sandstones investigated to the northeast. Anderson (1992) later followed these studies and investigated Upper Red Fork submarine fan deposits beyond the proposed shelf hinge line. He found the sandstone to be compositional similar to the sandstones above the shelf hinge line, but in contrast identified a larger abundance of plagioclase feldspar and minor abundance of microperthite. Puckette (1990) noted the same incorporation of microperthite, as well as granophyre fragments, in the Cherokee Skinner Sandstone proximal to Anderson's study area. Both proposed a predominant northeasterly source for sediment with additional minor sourcing from the southern Wichita Mountains. This fell in line with Dyman (1989) interpretation, who completed a quantitative petrographic analysis of the Desmoinesian sandstones throughout Oklahoma. Dyman (1989) determined that the Desmoinesian sandstones were spatially and temporal heterogeneous and derived from a mixture of sedimentary, igneous, and metamorphic source areas. His proposed major source areas for the sandstones included the craton, foreland blocks of the Ancestral Rocky Mountains, and orogenic terranes for southern Oklahoma (Wichita and Ouachita Uplifts). In addition to this, he allotted that a broad, north-trending quartz-rich belt of Desmoinesian sandstones coincided in part with exhumation of exposed quartz-rich sandstone beds within the Simpson Group on the Nemaha Uplift.

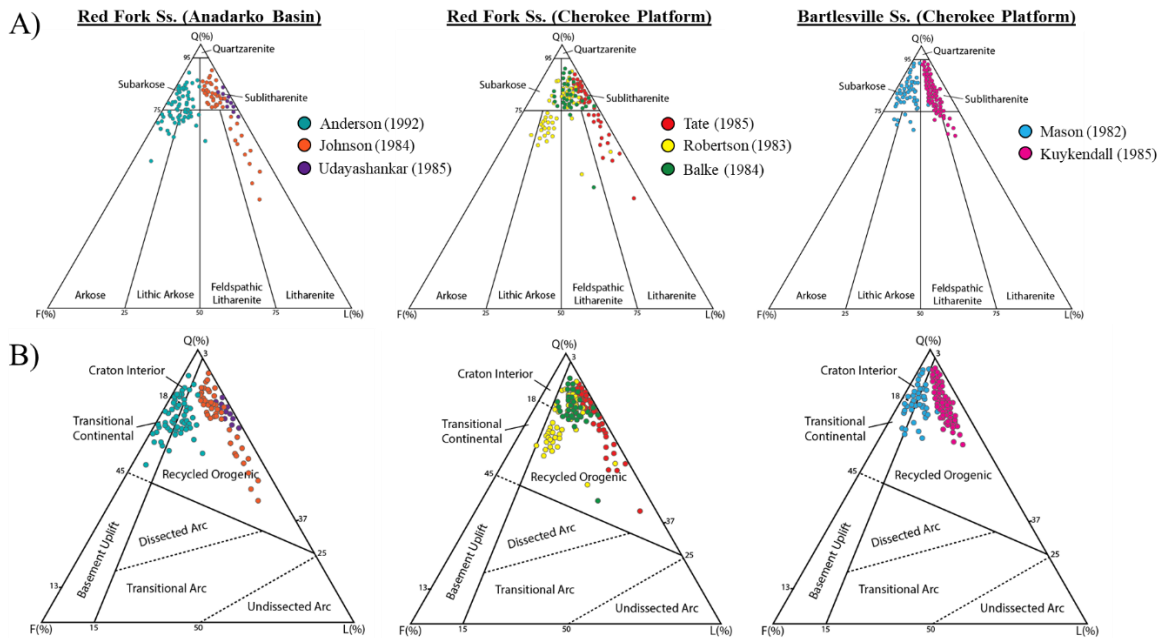


Figure 2. Compiled sandstone composition data (point counts) from the Red Fork and Bartlesville sandstones in surrounding areas on the Cherokee Platform and Anadarko Basin. **a)** Sandstone composition using Folk (1968) classification. **b)** QFL plot for inferred provenance type using Dickinson et al. (1983) classification.

2.2 New Insight into Appalachian Sediment Source and Dispersal

Although sandstone petrography has continued to provide unique information about provenance, more recent studies using detrital zircon geochronology of clastic strata in basins throughout the North American Craton has evolved our understanding of provenance and sediment dispersal during Pennsylvanian time. Most significant of these is perhaps a study done by Gehrels et al. (2011), in which a significant portion of detrital zircon ages corresponding to the Appalachian synorogenic orogenies was discovered in Paleozoic strata of the Grand Canyon. The identification of the Appalachians as a source of zircons in the Grand Canyon required a paradigm shift and an of a continental-scale sediment dispersal system extending from the

Appalachians to the location of the present Grand Canyon. This revelation resulted in a surge of studies to test the hypothesis of that proposed dispersal system extended from the Appalachians to basins across the North American Craton.

Thomas et al. (2017) is a comprehensive analysis of published zircon U-Pb ages and Hf signatures from Mississippian-Permian sandstones in the Appalachian foreland. The objective of this study was to define the provenance of Alleghanian synorogenic clastic wedges, as well as characterize the detritus available to more extensive intracontinental dispersal systems from the Appalachian margin. Results from the study determined that two major age components, Grenville (950-1300 Ma) and Taconic-Acadian (350-490 Ma), characterize the detrital zircon populations in the Alleghanian clastic wedges, with additional minor contributions from other ages. From this, Thomas et al. (2017) proposed that recycling from both the Taconic and Acadian clastic wedges along the Appalachian margin provided a large and readily available source of a wide range of ages of detrital zircons to Mississippian-Permian sediments in the Appalachian foreland and intracontinental dispersal systems throughout the North American Craton. Evidence supporting this hypothesis was further found in detrital zircons age signatures from Paleozoic strata throughout the North America Craton compiled in a study by Chapman and Laskowski (2019). In their study, Chapman and Laskowski (2019) determined that Appalachian derived detritus began moving westward across the North American Craton as early as the Devonian and became widespread in river systems throughout the craton by Pennsylvanian time. In addition, Chapman and Laskowski (2019) indicated that detrital zircons recovered from Pennsylvanian strata in the eastern, central, and western domains of the North America Craton showed slight spatial differences in age spectra. Western age spectra demonstrated a higher incorporation of Yavapai-Mazatzal (1600-1800 Ma) and Midcontinent Granite-Rhyolite (1300-1500 Ma) age zircons (interpreted source of the Ancestral Rockies), whereas central and eastern North America

age spectra show higher incorporations of Neoproterozoic/Pan-African (540-700 Ma) and Grenville (950-1300 Ma) age zircons, respectively.

Along the Midcontinent, Kissock et al. (2018) similarly interpreted that detrital zircon age signatures of Lower-Middle Pennsylvanian strata of the intracratonic Forest City and Illinois basins reflected both regional-scale fluvial systems that recycled underlying sedimentary strata and large-scale fluvial systems that likely supplied detritus shed from the Appalachian margin. In the study, Kissock et al. (2018) further inferred that Appalachian sourced systems were uniquely characterized by an abundance of detrital lithics and feldspars and could be divided into both a northern and central system based upon differences in detrital zircon age spectra. The northern Appalachians (Type 2 composite) was characterized by peak Acadian-Taconic and Neoproterozoic ages and the Central Appalachians (Type 3 Composite), similar to the Alleghenian clastic wedges investigated by Thomas et al. (2017), were characterized by peak Acadian-Taconic, Grenville, and Granite-Rhyolite Terrane ages. Regional-scale fluvial systems (Type 1 Composite) were characterized primarily as quartz-arenites with an abundance of Grenville age zircons. Other detrital zircon provenance work included in this study are those done by; Becker et al. (2005), West et al. (2008), Fyffe et al. (2009), Loan (2011), Pickell (2012), Willner et al. (2013; 2014), Siddoway and Gehrels (2014), Konstantinou et al. (2014), Henderson et al. (2015), Cole et al. (2015), Bradley et al. (2016), Xie et al. (2016), Thomas et al. (2016), and McGuire (2017).

CHAPTER III

GEOLOGIC BACKGROUND

3.1 Pennsylvanian Paleogeography

The paleogeography of the Pennsylvanian Sub-system was primarily constructed by tectonic activity associated with the final assembly of Pangea and variability in climatic conditions associated with Gondwanan glaciation. (Moore, 1979; Algeo and Heckel, 2008; Kissock et al., 2018; e.g.). This resulted in continually changing depositional patterns and sedimentary facies throughout the North American Midcontinent (Jenson, 2016; Rascoe and Adler; 1983, e.g.). The major tectonic and climatic events that largely controlled this variation can be summarized as: (1) orogenic uplift, which developed and shifted sediment sources, (2) closure of the Ouachita Embayment, which influenced dispersal of sediment, (3) accelerating subsidence of the Anadarko basin, and (4) flooding of the northern Midcontinent during the initiation of the Absaroka mega-sequence (Moore, 1979; Rascoe and Adler, 1983; Jordan 2008).

During the Pennsylvanian, evolution of numerous tectonic features occurred in rapid succession along the southern, eastern, and western margins of the Laurentian Craton. Along the southern margin, early stages of collision with Gondwana or a microplate (Perry, 1988) occurred during Late Mississippian to Early Pennsylvanian. This collision initiated inversion of the Southern Oklahoma rift zone and reactivation of Cambrian rift faults to the west (Hanson et 2013; Johnson, 1989). This intracratonic crustal flexure resulted in the uplift of the Wichita-Amarillo

mountains in the southern Oklahoma and the Texas Panhandle and initiated the growth and subsequent down-warping of the Anadarko basin (Johnson, 1989). The exhumation of the mountain belt provided thick accumulations of sediment (Granite Wash) to the southern portion of the Anadarko basin throughout the Middle Pennsylvanian to Early Permian (Moore, 1979; Johnson, 1989; Rascoe and Adler, 1983). To the west collision with Gondwana drove uplift of the Ancestral Rocky Mountains, which likely contributed significant detritus to the northwestern extent Anadarko shelf during the Early Pennsylvanian (Rascoe and Adler, 1983). Along the eastern margin of Laurentia, collision with northwest Africa led to continued growth and exhumation of the Appalachians (Alleghenian Orogeny) and a new pulse of detritus into foreland basins and beyond (Chapman and Laskowski, 2019; Thomas et al., 2017). Along the southern margin, uplift and northward thrusting of the Ouachita-Marathon belt occurred due to continued collision with the northern tip of South America (**Figure 3**). In Late Pennsylvanian, closure of the Ouachita embayment ensued and the mobile belt became a dominant source of sediment for the Anadarko and Arkoma basins in southern Oklahoma as principle sediment sources shifted from north-northeast to the south (Moore, 1979). Additional areas that underwent minor uplift, due to crustal flexure of the Midcontinent, were the Central Kansas and Nemaha Uplifts to the north, in present day Kansas and Nebraska, and the Ozark Uplift to the northeast in southwest Missouri and northern Arkansas. These uplifts influenced sediment distribution patterns throughout the Early to Middle Pennsylvanian and are presumed to have supplied locally derived detritus to areas along the Anadarko and Cherokee shelves (Moore, 1979; Johnson, 2009). Until the Early Desmoinesian the Nemaha Uplift separated the Anadarko basin from the Cherokee Platform and Arkoma basin, preventing the westward migration of sediment from the east.

Superimposed on these orogenic events were oscillating climatic conditions marked by cyclic sea-level fluctuations associated with the Absaroka megasequence, which began during the Late Mississippian. Sea-level changes during the megasequence are thought to occur in response

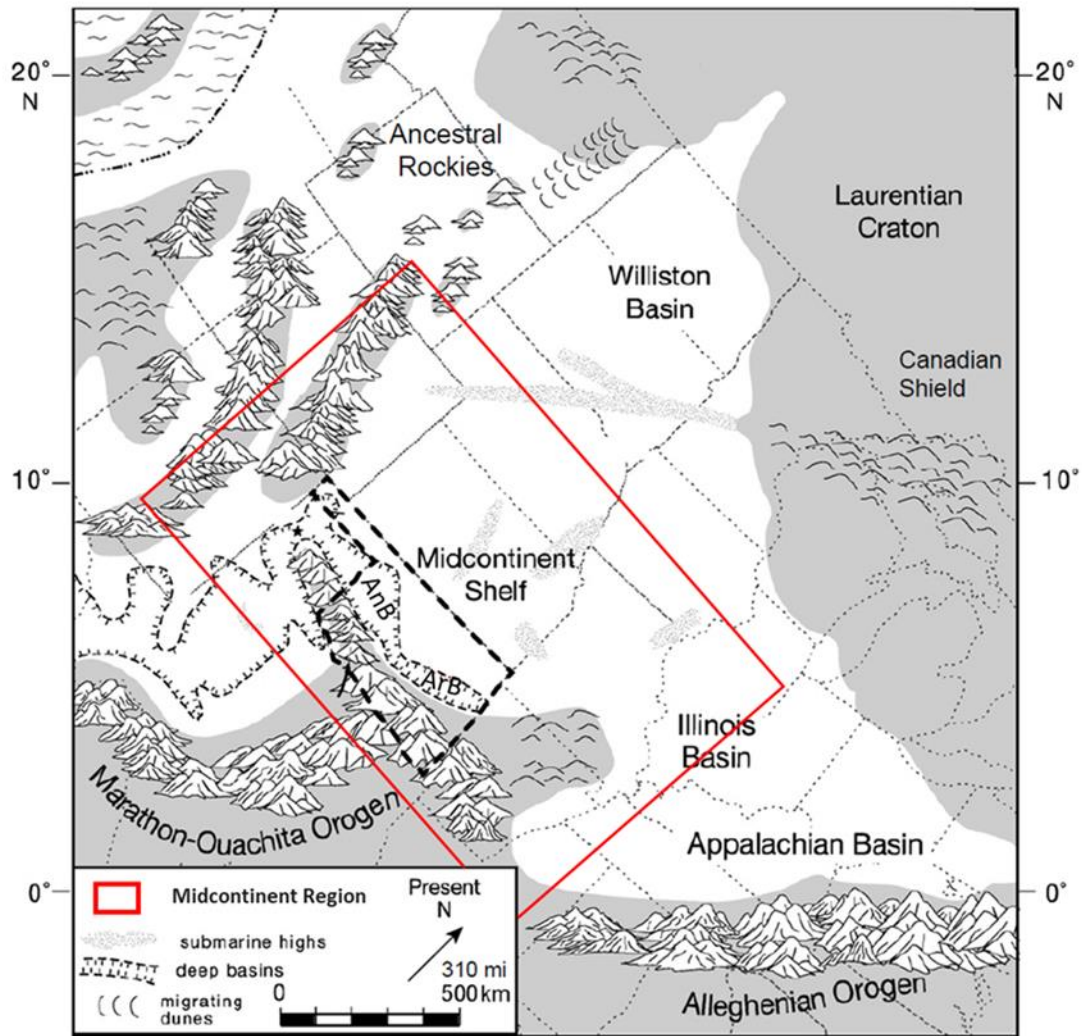


Figure 3. Paleogeographic reconstruction of the Middle-Late Pennsylvanian Laurentian Craton (modified from Algeo and Heckel, 2008).

to the waxing and waning of the Gondwana ice sheet modulated by Milankovitch orbital parameters (Algeo and Heckel, 2008). This resulted in high amplitude (up to 160 meters), high frequency (100 k.y.) sea-level rises and falls, which periodically flooded and exposed Pennsylvanian shelves on the Midcontinent (Algeo and Heckel, 2008; Jensen, 2016). This is reflected in Pennsylvanian cyclothem (Figure 5b) that indicate intermittent marine conditions alternated with widespread southward deltaic advances during the Early Desmoinesian (Jensen,

2016; Rascoe and Adler, 1983). In relatively low relief areas, on the Anadarko shelf and Cherokee platform, deltas formed and become marine-dominated or re-worked with slight rises in sea-level. Similarly, when sea-level dropped, deltaic and shallow marine shelf deposits were often incised by fluvial processes, allowing sediment to bypasses the shelf and accumulate in the Anadarko and Arkoma basins in the form lowstand deltas (Upper Skinner) and basin-floor fans (Red Fork) (**Figure 4**). Additionally, proximity to the paleoequator and the occurrence of coals support a sub-tropical to tropical humid climate for the Midcontinent. This climate influenced the magnitude and frequency of precipitation events, a major factor affecting rates of weathering, of subaerially exposed sediment on paleo-highs, and stream discharge (Cecil, 2003; Algeo and Heckel, 2008). Streams and large rivers on the North American Craton are postulated to have flowed westward during the late Paleozoic, influenced by dominant northeast and southeast trade winds (Gehrels et al., 2011; Chapman and Laskowski, 2019).

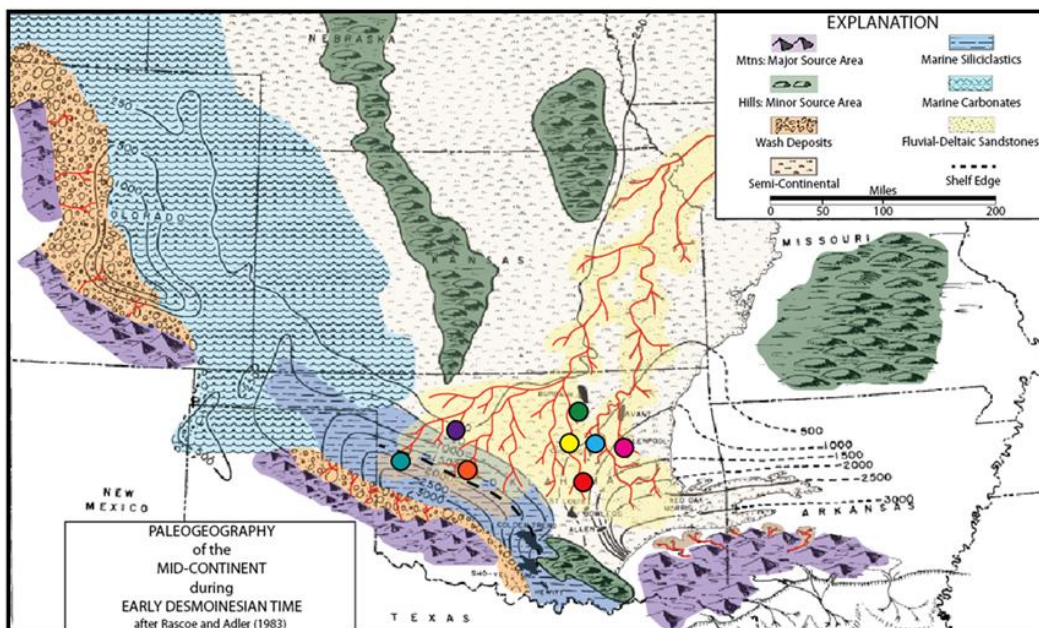


Figure 4. Early Desmoinesian paleogeography of the Mid-Continent (modified from Rascoe and Adler, 1983) illustrating the mapped extents of the Bartlesville and Red Fork sediment dispersal patterns. Colored markers represent the location of studies compiled in **Figure 2**.

3.2 Stratigraphic and Depositional Context

In Oklahoma and Kansas, the Desmoinesian series of the Pennsylvanian Subsystem is commonly divided into two groups: the carbonate dominated Marmaton Group and the siliciclastic dominated Cherokee Group. The boundary between these two groups is defined as the base of the regionally distributed Oswego Limestone (subsurface) and Fort Scott Formation (surface). The Cherokee Group is defined by all rocks below the Oswego-Fort Scott to the base of the Desmoinesian series. In northeastern Oklahoma, the Cherokee Group is further divided into the Cabaniss and Krebs groups, but the name Cherokee is often preferred and the section is widely referred to as the upper and lower Cherokee, respectively (Puckette, 1990).

Sediments of the Cherokee Group were deposited during the northward transgression of the Cherokee sea, interrupted by periods of southward delta progradation and shoreline retreat (Rascoe and Adler, 1983). This recorded intervals of 3rd order cyclic sedimentation that contain interbedded sandstone and shale “packages” bounded by transgressive limestone and subsequent highstand, marine (dark) shale beds (Ross and Ross, 1987; Jordan, 1957). These marker beds are easily recognizable across the southern Midcontinent and divide the Cherokee Group into the Prue, Skinner, Red Fork, Bartlesville, and Booch chrono-stratigraphic units (**Figure 5a**). The Verdigris, Pink, Inola, and Brown limestones, and the associated dark gray to black radiogenic condensed marine shales, are the chronostratigraphic and lithostratigraphic marker beds, respectively, that are used to subdivide the Cherokee Group. The top of the Pink Limestone lithostratigraphic marker is the boundary between the Red Fork and Skinner 3rd-order sequences and separate the upper and lower Cherokee intervals (Puckette, 1990). A summary of the detailed stratigraphy and depositional environments for the lower Cherokee Bartlesville and Red Fork sandstones follows.

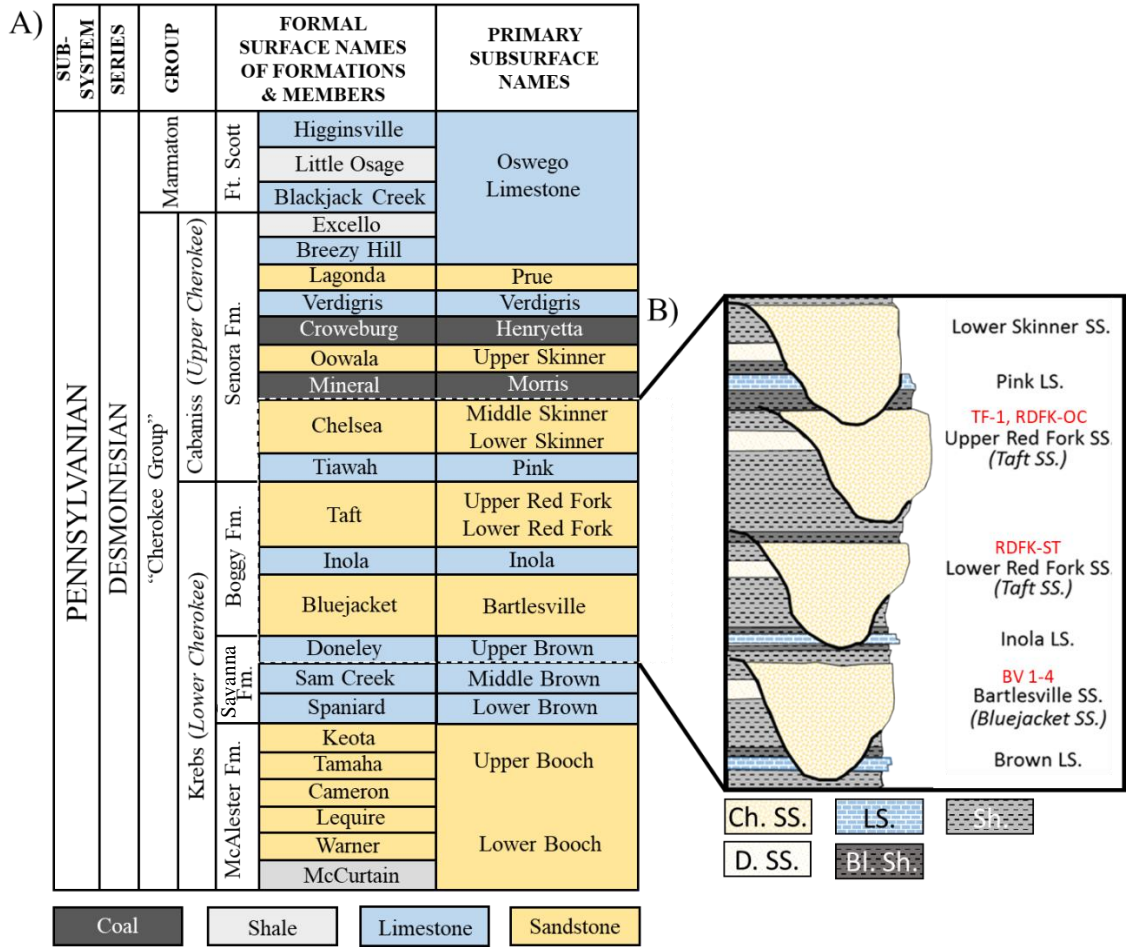


Figure 5. a) Stratigraphic column of the Midcontinent Desmoinesian series illustrating surface and subsurface nomenclature. **b)** Generalized sequence stratigraphy of the Cherokee Group as summarized by previous work mentioned here (Visher et al., 1971; Northcutt and Andrews, 1997; Andrews, 1997; e.g.). Channel sandstone (Ch. SS.), limestone (LS.), shallow marine shale (Sh.), deltaic sandstone (D. SS.), black shale (Bl. Sh.).

3.2.1 Bartlesville (Bluejacket) Sandstone

The Bartlesville Sandstone occurs in the lower Cherokee Boggy Formation and is defined as the interval from the base of the Inola Limestone to the top of the Brown Limestone.

Additionally, the Brown Limestone marks the boundary between the Boggy Formation and the underlying Savanna Formation, and is the initial transgressive sequence of the Cherokee Sea. The Bartlesville Sandstone is correlative with the surface equivalent Bluejacket Sandstone (Jordan,

1957), while subsurface equivalents include the Glenn Sandstone of Glenpool Field in Creek County, Oklahoma and the Salt Sandstone in Okmulgee, Oklahoma (Jordan, 1957).

The contact between the Bartlesville Sandstone and the underlying Brown Limestone is generally at the base of an incised valley, which often erodes down into the underlying Brown limestone and marine shales (Northcutt and Andrews, 1997) (**Figure 5b**). At the southern extent of the Bartlesville deposition, the contact appears gradational with the underlying marine shale, with the interval consisting of multiple lenticular sand bodies (Visher et al., 1971). Interpretations consider these sandstone bodies to be distributary-mouth bars deposited at the Bartlesville delta front (Northcutt and Andrews, 1997). The interval can generally be broken up into three progradational deltaic sequences that thicken to the southeast along an approximated shelf hinge line (Visher et al., 1971). To the northwest of the hinge line the interval thins and unconformably onlaps older strata (Northcutt and Andrews, 1997). The extent of Bartlesville deposition is limited to the Cherokee Platform and Arkoma basin east of the Nemaha Uplift. On the uplift the Bartlesville is absent either by nondeposition or erosion (Northcutt and Andrews, 1997). To the south and east of the Cherokee Platform, Bartlesville extent is limited by its outcrop in the Arkoma basin and along the western flank of the Ozark Uplift.

3.2.2 Red Fork (Taft) Sandstone

The Red Fork Sandstone interval occurs in the lower Cherokee Boggy Formation and is defined as the interval from the base of the Pink Limestone (Tiawah Limestone in outcrop) to the top of the Inola Limestone. The Inola Limestone markers the boundary between the Red Fork and underlying Bartlesville interval. In western Oklahoma, the Red Fork is additionally subdivided into the Upper and Lower Red Fork intervals by a locally extensive, disconformable, thin shale marker (Johnson, 1984). The Red Fork, for the most part, is the subsurface equivalent to the Taft Sandstone member (Jordan, 1957). However, the Taft Sandstone found in the southern part of the

Ozark outcrop belt, along the shores of Lake Eufaula, is highly conglomeratic and compositionally diverse from the Red Fork sandstones in central Oklahoma (Andrews, 1997). This indicates a potential source reversal to the southeast, similar to the upper Cherokee, and the sandstone as being uncorrelatable with the Red Fork sandstones identified trending from the northeast. (Andrews, 1997). Subsurface equivalents to the Red Fork Sandstone include the Earlsboro sandstone and Chicken Farm sandstone of central Oklahoma.

Sandstones of the Red Fork interval is predominantly of fluvial in the north and pass southward into deltaic and shallow marine environments in the Anadarko basin (Andrews, 1997). In central and northern Oklahoma, much of the sandstones consists of channel deposits that have incised directly into lower marine shales and limestone of the Inola transgressive sequence during sea-level lowstand (Robertson, 1983; Balke, 1984). On top of the Nemaha Uplift and along the Central Oklahoma fault zone, the Red Fork interval unconformably overlies Mississippian strata off structure and Mississippian through Early Ordovician strata on eroded structures indicating it was likely the initial southward prograding Cherokee fluvial-deltaic complex to overtop the positive structure and deposit sediment west into the subsiding Anadarko basin. Progradational sequences west of the Nemaha Uplift and Central Oklahoma fault zone consist of Red Fork delta front shales and sandstones overlain by channel sands (Andrews, 1997). The Red Fork interval thins to the north and east where it onlaps older strata and thickens to the southwest along a well-defined shelf-break (Anderson, 1992; Johnson, 1984). The shelf break represents the transition from dominantly deltaic to submarine lithofacies consisting of stacked sequences of submarine fans, channels, and turbidites (Anderson, 1992). Along the shelf-break, as many as 25 depositional units may be stacked, whereas on the northern shelf commonly two to three sand bodies are identified (Johnson, 1984).

CHAPTER IV

POTENTIAL SEDIMENT SOURCES

Provenance analysis based on dual detrital zircon geochronology and sandstone petrography requires detailed knowledge of the age, Hf isotopic signature, and sedimentological make up of potential source terranes. Earlier investigations provide this foundational knowledge for robust provenance analysis on the North American Craton (Gehrels et al., 2011; Thomas et al., 2017; Whitmeyer and Karlstrom, 2007; e.g.). The present configuration of the craton formed over billions years through a series of microcontinental collisions (Hoffman, 1989). These collisions and accretionary events formed 9 major provinces that are identified as potential sources of Paleozoic strata on the craton. They included the Superior, Wyoming, Trans-Hudson, Yavapai-Mazatzal, Midcontinent Granite-Rhyolite, Gondwanan-Pan-African accretions, Synrift Igneous, Grenville, and Appalachian synorogenic provinces (Whitmeyer and Karlstrom, 2007; Gehrels et al., 2011; Thomas et al., 2012; 2016; 2017) (**Figure 6**). In the following sections, potential sources of these province sediments are organized by geography. The locations of compiled detrital zircon U-Pb age data from previous work used in this study for provenance identification (including the composite type signatures from the Forest City and Illinois basins) are displayed in **Figure 8**.

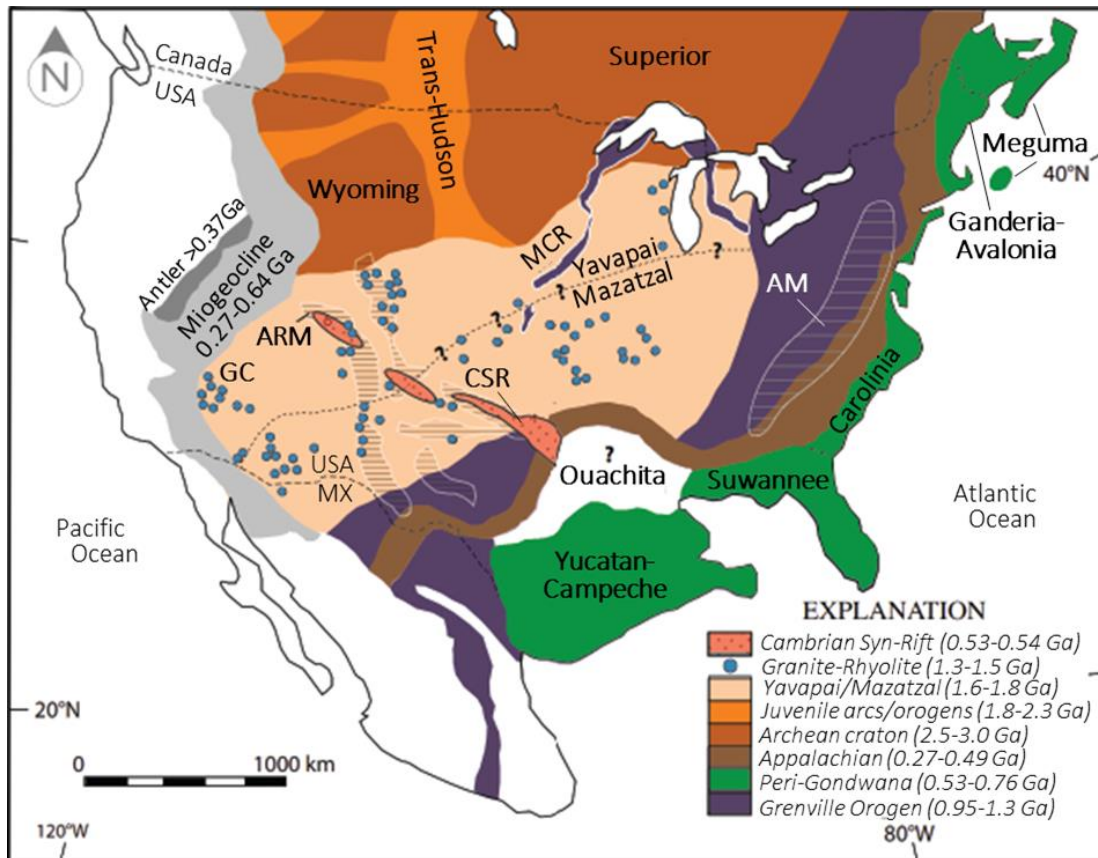


Figure 6. Basement map of major North American geologic provinces (modified after Chapman and Laskowski, 2019). Ancestral Rocky Mountains (ARM), Appalachian Mountains (AM), Cambrian Syn-Rift (CSR), Midcontinent Rift (MCR), Grand Canyon (GC).

4.1 Northern Provenance

The northern part of the North American Craton is occupied by the Canadian Shield which includes several distinct age provinces: Superior (2,700-3,500 Ma), Wyoming (2,500-2,700 Ma), Trans-Hudson (1,800-2,300 Ma), and Grenville (950-1300 Ma) (Whitmeyer and Karlstrom, 2007; Chapman and Laskowki, 2019; Gerhrels et al., 2011). These, as well as much of the Granite- Rhyolite and Yavapai-Mazatzal province of the Midcontinent, are covered by Paleozoic sedimentary rocks (Thomas et al., 2017). Sedimentary thickness and facies

distributions along with the present eroded limits of the Paleozoic cover indicate that much of the shield was covered before Mississippian time, therefore, eliminating the shield's magmatic and metasedimentary rocks as an available primary source for Pennsylvanian sediments (Sloss, 1988; Thomas et al., 2017). During the Neoproterozoic Iapetan rifting of Laurentia, the exposed craton was a source of zircon grains with ages from Superior to Grenville. These grains were deposited along sections of the rifted margin and later reworked by passive-margin transgression (Sloss, 1988; Konstantinou et al., 2013). These reworked sediments are recognized by their unique concentrations of 2,700-3,000 Ma zircons and common to early Paleozoic sedimentary rocks that cover large parts of the central North American Craton (Pickell, 2012; Konstantinou et al., 2013; Chapman and Laskowski, 2019). This makes it difficult to identify the Canadian Shield as probable source of these zircons, and other associated grains, without additional in-depth knowledge of the paleogeography and eroded limits of early Paleozoic sedimentary cover.

4.2 Eastern Provenance

The eastern margin of the North American Craton is characterized by the superposition of multiple provinces that comprise the Appalachian region. These provinces encompass a wide range of ages and they include the Grenville province, Iapetan synrift rocks, Gondwanan Accreted Terranes, and Appalachian Syn-orogenic terranes (Taconic, Acadian, and Alleghenian orogenies) (Thomas et al., 2017). Direct sourcing from these terranes, along with recycled material from early Paleozoic sedimentary cover and the Taconic and Acadian clastic wedges along the Appalachian front, are postulated to have dispersed detritus west across the craton during the orogenic uplift associated with the late Paleozoic Alleghenian orogeny (Gerhels et al., 2011; Chapman and Laskowski, 2019).

The Grenville province, a residual basement feature of the Elzevirian, Shawinigan, and Grenville orogenies, has a time of approximately 950-1300 Ma and encompasses the largest area

along the eastern margin of the craton (Rivers et al., 2012; Whitmeyer and Karlstrom, 2007). While the province is predominantly covered by early Paleozoic sedimentary cover, exposed external and internal basement massifs within the Appalachians provide the primary source of zircons with ages of 950-1300 Ma, as well as various ages from inliers of older, partially reworked, crystalline rocks (Thomas et al., 2017). Sediments derived from the igneous rocks of the Grenville orogen are known to yield ϵ_{Hf} values that range from -5 to 10 (Mueller et al., 2008; Bickford et al., 2010). The Grenville ages of 950-1300 Ma generally dominate sediments in the Taconic clastic wedges of the Appalachian Foreland (Thomas et al., 2017).

Along with the Grenville internal basement massifs, accreted terranes of Gondwanan affinity are distributed along the internal parts of the Appalachians and correspond to the Pan-African-Brasiliano events in Gondwana. Exposed terranes are primarily focused in the northern Appalachians with the three major composite terranes Ganderia, Avalonia, and Maguma extending along the orogen from the New York promontory to the Newfoundland embayment. These terranes were accreted by the late Paleozoic (Willner et al., 2013; 2014; Thomas et al., 2017). Southward, the minor composite of the Carolina terrane comprises the internal part of the Appalachian orogen, from the Pennsylvania embayment southward to the Alabama promontory (Hibbard, 2000). These Gondwanan terranes have Neoproterozoic metavolcanic, metasedimentary, and plutonic basement rocks with ages of 520-800 Ma (West et al., 2008; Fyffe et al., 2009; Loan, 2011; Willner et al., 2013; 2014; Bradley et al., 2016; Henderson et al., 2016;). Ages of 760-530 Ma and older components of Gondwana, including ages of 2730-2550 Ma and 2200-1140 Ma, generally dominate Neoproterozoic to Cambrian sedimentary rocks (Willner et al., 2013; Henderson et al., 2016), but are relatively absent in late Paleozoic clastic wedges in the Appalachian foreland basin (Thomas et al., 2017) (**Figure 7**). While indistinguishable from Laurentia rocks, such as the Iapetan Synrift rocks on the Iapetan rifted margin (530-765 Ma), igneous and sedimentary rocks from the Gander and Avalon terranes indicate that Gondwana

derived sediments generally yield ϵ_{Hft} values that are highly variable and somewhat more evolved (Willner et al., 2013).

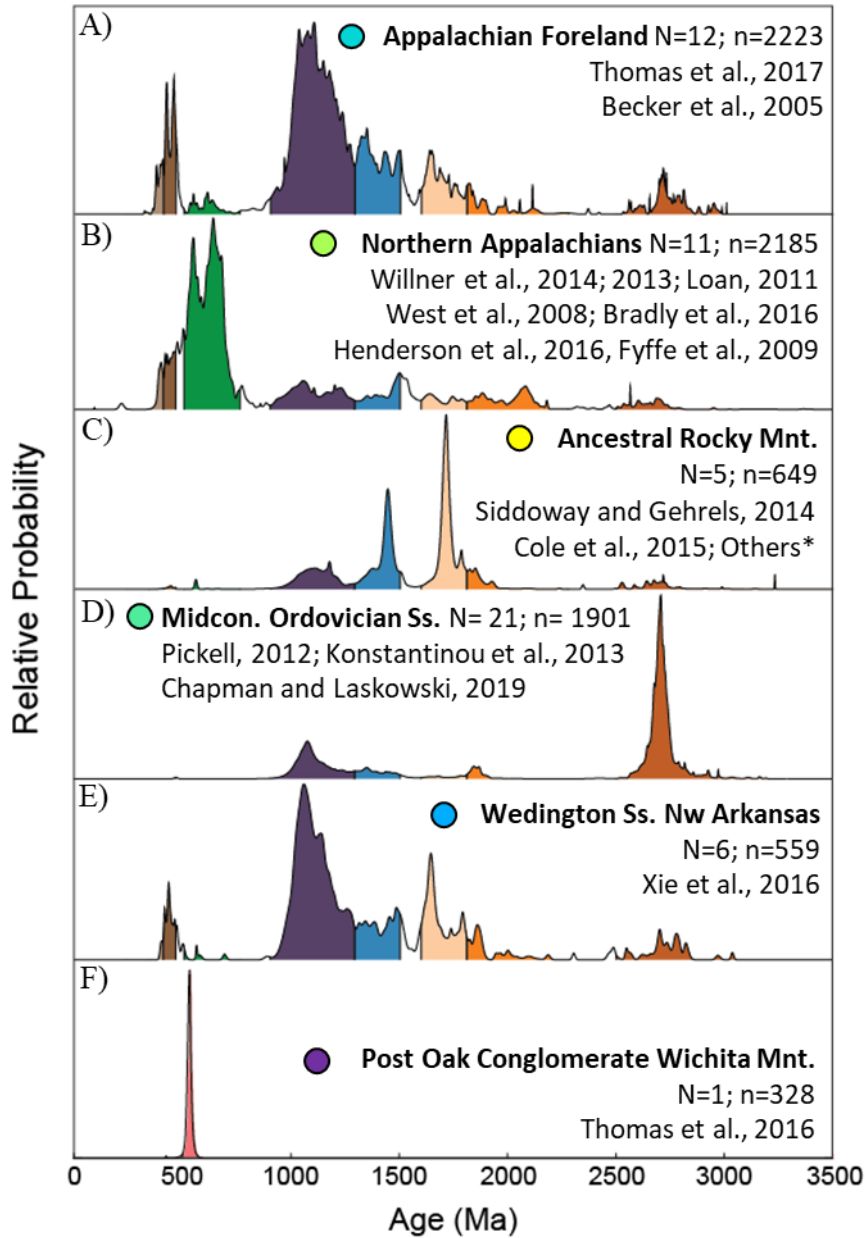


Figure 7. U-Pb probability density plots of samples from the **a)** Appalachian Foreland, **b)** Northern Appalachian Peri-Gondwanan Terranes, **c)** Ancestral Rocky Mountains and Grand Canyon, **d)** Midcontinent Ordovician quartzarenites, **e)** Weddington Sandstone on the Arkansas Shelf, **f)** Post Oak Conglomerate in the Wichita Mountains of southern Oklahoma. Plots are colored coded to the North American provinces observed in **Figure 6**.

The Taconic, Acadian, and Alleghenian synorogenic terranes are also distributed along the eastern margin of the craton and record a succession of arc-accretion events that occurred during the Ordovician (490-420 Ma), Devonian (420-350 Ma), and Mississippian-Pennsylvanian (330-270 Ma), respectively. Eroded roots of the magmatic arcs dominate the Appalachian foreland clastic wedges, which are potential sources for late Paleozoic recycling (Thomas et al., 2017). These clastic wedges are generally dominated by igneous rocks of the preceding synorogenic plutons, along with a variety of ages from inliers of older, reworked, crystalline rocks (Thomas et al., 2017). Sediments of the Pennsylvanian age Alleghenian clastic wedges are concentrated with zircons ages of the Grenville province and the Taconic and Acadian synorogenic plutons, but contain smaller populations of zircons from the Alleghenian synorogenic plutons and other pre-Alleghanian sources (Becker et al., 2005; Thomas et al., 2017).

4.3 Western Provenance

It is postulated the Pennsylvanian western sources are postulated to have contributed minimal detritus to the central craton primarily due to the prevailing northeast to southwest trade winds (Chapman and Laskowski, 2019). However, two proximal sediment sources, the Ancestral Rockies and Transcontinental Arch, could have contributed small volumes of arkosic and metamorphic lithic fragment-rich-detritus to the western portions of the Anadarko basin during the earliest Pennsylvanian (Rascoe and Adler; 1983; Dyman, 1989; Johnson, 1989). As a result of ongoing uplift during much of the Pennsylvanian and continuing into Early Permian, the Ancestral Rocky Mountains generated sediment that was likely transported by mountain fed rivers to the western margin of the craton (Gehrels et al., 2011; Chapman and Laskowski, 2019). The detrital grains sourced from the Ancestral Rockies record derivation from Precambrian (Yavapai-Mazatzal (1657-1781 Ma)) basement and smaller portions of 1300-1500 Ma granitoids exposed in the mountains (Gehrels et al., 2011; Siddoway and Gehrels 2014). Just to the east of the Ancestral Rocky Mountains, in present day northwestern Kansas and Nebraska, the

Transcontinental Arch simultaneously uplifted to a broad, low-relief topographic high exposing metaquartzite (Rascoe and Adler; 1983;). However, exposure of the Transcontinental Arch's metamorphic terranes likely only spanned a short time during the Early Pennsylvanian (Morrowan-Atokan) before major transgression and onlapping of early Desmoinesian strata.

4.4 Midcontinent Provenance

In the Midcontinent, several sources existed during the Pennsylvanian that provided proximal detritus to the Anadarko and Arkoma basins, as well as adjacent shelf areas. In northern Oklahoma and southern Kansas, late Paleozoic uplift of the Nemaha Ridge exposed Precambrian crystalline basement, until transgressive overlap of the Desmoinesian Cherokee-Marmaton succession. This basement material includes various assemblages of metamorphic, plutonic, and volcanic rocks that range in age from 1,400-1,700 Ma (Whitmeyer and Karlstrom, 2007; Bickford et al., 1981). Farther east, faulting and uplift of the Ozark dome exposed similar age Precambrian through Mississippian rocks southwestward from northern Missouri into the Arkoma foreland basin and Ouachita fold-and-thrust belt. Granitic basement in the Francois Mountains, southeastern Missouri, show a range of ages in two groups from 1317-1323 Ma and 1462-1466 Ma (Thomas et al., 2012), with $\epsilon_{\text{Hf}}(t)$ values suggesting the granitic basement evolved from underlying Yavapai-Mazatzal juvenile crust on the central craton (Goodge and Vervoort, 2006). Additionally, exposed Upper Cambrian-Late Mississippian strata along the uplift could have provided significant quantities of recycled grains with a broad range in ages. In the south, proximal turbidite and basin-floor fan deposits of feldspathic and quartzose-chert conglomerates, including the classic "Granite Wash", are attributed to rocks exposed along the Southern Oklahoma Fault System and Ouachita Fold Belt. In the Wichita Mountains, Paleozoic sandstones directly above an unconformable contact with the Wichita Granite Group have strongly unimodal U-Pb ages from 540-520 Ma and juvenile Hf values of 4.7 to 10.1 (Thomas et al., 2016). In contrast Paleozoic sandstones on the flank of the Arbuckle anticline have detrital grains with ages

that correspond dominantly to the Superior (~2700 Ma) province and secondarily to the Granite-Rhyolite (1480-1320 Ma) and Grenville provinces (Thomas et al., 2016). Similarly, exposed Ordovician-Mississippian strata along the Ouachita Fold Belt provide detrital zircon signatures characterized by a dominance of Grenville province ages along with secondary concentrations of Granite-Rhyolite and Superior province ages (McGuire, 2017).

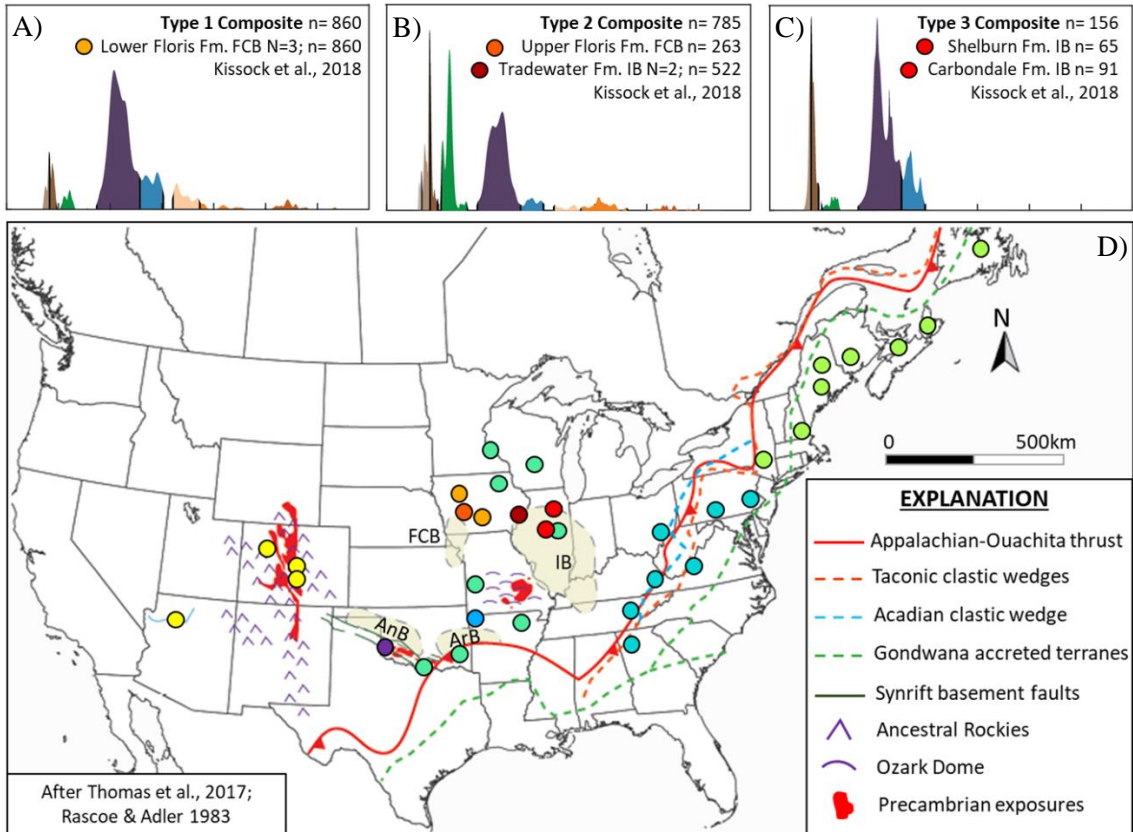


Figure 8. Top: U-Pb probability density plots of samples from the Illinois and Forest City basins; **a)** type 1 composite, **b)** type 2 composite, **c)** type 3 composite. Bottom: **d)** regional map of potential provenance elements on the North American Craton (modified after Thomas et al., 2017 and Rascoe and Adler, 1983) with the location of samples from **Figure 7** and the Illinois and Forest City basins presented here.

CHAPTER V

METHODOLOGY

5.1 Detrital Zircon Geochronology

Over the past few decades', detrital zircon geochronology has emerged as a standard, if not the primary, tool for sediment provenance analysis, largely due to the advancement of in situ analytical techniques yielding rapid and precise (1-2 sigma uncertainty) U-Pb and hafnium isotope analysis (Saylor and Sundell, 2016; Thomas, 2011; Gehrels et al., 2008). Applications of detrital zircon geochronology include: improved ability to accurately characterize unknown provenance proportions, unmixing highly complex sediment source distributions, correlating between sedimentary units, improved sediment budgeting and routing models, and determining maximum depositional age (Saylor and Sundell, 2016; Saylor and Sundell, 2017; Thomas, 2011). These applications have benefited from growing samples sizes, due to significantly decreased analytical cost, which permits a greater ability to complete robust intersample comparisons, identification of small subpopulations (sediment sources), and quantification of relative subpopulation proportions (relative %) (Saylor and Sundell, 2016; Saylor and Sundell, 2017; Saylor et al., 2017). Teamed with detailed quantitative and qualitative petrographic analysis, these applications can be practically applied to the prediction of spatial and temporal changes in rock fabric, which plays an essential role in siliciclastic reservoir quality. This study attempted this through a unique workflow (**Figure 9**), which incorporates both detrital zircon geochronology

and sandstone petrography to reconstruct potential sediment dispersals paths that can be used in future investigations to accurately reconstruct depositional models and improve predictions for clastic-reservoir occurrence and quality. Nonetheless, it is important to remember that provenance estimation made by these methods involves some degree of uncertainty and therefore predictions are purely made on the basis of highest probability (likeliness) of occurrence and not actuality.

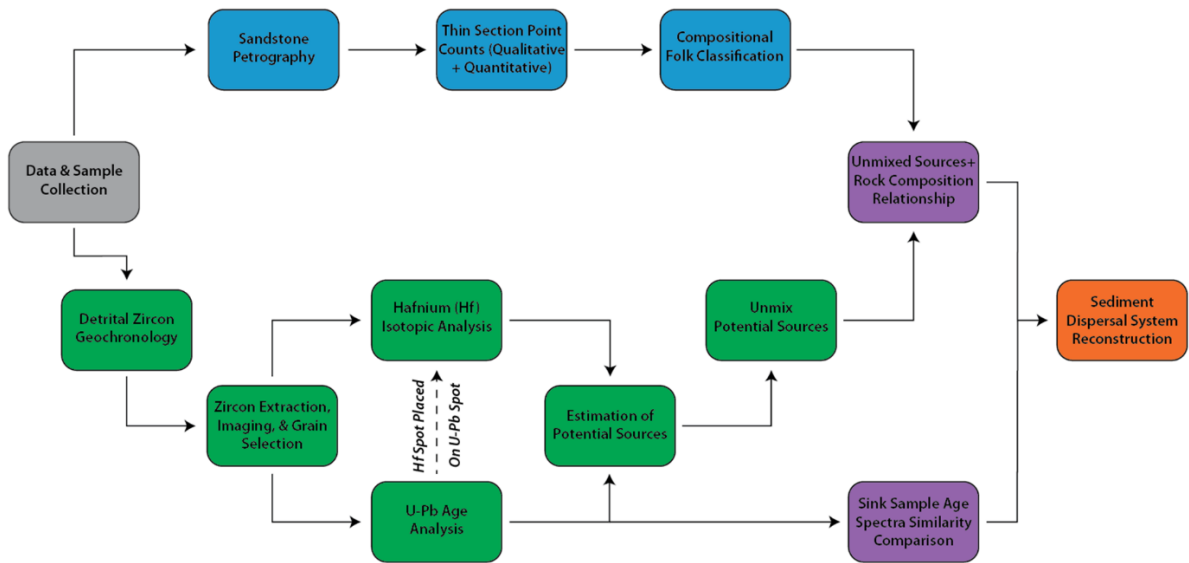


Figure 9. Flowchart describing the workflow for this investigation (left to right) and the methods used.

5.1.1 Sample Collection and Preparation

Sampling was designed to collect the Bartlesville/Bluejacket and Red Fork/Taft sandstones at selected locations on the Cherokee Platform, northern Oklahoma and in the Anadarko Basin. Locations were chosen based on accessibility and proximity to the petrologic studies previously conducted on the sandstones by students at Oklahoma State University. This was done in an effort to draw a necessary correlation between provenance observations made in

this study and the detrital composition and depositional trends previously observed for the two sandstone reservoirs. In total, four samples were collected with three designed for analysis of both detrital zircons and sandstone petrography, and one for petrographic analysis alone. One sample of Bluejacket Sandstone was taken from the prominent outcrop located along OK Highway 20 west of Pryor, Oklahoma (**Figure 10**). Approximately 10kg of the coarsest grain sized material was collected from various locations along the outcrop. Stratigraphically above this section, and four miles to the west, one sample of very fine grained Red Fork sandstone (referenced as Red Fork Outcrop in this study) was taken just below the Pink Limestone contact. This sample was chosen to be analyzed for sandstone petrography alone based upon its similarity and proximity to the Bluejacket sample. In addition to this sample, two additional Red Fork Sandstone samples were collected and run for detrital zircon analysis. One sample was collected from the Taft Sandstone, previously referenced by Andrews (1997), outcropping near Taft, Oklahoma in Muskogee County. The second Red Fork sample came from lateral drill cuttings taken from the 1HX Saratoga 1720 well located in section 8, T.14N., R.14W., South Thomas Field, Custer County, Oklahoma. This second sample is from an area immediately northeast (landward) of the Lower Red Fork shelf-break identified by Johnson (1984). Red Fork samples were taken from a very fine- to fine-grained sandstone contacted approximately half-way into the lateral that landed in section 20, T.14N., R.14W., with a true vertical depth (TVD) of 10,865 feet. Cuttings were interpreted to be from an incised valley-fill sandstone within the Lower Red Fork interval, previously characterized and mapped by Johnson (1984) (**Figure 11**).

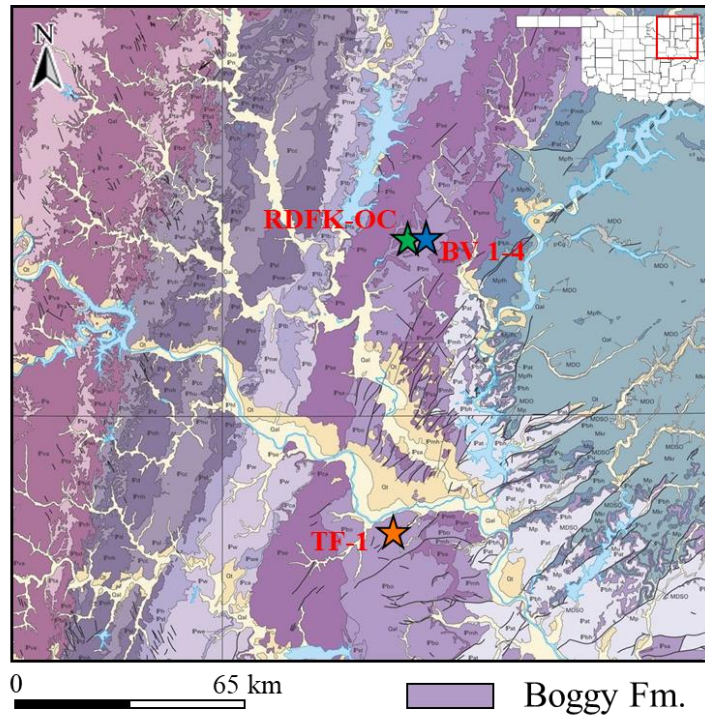


Figure 10. Geologic map of northeast Oklahoma (modified from Heran et al., 2003). Map shows the location of outcrop samples RDFK-OC, BV 1-4, and TF-1.

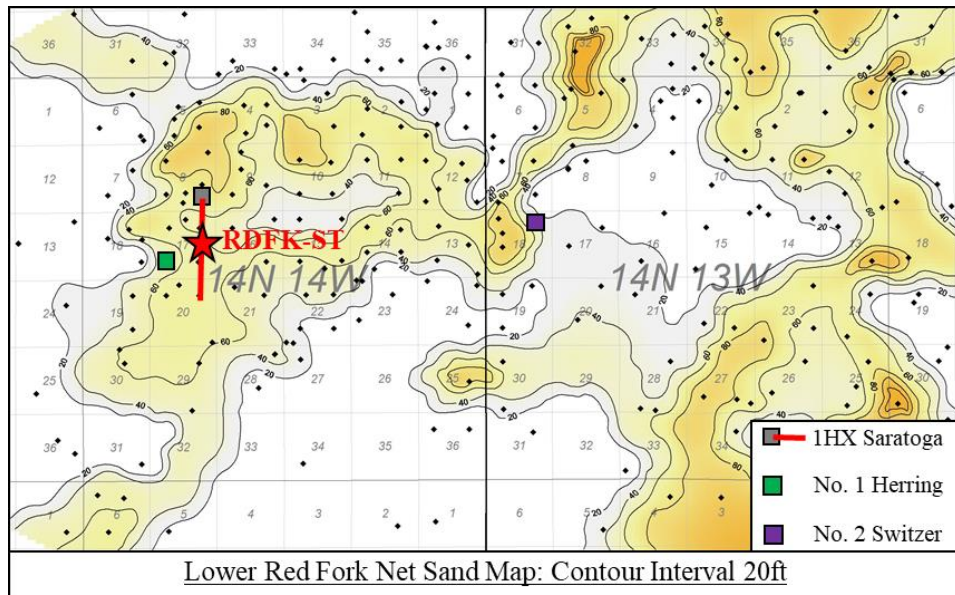


Figure 11. Net sandstone isopach within the Lower Red Fork channel encountered by the 1HX Saratoga, No.1 Herring, and No.2 Switzer wells in South Thomas Field.

Once collected, outcrop samples were transported to Oklahoma State University where they were prepared for zircon extraction and thin sectioning. Prior to zircon separation and extraction, the exterior of outcrop samples were cleaned of contamination using a rock saw, deionized water, and a wire brush, while lateral drill cuttings from the 1HX Saratoga 1720 were soaked in acetone to remove drilling mud and residual oil saturation. Once cleaned, 5-10 kg of each sample were broken into $\frac{3}{4}$ inch pieces using a rock hammer then crushed and disaggregated using a SPEX Shatter Box. Crushed samples were sent to the University of Arizona LaserChron Center for separation and mounting using procedures outlined by Gehrels et al. (2008) and Gehrels and Pecha (2014). Zircon crystals were extracted by traditional methods of separation with a Wilfley table, heavy liquids, and a Frantz magnetic separator. Samples were processed to retain as many zircons as possible from the original sample in the final heavy mineral fraction. A representative split (generally hundreds of grains) of the final, retained zircon yield was mounted in a 1 inch-diameter epoxy plug along with SL (Sri Lanka), FC-1, and R33 primary zircon standards and additional Hafnium zircon standards Mud Tank, Temora, 91500, and Plešovice. Mounts are sanded down to a depth of ~ 20 μm , polished and imaged prior to analysis. Cathodoluminescence (CL) and back-scattered electron (BSE) images were generated for every sample (**Figure 12**). Images were used to locate laser pits in homogeneous portions of crystals where multiple age zones were identified and to identify any non-zircon crystals retained after the final mineral fractionation.

5.1.2 U-Pb Age Analysis

U-Pb geochronology of zircons was conducted by laser ablation-inductively coupled mass spectrometry (LA-ICPMS) at the University of Arizona LaserChron Center using methods described by Gehrels et al. (2008, 2011) and Gehrels and Pecha (2014). The analysis was conducted with a Photon Machines Analyte G2 excimer laser coupled to a Thermo Element 2 HR

ICPMS. Analyses were conducted with a 20 μm beam diameter, which excavated a pit of $\sim 12 \mu\text{m}$ depth during a ~ 35 second analysis.

Between 117 and 220 analyses were conducted on each sample mount. A minimum number of 117 was chosen in order for each sample analysis to have a 95% confidence that all grain age populations representing $>5\%$ of the total grains would be included in the analysis (Vermeesch, 2004). Grains were selected at random and were only rejected on the basis of small size (less than 20 μm), the presences of cracks or inclusions, and/or complex zonation.

Ages were calculated from the three measured ratios of $^{206}\text{Pb}/^{238}\text{U}$, $^{206}\text{Pb}/^{207}\text{Pb}$, and $^{207}\text{Pb}/^{235}\text{U}$. Measurements were made via six corrections as outlined by the Arizona LaserChron Lab: (1) calibration of $^{206}\text{Pb}/^{238}\text{U}$ and $^{206}\text{Pb}/^{207}\text{Pb}$ isotopic and elemental fractionation relative to FC-1 (primary) and SL and R33 (secondary) standards; (2) subtraction of ^{204}Hg based on measurement of ^{202}Hg and natural $^{202}\text{Hg}/^{204}\text{Hg}$ to yield ^{204}Pb intensity; (3) Pb correction based on the measured $^{206}\text{Pb}/^{204}\text{Pb}$ and assumed composition of common Pb using Stacey and Kramers (1975); (4) calculations utilizing decay constants of Steiger and Jager (1977) and Hiess et al. (2012); (5) propagation of internal uncertainties of $^{206}\text{Pb}/^{238}\text{U}$ and $^{208}\text{Pb}/^{232}\text{U}$ based on regression scatter and $^{206}\text{Pb}/^{207}\text{Pb}$ and $^{206}\text{Pb}/^{204}\text{Pb}$ based on standard deviation; and (6) propagation of uncertain external uncertainties (fraction calibration, age of primary standard, common Pb composition, and decay constants)(Horstwood et al., 2016).

For interpretation, data were filtered to exclude ages with $>20\%$ discordance, $>5\%$ reverse discordance, $>10\%$ uncertainty, or high common Pb. The selection criterion for using $^{206}\text{Pb}/^{238}\text{U}$ age verses $^{206}\text{Pb}/^{207}\text{Pb}$ age as “best age” was set at 900 Ma, and $^{206}\text{Pb}/^{207}\text{Pb}$ ages were used for U-Pb dates over 900 Ma. Data were presented graphically on U-Pb relative probability density plots and normalized age-probability diagrams utilizing the Isoplot 3.0 program from Ludwig (2003), as well as additional programs provided by the Arizona

LaserChron Center (<http://www.laserchron.com>). Relative probability density plots were constructed separately for each sample by summing all ages and their uncertainties and normalized age-probability diagrams were constructed by summing all relevant analyses and uncertainties and then dividing by the number of analyses such that each curve contains the same area. Ages of peaks in age-probability diagrams were calculated using the University of Arizona Excel based 'Age Pick' program. Greatest significance was placed on ages of peaks containing continuous age probability from at least three analyses at the 1σ level.

Comparison of detrital zircon age spectra was aided by multidimensional scaling (MDS) using methods described by Saylor et al. (2017). MDS of detrital zircons facilitates the comparison of detrital age distributions by producing a Cartesian plot in N- dimensions through conversion of intersample dissimilarity (distance) to disparity via linear transformation and iterative reengagement in Cartesian space (Saylor et al., 2017). To accomplish this, MDS seeks to minimize the stress ("misfit") between distance and disparity, with low stress indicating a reasonable transformation or linear correlation between distance and dissimilarity. Stress is calculated as is the disparity between the *i*th and *j*th element and the disparity is calculated as a linear (1:1) transformation of the input dissimilarities (Saylor et al., 2017; Vermeesch, 2013). In an MDS plot, samples are represented as a point, typically in a two- or three-dimensional Cartesian space, with greater distances between two points indicating greater dissimilarity between the two individual U-Pb age spectra (Saylor et al., 2017). In this study, metric nonclassical MDS was implemented using the DZmds MATLAB algorithm developed at the University at Houston and referenced by Saylor et al. (2017). Dissimilarity was calculated as the Kolmogorov-Smirnov (K-S) Test D value and coefficient of nondetermination (compliment of the Cross-correlation coefficient (1-R²) based on PDPs). Because the K-S Test D value and coefficient of nondetermination are calculated differently (Saylor and Sundell, 2016), the resulting MDS plots are not expected to be identical and therefore provide two different models

for comparison. Both are plotted in 3-dimensions using metric squared stress, where stress is normalized to the sum of the 4th power of dissimilarities. Criterion were selected to minimize both the number of dimensions and the stress. Plots were interpreted in terms of relative grouping of sample and potential source points and the similarity (distance) between samples and potential sources, in terms of closest and second closest neighbor, with greatest weight given to the similarity trends seen in MDS plots derived from both metrics.

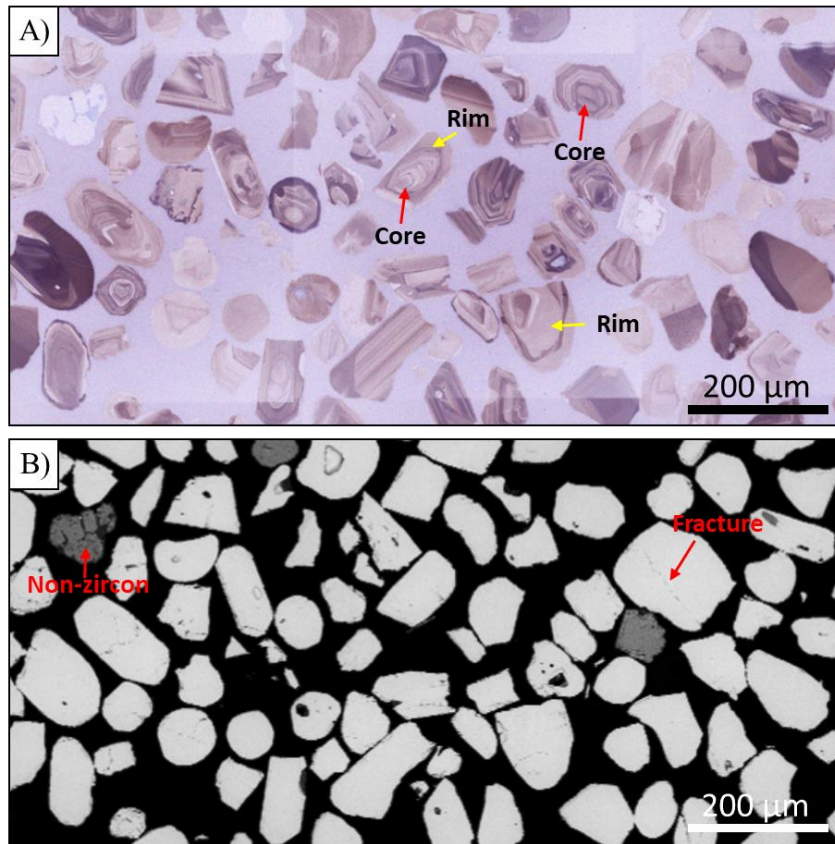


Figure 12. a) Cathodoluminescence (CL) image of zircons from subsample BV 4, notice the complex zonation in some grains. **b)** back-scattered electron (BSE) image of zircons from subsample BV 4, notice the difference in brightness between the darker non-zircon and nearby zircons (light).

5.1.3 Hafnium Isotopic Analysis

During the crystallization process, it is commonly understood that zircons take up relatively large amounts of hafnium (Hf) (~1%), but exclude lutetium (Lu). Therefore, knowing that the isotope ^{176}Hf is the daughter of radioactive ^{176}Lu , the measured $^{176}\text{Hf}/^{177}\text{Hf}$ ratio can be used to determine the relative composition of the magma from which the zircon crystallized. When two sediment sources have overlapping zircon crystallization ages, compositional differences in magma, measured from the $^{176}\text{Hf}/^{177}\text{Hf}$ ratio, can be invaluable in distinguishing between zircons derived from each of the two unique sources. In this investigation, Hf signatures are necessary for estimating the source of zircons with ages from 530-540 Ma. These zircons occur in both Cambrian igneous rocks of the Southern Oklahoma Wichita Mountains and Pan-African-Gondwanan exposures within the Northern Appalachian Mountains, but have distinct Hf signatures as identified by Thomas et al. (2016) and Thomas et al. (2017).

In this investigation, Hafnium isotope analyses was conducted at the University of Arizona Laserchron Center using methods described by Gehrels and Pecha (2014) and Thomas et al. (2017) utilizing a Nu HR ICPMS coupled to a Photon Machines Analyte G2 excimer laser. Depending on the distribution of the computed U-Pb ages, 15 or 30 analyses were conducted on each sample with grains selected to represent each of the main age groups and avoid grains with discordant ages. Analyses were conducted on top of the U-Pb pit in attempt to link the Hf and U-Pb data. Acquisition parameters were optimized for laser ablation using a solution of JMC475 with varying amounts of Lu and Yb and seven zircon standards (Mud Tank, 91500, Tempora, R33, FC52, Plesovice, and Sri Lanka (SL)) mounted with unknowns. Standards were analyzed at the beginning and end of each sample analysis. Solutions, standards, and unknowns analyzed during a session were reduced together to achieve minimum offset of the measure $^{176}\text{Hf}/^{177}\text{Hf}$ of standards relative to the known values. The Bartlesville sample (BV 1-4) and the Red Fork (RDFK-ST) and Taft (TF-1) samples were run as separate sessions and therefor have unique

reduction values. Results are reported as the mean and 1σ standard error. Hf isotope geochemical results are reported in epsilon units (ϵ) and reported as the mean and 1σ standard error. ϵHf results are reported as $\epsilon\text{Hf}(t)$, evaluated at the timing of crystallization (t) based on the grain U-Pb pit age.

5.2 Sandstone Petrology

Petrographic analysis of each sample was conducted to determine the detrital mineralogical compositions for comparison and correlated with computed detrital zircon U-Pb age peaks and $\epsilon\text{Hf}(t)$ values. The correlation was used to observe relationships between detrital zircon provenance estimations and sandstone detrital composition and fabric. Thin sections cut from each sample were examined for quantitative and qualitative mineralogy of detrital constituents using the well-established methodology of point counting. Since thin sections could not be cut for the RDFK-ST drill cuttings, point counts were taken from the No.1 Herring and No. 2 Switzer cores previously described by Johnson (1984). Both cores are located within a few miles east and west of the 1HX Saratoga 1720. More than 300 points were counted for each thin section. For reporting purposes, the amount of each mineral was averaged for samples with multiple sections. For interpretation, observed data were normalized independently and plotted together on Folk QRF (Folk, 1968) and provenance type (Dickinson et al., (1983) ternary diagrams shown in **Figure 13**.

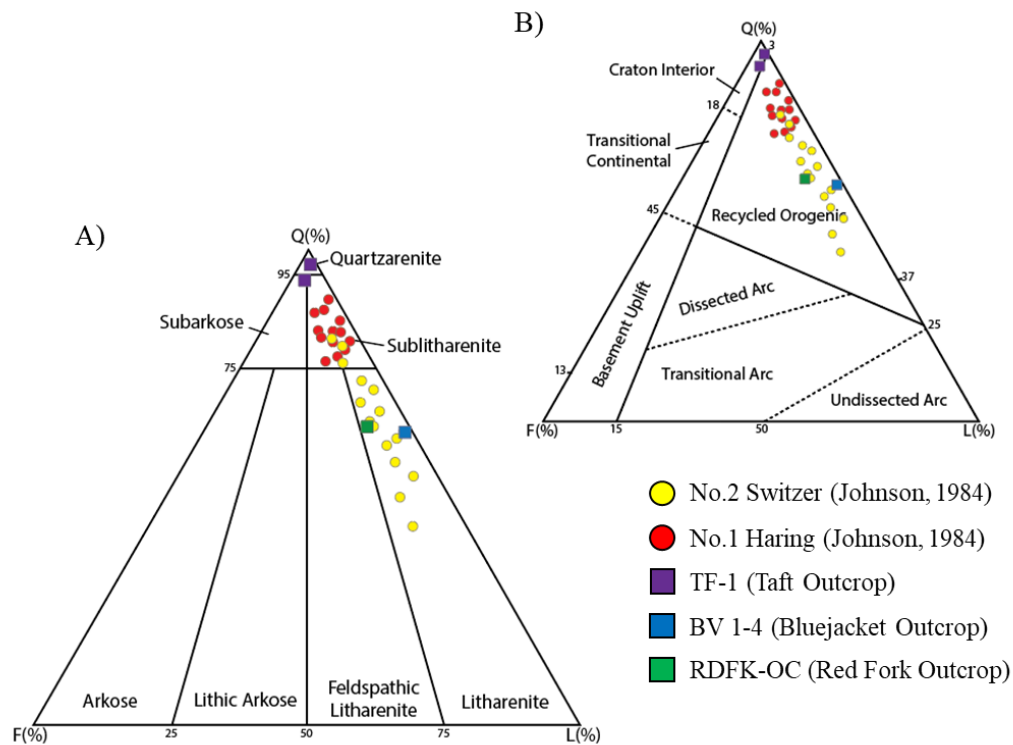


Figure 13. Compiled point counts from samples analyzed in this study along with point counts from the No.1 Switzer and No.1 Hearing cores analyzed by Johnson (1984). **a)** Sandstone composition using Folk (1968) classification. **b)** QFL plot for inferred provenance type using Dickinson et al. (1983) classification.

CHAPTER VI

RESULTS

6.1 Detrital-Zircon U-Pb Type Signatures

In order to better facilitate the comparison between Cherokee sandstones analyzed in this study, and clastic strata investigated in previous basin studies, two type signatures were defined based on the presence and relative abundance of detrital zircon age populations and detrital constituents. This was done following the Kissock et al. (2018) type signature classification system in order that the contrasting Cherokee sandstones could be easily compared based upon their matching type signatures, with similar age sandstones investigated in the Illinois and Forest City basins. Similarly, Grenville-age zircon (980-1300 Ma) populations were ignored in this characterization, due to their persistent presence and abundance in most Paleozoic sandstones, including the Cherokee sandstones analyzed, which limits their utility in provenance interpretation (e.g., Gehrels et al., 2011; Thomas et al., 2017). However, despite this, age-spectra comparisons facilitated by MDS fully consider both the presence and relative abundance of the Grenville-age populations. Type 1 signatures are characterized by the dominance of a Yavapai-Mazatzal (1600-1800 Ma) population, lesser abundances of Granite-Rhyolite (1300-1500 Ma) and Neoproterozoic (530-760 Ma) populations, and a minimal Appalachian (270-490 Ma) population. In contrast, Type 2 signatures are dominated by a significant Neoproterozoic population, a slightly smaller Appalachian population. In contrast, Type 2 signatures are dominated by a significant Neoproterozoic population, a slightly smaller Appalachian population,

And very minimal amounts of all other population. Compositionally, sandstones of both signatures differ with respect to the presence, or lack, of lithic fragments. Type 1 sandstones are characterized as having >90% monocrystalline quartz and minor amounts of lithics (<2%), whereas Type 2 sandstones are characterized by a large presence (>28%) of lithics dominated primarily by populations of metamorphic rock fragments. Full classification of both type signatures, along with the classification of type signatures from Kissock et al. (2018), are presented in **Table 1**.

Type Signature	Detrital Zircon Age Signature	Sandstone Composition	Stratigraphic Position
Kissock et al., 2018			
Type 1	Dominant Populations: Appalachian (5-16%), Midcontinent (15-35%) *includes concentrations of Yavapai-Mazatzal (1600-1800 Ma), Superior (6-17%)	Very fine- to fine-grained, quartzarenite with minor mica and carbonate lithics	Lower parts of both basins, often near the basal Pennsylvanian unconformity
Type 2	Dominant Population: Appalachian (5-16%), Neoproterozoic (15-36%)	Fine- to coarse-grained, dominantly subarkose or sublithic to lithic arkose or feldspathic litharenite, ~5%–10% mica, feldspar, lithic grains	Throughout the Illinois Basin and in the upper part of the Forest City Basin
Type 3	Dominant Populations: Appalachian (15-26%), Midcontinent (10-17%) * <i>lacks concentration of grains >1550 Ma</i>	Fine- to coarse-grained, dominantly subarkose or sublithic to lithic arkose or feldspathic litharenite, ~5%–10% mica, feldspar, lithic grains	Stratigraphically highest samples in the Illinois Basin; not found in Forest City Basin
This Study			
Type 1	Dominant Populations: Yavapai-Mazatzal (38%)	Fine- to coarse-grained, quartzarenite to subarkose, 1-2% chert, 1-4% plagioclase feldspar	Middle Desmoinesian on the Cherokee Platform/Arkoma Shelf
Type 2	Dominant Populations: Appalachian (14-15%), Neoproterozoic (33-43%)	Very fine- to fine-grained, sublitharenite to litharenite, 29-63% rock fragments, >8% metamorphics, 1-6% mica	Middle Desmoinesian on the Cherokee Platform/Arkoma shelf and Anadarko shelf margin

Table 1. Compositional characteristics of type signatures from this study and those from Kissock et al, 2018.

6.1.1 Type 1 Signature

Taft Sandstone (TF-1)

Sample TF-1 is a mature, moderately-sorted, medium- to coarse-grained sandstone with grains ranging from subrounded to rounded. Primary detrital constituents consist of monocrystalline quartz (95%), chert (3%), and plagioclase feldspar (2%). Quartz grains commonly contain syntaxial quartz overgrowths. Grains demonstrate both angular and subrounded morphologies indicating both allogenic mechanical smoothing and authigenic overgrowth. Detrital zircon analyses yielded 211 concordant ages ranging from 376 to 3315 Ma, with the dominant concentration of ages consisting of Yavapai-Mazatzal Terrane (38%), with a dominant peak at 1680 Ma. A secondary concentration of ages consisted of Grenville Province (30%), with dominant peaks at 1003, 1043, and 1088 Ma, while minor components consisted of the three age groups characterized as Appalachian synorogenies (5%), Neoproterozoic Terranes (9%), and Granite-Rhyolite Terranes (8%).

6.1.2 Type 2 Signature

Bluejacket Sandstone (BV 1-4)

Sample BV 1-4 is a well-sorted, very fine- to fine-grain litharenite sandstone with grains ranging from subangular to subround. Detrital constituents consist primarily of monocrystalline quartz (64%) and metastable rock fragments (29%). Rock fragments were primarily characterized as low-grade metamorphics (24%) consisting predominantly of mica schist, schistose quartzite, and polycrystalline quartz. In comparison, feldspars (7%) make up a relatively small fraction of detrital constituents but consist of both plagioclase and microcline that were commonly identified undergoing dissolution and therefore could have made up a larger portion of detrital grains prior to burial. Other minor constituents included both muscovite and biotite that ranged on the scale of 0.8 to 2.5 mm in size and make up approximately 2% (unnormalized) of the sandstone sample.

Due to a high yield of grains resulting from the fractionation of detrital zircons, analysis of BV 1-4 was divided into four separate analytical samples (numbered 1-4) which were cumulated at the end to result in 452 concordant U-Pb ages and 60 ϵ_{Hf} values. The cumulative sample resulted in a dominant concentration of Neoproterozoic ages (33%) with the majority falling between 515 and 699 Ma with peaks at 545 and 616 Ma. Secondary concentrations consisted of Grenville (28%) and Appalachian (15%) ages with dominant peaks at 1098 and 416 Ma respectively. A minor Yavapai-Mazatzal peak, consisting of 14 grains, is also observed at 1633 Ma.

Red Fork Sandstone South Thomas Field (RDFK-ST)

As previously mentioned, due to the inability to develop thin sections from the 1HX Saratoga 1720 cuttings, petrographic analyses of the Lower Red Fork Sandstone targeted by the well were taken from previous point counts conducted on the No. 1 Herring and No. 2 Switzer cores by Johnson (1984). Through the correlation of gamma-ray log signatures and mapping of net-sandstone trends within the South Thomas field it was determined that the massively bedded, channel sandstones penetrated by the No. 1 Herring and No. 2 Switzer wells correlated laterally with the channel sandstone targeted by the 1HX Saratoga 1720. In his study, Johnson (1984) characterized the sandstones as mostly very fine grained lith- to sublitharenites with a primary quartz end member ranging from 28-63%. Volcanic, metamorphic, and sedimentary rock fragments were identified in varying abundances, ranging from 4-40% of the entire detrital fraction. Johnson (1984) did not specifically classify the grains, but noted a dominance of mud fragments. Feldspars were observed in least abundance, composing $\leq 5\%$ of grains. Detrital zircon analysis of sample RDFK-ST resulted in 217 concordant U-Pb ages and 30 ϵ_{Hf} values, with 13 U-Pb ages rejected for values less than the minimum depositional age of the sandstone (~ 300 Ma). The final yield of 204 filtered ages range from 329-2795 Ma with a dominant concentration of Neoproterozoic (43%) ages, with peaks at 549 and 610 Ma. Secondary

concentrations consist of Appalachian (14%) and Grenville (19%) ages. All of other ages make up 24% of the final fraction with minor peaks (>5 grains) at 2092 and 1877 Ma.

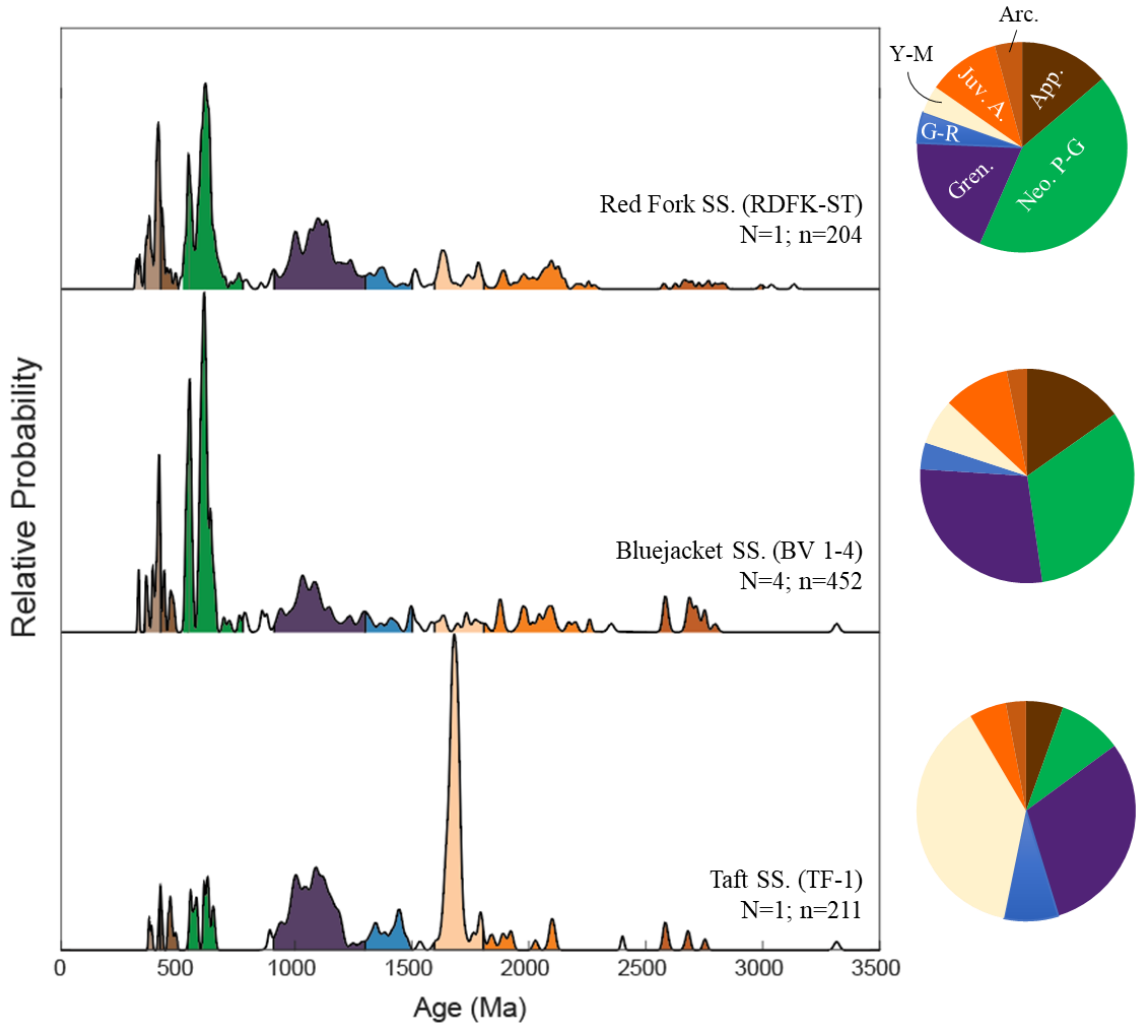


Figure 14. Relative age-probability (left) and relative frequency (right) plots of results from U-Pb analysis of detrital zircons. Plots are colored coded to the North American provinces displayed in **Figure 6**. Appalachian (App.), Neoproterozoic Peri-Gondwana (Neo. P-G), Grenville (Gren.), Granite-Rhyolite (G-R), Yavapai-Mazatzal (Y-M), Juvenile Arcs/Orogens (Juv. A.), Archean Craton (Arc.).

Red Fork Sandstone Outcrop (RDFK-OC)

Sample RDFK-OC was examined using petrographic analysis alone, but based on its vertical and lateral proximity and internal sedimentological similarities to BV 1-4, it was characterized here as a Type 2 sandstone. The sandstone is a very fine grained, well-sorted, litharenite with grain shapes ranging from subangular to subround. Primary detrital constituents are monocrystalline quartz (62%) and metastable rock fragments (37%). Rock fragments are primarily metamorphic (36%) consisting of mica schist and schistose quartzite, same as those identified in the Bartlesville outcrop samples. Additionally, sedimentary rock fragments (1%) were identified as recycled mud and silt (shale) clasts. Similar to BV 1-4, feldspars make up only a trace (~1%) of detrital constituents and were commonly partially dissolved. When compared to BV 1-4, other mineral constituents include a relatively large portion (6% unnormalized) of both biotite and muscovite mica.

6.2 Multidimensional Scaling (MDS)

As previously mentioned, multidimensional scaling was used to facilitate comparisons between detrital zircon age signatures in this study and composite signatures from Paleozoic strata and time-equivalent sandstone units of the potential provenance regions discussed. This was done in order to quantify age spectra similarities for improved provenance estimation and to determine possible sediment dispersal pathways. Comparisons were drawn between the composite signatures presented in **Figure 7** and the composite type signatures from the Forest City and Illinois basins. The direct results from the MDS analysis are presented here but implications are discussed in the preceding chapters.

MDS shows a systematic variation between the different basin sample Type signatures and source regions on the North American Craton. For the Type 2 sandstones, there is a systematic increase in similarity with the Type 2 basin samples in the Forest City basin (FCB-T2) and Northern

Appalachian (NA) sources, as well as a decreasing similarity with Type 2 basin samples in the Illinois basin (IB-T2) and the Appalachian foreland (AF) sources seen in both models (**Figure 14**). Both models also show a lack in similarity (dissimilarity) between the Type 1 and Type 2 sandstones in this study, with decreasing similarity between the Type 1 sandstone in this study and those in the Forest City basin. The Type 1 Taft sandstone shares equal similarity with the Ancestral Rocky Mountain sources and the Mississippian Weddington Sandstone of northwest Arkansas in the KS Test D model (**Figure 14c&d**) but shows decreasing similarity with the Weddington Sandstone in the Cross-Correlation model (**Figure 14a&b**). This reflects a mixture of potential sediment sources whether or not they are directly correlated with sources in the Ancestral Rockies and/or recycling from the Weddington Sandstone. In contrast, the Type 1 Forest City basin samples show increasing similarity with Illinois basin Type 2 samples and Central Appalachian sources. In both models, all three samples show decreasing similarity with both basin samples and sources of the North Appalachians, Ancestral Rockies, and recycled Midcontinent Ordovician quartzarenites (MO).

6.3 Hafnium Isotope (U-Pb- ϵ Hf(t)) Distribution

To aid in the visualization and interpretation of Hf results, combined U-Pb ages and ϵ Hf(t) values are plotted as two-dimensional (2D) and three-dimensional (3D) bivariate kernel density estimates (KDEs) using methods described by Sundell et al. (2019) and implementation of the HafniumPlotter MATLAB algorithm developed at the University of Arizona. Construction of bivariate KDEs is done following the same basic method of a standard one-dimensional (1D) KDE but over a 2D grid (U-Pb ages on the x-axis, and ϵ Hf(t) values on the y-axis) with density values on the z-axis (Sundell et al., 2019). This facilitates the visualization of complex 2D geochronology data as density plots that allow for identification of robust data clusters and non-arbitrary contouring of those clusters (usually set at 1σ and 2σ uncertainty). To construct a bivariate KDE, the HafniumPlotter algorithm takes each data point on a 2D scatter plot and

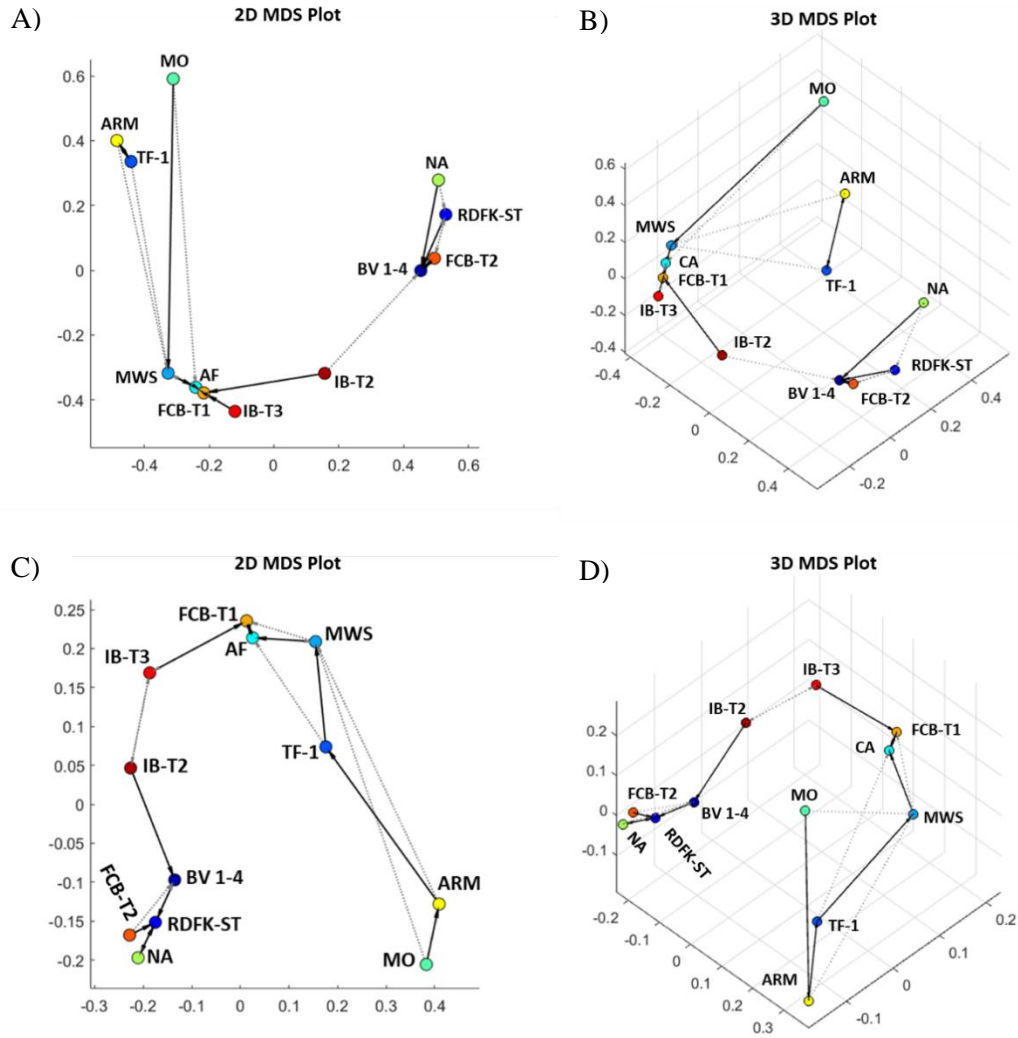


Figure 15. a) 2D and b) 3D MDS plots calculated using the coefficient of nondetermination. c) 2D and d) 3D MDS plots calculated using KS Test D value. Plots include data from the Appalachian Foreland (AF), Northern Appalachians (NA), Ancestral Rocky Mountains and Grand Canyon (ARM), Midcontinent Ordovician quartzarenites (MO), Mississippian Weddington Sandstone (MWS), Forest City Basin Type 2 (FCB-T2) and Type 1 (FCB-T1) sandstones, and Illinois Basin Type 2 (IB-T2) and Type 3 (IB-T3) sandstones. Solid arrows point to closest neighbor (greatest similarity), dashed arrows point to second closest neighbor.

converts it into a 2D Gaussian with separate kernel bandwidths for the x-axis (U-Pb age) and y-axis ($\epsilon_{\text{Hf}}(t)$) values determined by optimization (using Botev et al., 2010) or arbitrary selection (Sundell et al., 2019). Here constructed bivariate KDEs are computed over a specified square grid of 512×512 cells and normalized such that the volume area integrates to one. Kernel bandwidths were set at 50 Ma for the x-axis and 2ϵ for the y-axis and contours are calculated at 68% (1σ) and 95% (2σ) peak density. Due to the differences in age peaks, therefore differences in the grain placement the of Hf analyses, the type 1 Taft sample is plotted separately from the type 2 Red Fork and Bluejacket samples. Results are referenced to similarities (and dissimilarities) in density contours of U-Pb- $\epsilon_{\text{Hf}}(t)$ values from the Appalachians (Thomas et al., 2017), Gondwana Gander-Avalon terranes (Wilner et al, 2013; 2014), Southern Oklahoma Igneous Rocks (Thomas et al., 2016), Midcontinent Granite-Rhyolite (Goodge and Vervoort, 2007), and Yavapai-Mazatzal terranes of the Ancestral Rockies (Bickford et al., 2008).

The primary focus of the analysis of the Taft sandstone was to test the $\epsilon_{\text{Hf}}(t)$ values of peak ages between 1300-1500 Ma and 1600-1800 Ma, corresponding to the Laurentian Craton Midcontinent Granite-Rhyolite and Yavapai-Mazatzal provinces, respectively. The highest density of grains is focused between 1651 and 1715 Ma and yield highly juvenile $\epsilon_{\text{Hf}}(t)$ values of 4.0 to 9.5 (**Figure 15a**). This density shows overlapping similarities with the U-Pb- $\epsilon_{\text{Hf}}(t)$ values from crustal rocks in the Ancestral Rockies (Bickford et al., 2008) at both the 1σ and 2σ level but with a slight offset (younger) peak age and a more concentrated range in $\epsilon_{\text{Hf}}(t)$. This is likely a result of dissimilarities in source and/or crustal material. $\epsilon_{\text{Hf}}(t)$ from the 1300-1500 Ma zircons show juvenile to slightly intermediate values from 3.2 to 6.1 that lie within 1σ density of crustal material consistent with Midcontinent Granite-Rhyolite granite emplaced in central Yavapai basement (Goodge and Vervoort, 2007). Crustal evolution trends show values near similar to that of the 1651 to 1715 Ma zircons analyzed, suggesting recycling of crust with similar crustal residence ages. Younger grains (<1300 Ma) show both the continued addition of juvenile crust

and more evolved crustal material, with indications of vertical ‘mixing’ trends. This is typical of U-Pb- ϵ Hf(t) signatures from younger grains on both the Laurentian (Thomas et al., 2017) and Gondwanan cratons (Willner et al., 2013; 2014), which can be seen at the 2σ level in **Figure 15b**.

In contrast to the Taft sample, the objective for Type 2 Bluejacket and Red Fork samples was to analyze younger age peaks corresponding to the Appalachian, Southern Oklahoma Igneous, Neoproterozoic Gondwanan, and Grenville provinces. Cumulative ϵ Hf(t) shows juvenile to evolved crustal values that widely range from -18.3 to 10.5. Grains ranging from 339 to 438 Ma make-up the highest peak intensity with the majority of grains falling within -6.0 to 2.2 ϵ Hf(t) (**Figure 16a**). Similarities in U-Pb- ϵ Hf(t) values can be drawn between the 1σ density contour of these grains and those from Pennsylvanian strata along the Appalachians (Thomas et al., 2017). The Neoproterozoic age grains show a similar peak intensity in ϵ Hf(t) values, but with a wider overall range in values from -18.3 to 10.5. This is constant with the distribution of U-Pb- ϵ Hf(t) values from the Gondwana Gander-Avalon terranes (Willner et al., 2013; 2014) at the 1σ and 2σ level (**Figure 16b**). Similarly, older grains from 1045 to 1063 Ma show a greater correlation with U-Pb- ϵ Hf(t) values from the Gander-Avalon terranes in comparison to the Pennsylvanian strata along the Appalachians, with the majority of values ranging from -0.9 to 4.0. Overall, the younger grains (<1300 Ma) from the cumulative samples seem to follow trend with those from the Taft sample.

Type 1 (TF-1) Sandstone

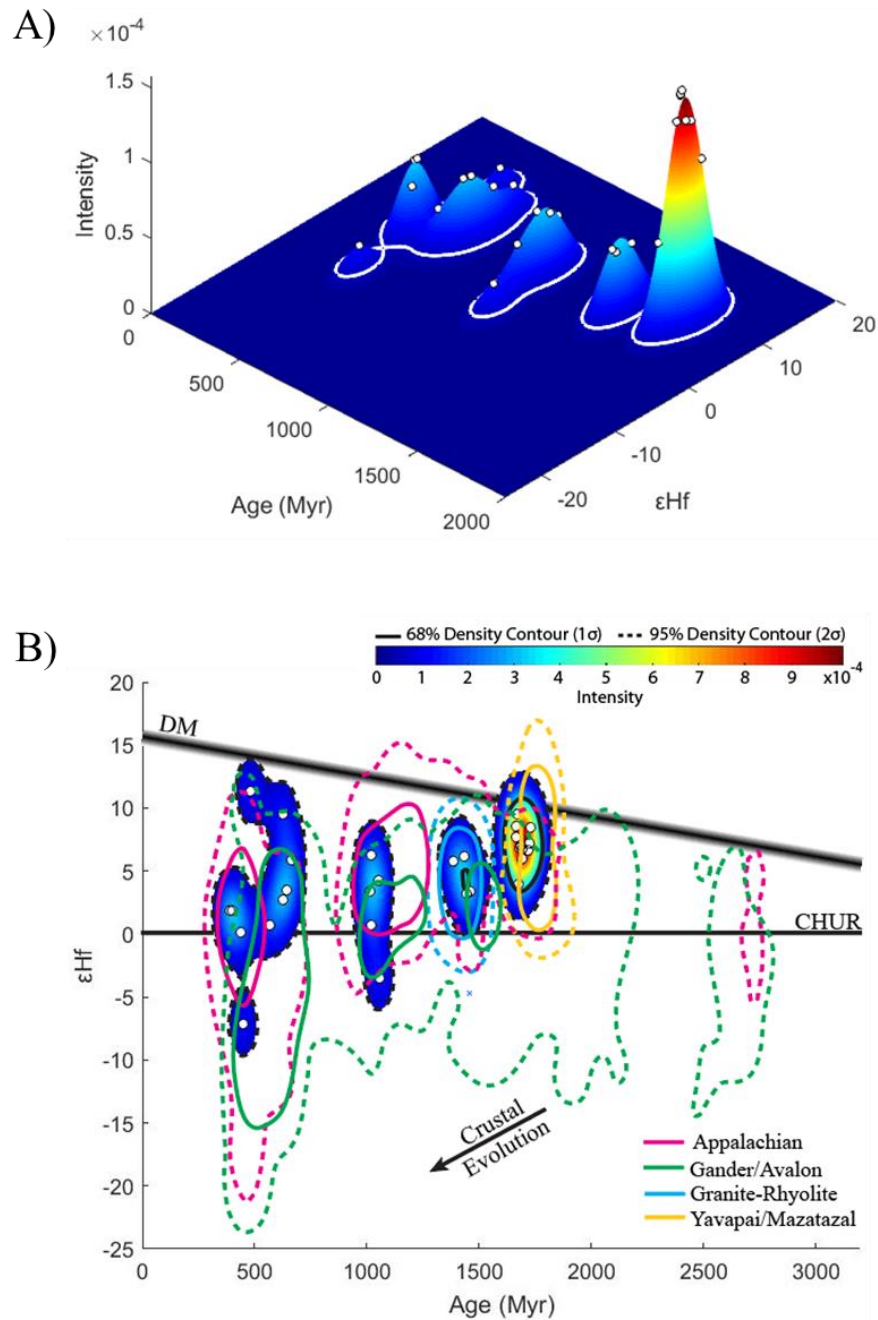


Figure 16. U-Pb- $\epsilon\text{Hf}(t)$ results from the Taft (TF-1) sandstone plotted as bivariate kernel density estimates; **a)** three-dimensional (3D) plot and **b)** Two-dimensional (2D) view of the 3D plot in **(a)**. The 2D plot compares results from the Appalachians (Thomas et al., 2017), Gondwana (Gander and Avalon terranes) (Willner et al., 2013; 2014), Yavapai-Mazatzal rocks of the Ancestral Rockies (Bickford et al., 2008), and Midcontinent Granite-Rhyolite (Goodge and Vervoort, 2007). Contours are plotted at 68% and 95% of peak density.

Type 2 (RDFK-ST + BV1-4) Sandstone

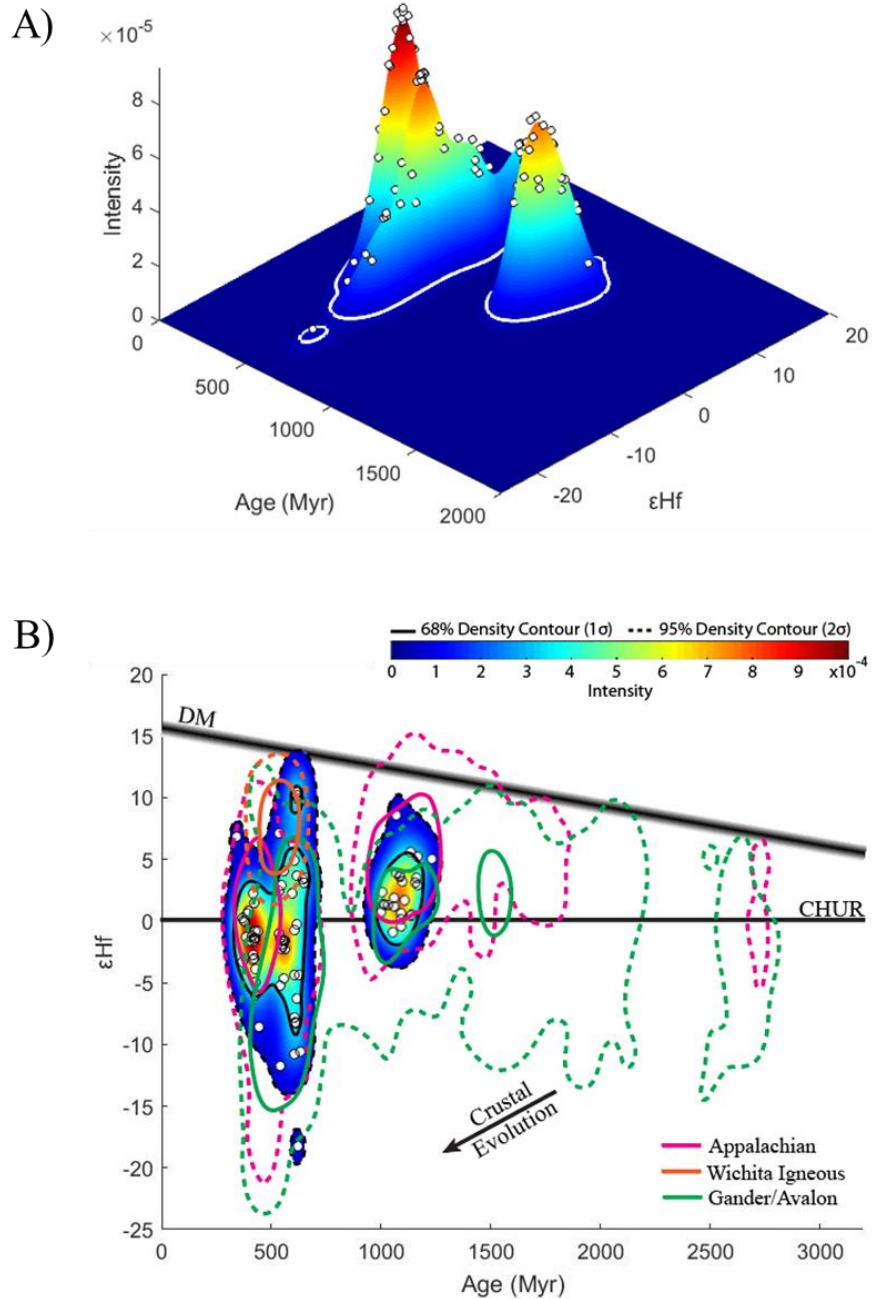


Figure 17. Combined U-Pb- $\epsilon\text{Hf}(t)$ results from the Red Fork (RDFK-ST) and Bluejacket (BV 1-4) sandstones plotted as bivariate kernel density estimates; **a**) three-dimensional (3D) plot and **b**) Two-dimensional (2D) view of the 3D plot in **(a)**. The 2D plot compares results from the Appalachians (Thomas et al., 2017), Gondwana (Gander and Avalon terranes) (Willner et al., 2013; 2014), and southern Oklahoma Cambrian igneous rocks in the Wichita Mountains (Thomas et al., 2016). Contours are plotted at 68% and 95% of peak density.

CHAPTER VII

DISCUSSION

7.1 Provenance Interpretations

7.1.1 Type 1 Provenance

Results from the paired detrital zircon geochronology and sandstone petrography strongly suggest that the Type 1 Taft Sandstone was primarily sourced locally, from the interior of Laurentian craton. This is concluded from two key observations: 1) the abundance of monocrystalline quartz grains relative to other grain populations, and 2) the lack of zircon grains with ages younger than 950 Ma. The minimal fraction of lithic grains, in conjunction with the relative abundance and roundness of the monocrystalline quartz population, indicates some order of sediment recycling from the cratonic interior. Considering the Taft Sandstone belongs to a fluvial system, the moderate sorting and size of grains suggest sediment was likely more locally sourced rather than transported over a great distance. Since Pennsylvanian sandstones on the Midcontinent are notorious for large populations of detrital zircons <950 Ma in age, which are minimal in the Taft Sandstone, local sourcing would have to be predominantly recycled from pre-Pennsylvanian strata. However, a small proportions of Neoproterozoic grains identified in the Taft sample does suggest either mixing with potential drainage systems from the Appalachians and/or the potential for minor recycling of early Pennsylvanian strata in filled intracratonic basins on the Midcontinent (Kissock et al., 2017).

Based on the geographic location of the Taft sample, there are two more probable

recycled source candidates: early Paleozoic quartzarenites and/or late Mississippian clastics of the Midcontinent region. The early Paleozoic quartzarenites in the Midcontinent, such as the Ordovician St. Peters sandstones, are widespread and provide clean, mature quartzarenite deposits (Konstantinou et al., 2013). Despite the compositional similarity, detrital zircon U-Pb signatures of those sandstones show a dominant population of Superior province ages (Pickell, 2012; Konstantinou et al., 2013; Chapman and Laskowski, 2019), making them an unlikely sediment source for the Taft Sandstone. However, late Mississippian clastics on the Arkansas shelf contain nearly identical zircon populations as the Taft signature (Xie et al., 2016). The small percentage of chert grains in the Taft Sandstone would also suggest minor recycling from early Mississippian chert-bearing carbonates on the Midcontinent. Furthermore, Mississippian strata were likely exposed on topographic highs adjacent to the Arkoma basin and could have been a significant source of sediment during the Middle Pennsylvanian time. However, additional sources are needed to account for the discrepancy in the abundance of grains corresponding to the Yavapai-Mazatzal province.

As previously discussed, most of the Yavapai-Mazatzal terrane remained covered during Middle Pennsylvanian, except on basement uplifts associated with the Midcontinent Rift System, Transcontinental Arch, and Ancestral Rocky Mountains (Rascoe and Adler, 1983). Yavapai-Mazatzal grains from the Taft Sandstone have a strong unimodal distribution with a peak at 1680 Ma. This tight age cluster in combination with peak grains demonstrating highly concentrated, juvenile, $\epsilon_{\text{Hf}}(t)$ values suggest a unimodal source of the Yavapai-Mazatzal population. While MDS suggests a source region analogous with the Ancestral Rockies, this is a highly improbable source of grains in the Taft sandstone since Yavapai-Mazatzal clusters connected with the region have a slightly higher composite peak age at ~1715 Ma and are generally accompanied by a higher concentration of Granite-Rhyolite grains (Cole et al., 2015; Gehrels et al., 2011; Siddoway and Gehrels, 2014) than observed in the Taft Sandstone. Additionally, paleocurrent trends, along

with mapped extents of the Cherokee sandstones, does not support the eastern movement of sediment across the Midcontinent during the early Desmoinesian. The only other known local exposure of the Yavapai-Mazatzal province rocks during the Pennsylvanian is the Nemaha Ridge (Whitmeyer and Karlstrom, 2007), which is a buried structural zone with granitic highs in the Precambrian basement associated with the Midcontinent rift system. While not presently exposed, the ridge consists of various assemblages of granite, rhyolite, and quartzite which range in age from ~1370 to 1650 Ma (Bickford et al., 1981). The absence of early Pennsylvanian strata on the arch of the uplift in northeast Kansas suggests the ridge was a high during deposition of the Taft Sandstone. Additionally, regional fluvial system sourced from exhumed basement material on the ridge could explain the presence of coarse grained feldspars in the Taft sample. However, these grains likely would have had to be accompanied by a larger fraction of metasedimentary quartzite to account for the large population of Yavapai-Mazatzal age grains.

Another potential source, that has not been previously proposed, is Yavapai-Mazatzal juvenile crust (1650 -1690 Ma) presently underlying the Ozark Dome (Whitmeyer and Karlstrom, 2007). While current sedimentary cover suggests that the Ozark Dome remained predominantly covered by early Paleozoic to late Mississippian strata during the Pennsylvanian, underlying Yavapai-Mazatzal granites and rhyolites are dated at 1637 to 1690 Ma (Bickford et al., 1981; Whitmeyer and Karlstrom, 2007), placing them well in the range of the peak age observed in the Taft Sandstone. However, the only identified exposure of granitic basement on the Ozark Dome belongs to intrusive Midcontinent granites and rhyolites in the St. Francois Mountains of eastern Missouri (Bickford et al., 1981; Thomas et al., 2012). A-type granites in the region are measured to have crustal residence ages that match the age of pre-existing Yavapai-Mazatzal juvenile crust on the central craton (Goodge and Vervoort, 2007). Similarly, $\epsilon_{\text{Hf}}(t)$ values from Granite-Rhyolite zircons in the Taft Sandstone have a crustal residence ages that match the age of the Yavapai-Mazatzal populations analyzed from the sandstone. This suggests these Granite sourced

zircons were derived largely from, and likely emplaced in, similar age (pre-existing) crustal material (Goodge and Vervoort, 2007). This is supported by data from Goodge and Vervoort (2007) and Bickford et al. (1981) which support the probability that Midcontinent granitoid intrusions emplaced portions of the overriding Yavapai-Mazatzal juvenile crust on and around the Ozark Dome. Uplift and accompanying exhumation of the Ozark Dome could have eroded subaerially exposed limits of the emplaced crust leaving the present day exposures of granitoid intrusions in the St. Francois Mountains. However, this does not imply that the Ozark Dome was the sole source of these grains, as Midcontinent Granite-Rhyolite and Yavapai-Mazatzal populations are also abundant in late Mississippian shelf siliciclastics (Xie et al., 2016).

In summary, the broad range in ages and the difference in relative abundance for each age group of the Taft Sandstone suggest that it is likely that there were multiple sources located on the interior craton. Contributions of zircons from those sources changed during the Middle Pennsylvanian which suggest the early Desmoinesian Type 1 deposits are predominantly localized along the western flank of the Ozark Dome. The primary sources of the Taft Sandstone are recycled late Mississippian clastics on the Midcontinent shelf, and granitic rocks from either exposed Yavapai-Mazatzal and Granite-Rhyolite basement on the Nemaha ridge or Ozark Dome.

7.1.2 Type 2 Provenance

Type 2 sandstones represent deposition by northeast to southwest flowing fluvial sediment systems active in the Midcontinent region during the early Desmoinesian. Detrital zircon geochronology data from the measured samples show similar age distributions with majority of zircon grains having Neoproterozoic and Acadian synorogenic ages. In addition, compiled point counts show that all samples have abundant metamorphic rock fragments (predominantly mica schist) and trace amounts of both muscovite and biotite mica. Considering that older strata on the Midcontinent, including basement rocks, are virtually devoid of both

Neoproterozoic ages and metamorphic rocks supports the idea that the early Desmoinesian marked the emergence of a novel, post-Mississippian, sediment source to the Midcontinent. Grains were likely transported from distant sources as indicated by grain maturity (fine-grained and sub-rounded). This, along with highly negative $\epsilon_{\text{Hf}}(t)$ values from 530-540 Ma, further suggest the Cambrian syn-rift igneous rocks exposed in the Wichita Mountains were not a major contributor of sediment for Type 2 sandstones on the Anadarko shelf, as previously postulated (Thomas et al., 2016).

Considering the evidence for south-southwest paleoflow directions and westward transport of sediment during the Pennsylvanian (Rascoe and Adler, 1983; Kissock et al., 2018; Chapman and Laskowski, 2019), the two most probable source candidates for the Type 2 sandstones on the Midcontinent is recycled clastics from the Appalachian foreland and/or peri-Gondwanan metasedimentary terranes to the east and northeast of the Laurentian craton. However, as previously discussed, Neoproterozoic ages are largely absent in Paleozoic clastic wedges along the central and southern portions of the Appalachian foreland (Thomas et al., 2017), which would preclude them as a prominent source region. Furthermore, MDS indicates that detrital zircon signatures from the Appalachian foreland show increased systematic dissimilarities with the Type 2 sandstones in comparison with compiled detrital zircon data from source rocks along the north portions of the Appalachian orogeny. This is likely due to the relative enrichment of Neoproterozoic age zircons in Cambrian and Ordovician strata in portions of the northeast Appalachian orogeny, where they sit on peri-Gondwanan basement comprised of the Gander and Avalonia terranes (Willner et al., 2014). Today these terranes are exposed from southeastern New England to Newfoundland and consist of varying volcanic, plutonic, and metasedimentary assemblages (Willner et al., 2013; 2014). This includes the Gander Group mica schist which has similar U-Pb ages as well as Hf distributions to the Neoproterozoic and Grenville age population in the composite Type 2 sandstones. In addition, plutons of the Acadian

orogeny are more common in the northern Appalachians than the southern Appalachians (Thomas et al., 2017), which would account for the abundance of Acadian synorogenic zircons contemporaneous with Neoproterozoic populations. Deformation associated with the Alleghenian orogeny could have exhumed these potential source rocks, providing a viable source of metamorphic rock fragments and other lithic detrital grains found prominent in early Desmoinesian sandstones of the Midcontinent.

7.2 Middle Pennsylvanian Sediment Delivery Pathways

The provenance analysis of Desmoinesian sandstones on the southern Midcontinent provides new constraints for the ongoing debate about Middle Pennsylvanian sediment dispersal patterns on the Laurentian Craton. Similarities and differences in compiled sandstone compositions and U-Pb detrital zircon signatures from early-middle Pennsylvanian sandstones on the Laurentian Craton support both transcontinental westward-flowing fluvial systems from an Appalachian provenance and small-scale drainage systems with local Midcontinent provenance associated with structural highs. Unfortunately, only limited early-middle Pennsylvanian detrital zircon data have been published, which causes uncertainties and hinders a more detailed reconstruction of sediment dispersal pathways west and south of the sample locations in this study.

Several studies, including here, have proposed that early Desmoinesian sandstones (Cherokee Group) on the southern Midcontinent show spatial variabilities in both feldspar and lithics, a significant portion being metamorphic rock fragments (reaching > 25%), and generally plot in the range of sublitharenite to subarkose (Dyman, 1989; Anderson 1991; Mason 1982; Kuykendall, 1985; e.g.). The reduction in feldspar in some sandstones can be attributed to both long transport distance and chemical weathering in a tropical setting, or dissolution of the metastable grains post deposition. Yet, this interpretation is inconsistent with the abundant

preservation of metamorphic fragments. However, this study has identified several sources on the Midcontinent that can account for this spatial variability and preservation of feldspars, but not the availability of metamorphic grains. This would suggest a separate source of these grains from distant sources outside the Midcontinent. Similarly, coeval Pennsylvanian sandstones to the east in the Forest City and Illinois intracratonic basins and the Appalachian foreland are also characterized as by a relatively high percentage of lithics, although there is no of mention metamorphic percentages (Kissock et al., 2018; Thomas et al., 2017). However, Type 2 classified, coeval, sandstones in the Forest City and Illinois basins are additionally characterized by significant proportions of mica (~5-10%) and Neoproterozoic age zircons, similar to the Type 2 sandstones in this study. These Type 2 sandstones share systematic similarities with Paleozoic sandstones and older material exposed along the northern Appalachians, which contain assemblages of metasedimentary rocks.

Considering that sedimentation in those areas was simultaneous and continuous throughout the Middle Pennsylvanian, these comparisons concluded that the Type 2 Desmoinesian sandstones in the Illinois, Forest City, Anadarko, and Arkoma basins were likely derived from similar sources and transported by shared drainage systems. Additionally, field observations and subsurface mapping provide evidence for southwestward-flowing river systems that extend up to the southern extent of the Forest City basin (Visher et al., 1971). It is inferred that this trend represents the continued westward migration of the transcontinental fluvial systems with headwaters in the southeastern New England across the Laurentian Craton during the middle Pennsylvanian, as proposed by Kissock et al. (2018). The southwestward system likely flowed through the Michigan basin and the Mabash Valley fault system before passing through the northern extent of the Illinois basin, followed by the Forest City basin, and merged with local drainage systems on the southern Midcontinent, before it finally entered the marginal marine and deltaic environments of the Anadarko shelf and Arkoma shelf (**Figure 18**). Linkage of drainage

systems from the northeast with the Anadarko basin supports the overtopping of the Nemaha Ridge during the Early Desmoinesian or at least by the time the Red Fork and time-equivalent fluvial systems were active on the Midcontinent.

Continued deformation of the eastern margin of Laurentia during the middle Pennsylvanian exhumed the central and southern Appalachians which likely increased sediment flux into the Appalachian foreland (Thomas et al., 2017; Kissock et al., 2018). Kissock et al., (2018) proposed that overfilling of the basin during the middle Pennsylvanian allowed the western migration of sediment from those regions to reach the Illinois basin during the early-middle Desmoinesian. However, comparison with detrital zircons signatures from the western flowing systems in the Illinois basin (Type 1 composite) and signatures from the Appalachian Foreland suggest the westward flowing systems with headwater in the central and southern Appalachians were either impeded by the Ozark Uplift or did not reach the southern Midcontinent during the early-middle Desmoinesian. Farther west, late Paleozoic strata in the Grand Canyon have detrital zircon age populations that are similarly interpreted to reflect drainage systems from the Appalachians (Gehrels et al., 2011), but essentially lack Neoproterozoic ages seen in the Type 2 sandstone that would support linkage with the southwestward transcontinental systems proposed here. By early Permian time, however, strata in the Grand Canyon record minor populations of Neoproterozoic age grains (Gehrels et al., 2011). This trend is inferred to represent the continued westward migration of the transcontinental fluvial systems with headwaters in the northern Appalachians across the central craton during the middle Pennsylvanian to early Permian time (Kissock et al., 2018). It is proposed that increased influx of Appalachian derived sediment to the southwestern margin likely coincided with flooding of the Midcontinent during the middle to late Pennsylvanian and the shifting of sediment sources from north to south (Moore, 1979; Rascoe and Adler, 1983; Jordan 2008).

Contemporaneous with the emergence of transcontinental systems with headwaters in southeast New England during the middle Pennsylvanian, regional-scale fluvial systems persisted on the southern Midcontinent. Subtropical climates, along with the progressive uplift of structural highs, provided conditions conducive to high rates of erosion. During this time Mississippian and older strata, as well as exposed basement material, were likely eroded from adjacent topographic highs and the resulting sediments deposited into the Arkoma and Anadarko basins (Moore et al., 1979; Johnson, 2008; Dyman, 1989). This is reflected in Type 1 fluvial systems on the Arkoma shelf that have characteristics of smaller scale drainage systems with headwaters on the Ozark Uplift. Exhumation of late Mississippian strata on the Uplift is inferred to have contributed the majority of recycled quartz to portions of the eastern Arkoma basin. Small populations of Neoproterozoic grains suggest the regional-scale fluvial systems either mixed with the transcontinental fluvial systems entering the basin from the northeast or eroded into and recycled early Pennsylvanian sands. This could account for the small fractions (<1%) of metamorphic fragments identified in the Taft sandstone. Mixing could have involved regional-fluvial systems sourced from the Nemaha ridge. However, considering the age equivalency of the Red Fork and Taft Sandstone units, and the simultaneous deposition with fluvial-systems from the northeast, it is unlikely that fluvial systems from the ridge flowed eastward across the Arkoma shelf. Furthermore, detrital zircon data in this study does not support previous postulations that exhumation of exposed Yavapai-Mazatzal age metasedimentary rocks on the ridge was a major contributor of metamorphic fragments to the southern Midcontinent during the Pennsylvanian (Xie, 2016). Thus, new data presented here provides additional support and constraints on the interpretation for multiple dispersal paths for sediment derived from the Appalachians and transported southwestward across the Laurentian continent (Gehrels et al., 2011; Kissock et al., 2018; Chapman and Laskowski, 2019; e.g.), as well as constraints on the interpretation of dispersal pathways for regional fluvial systems on the Midcontinent during the Middle Pennsylvanian (Rascoe and Adler, 1983; Moore, 1979; Johnson, 2008; e.g.).

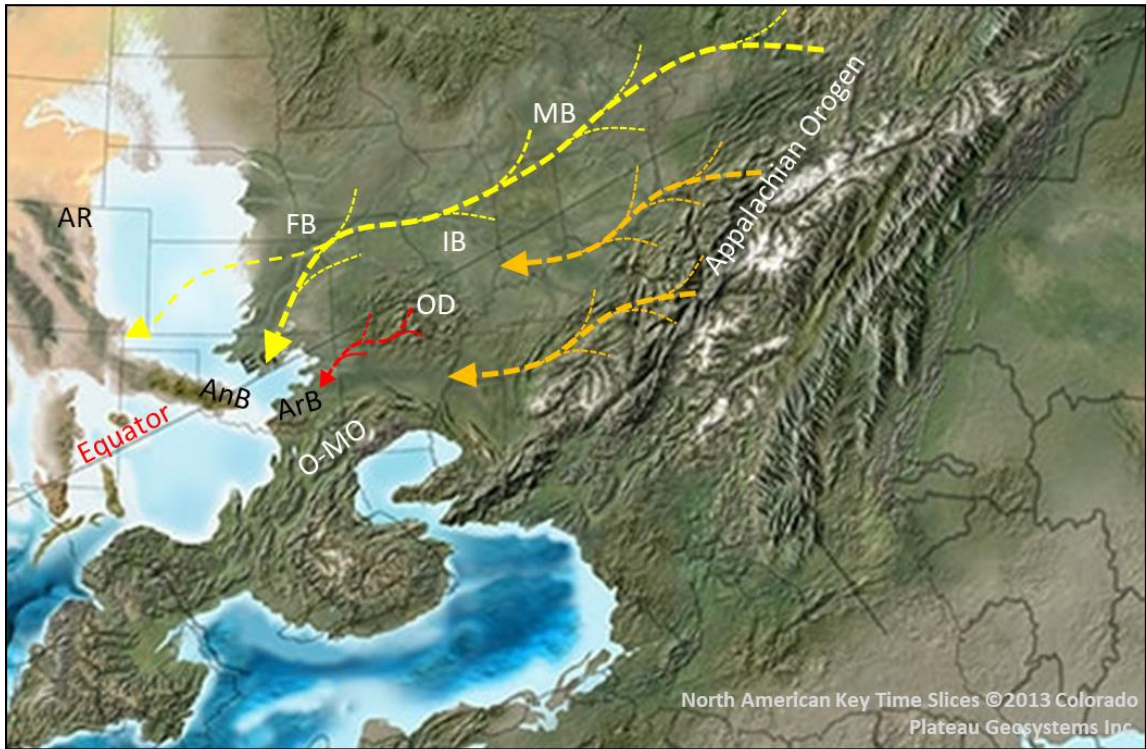


Figure 18. Middle-Late Pennsylvanian paleogeography reconstruction (from North American Key Time Slices ©2013 Colorado Plateau Geosystems Inc.) and possible configuration of inferred sediment dispersal patterns in the Desmoinesian. Yellow = dispersal path of fluvial systems from the northern Appalachians, orange = transverse dispersal paths from the central and southern Appalachians (Kissock et al., 2018), red = regional drainage paths from the Ozark Dome. Michigan Basin (MB), Illinois Basin (IB), Forest City Basin (FB), Anadarko Basin (AnB), Arkoma Basin (ArB), Ozark Dome (OD), Ouachita-Marathon Orogeny (O-MO), Ancestral Rocky Mountains (AR).

CHAPTER VIII

CONCLUSIONS

In this study, 867 new detrital zircon U-Pb ages and 120 new $\epsilon\text{Hf}(t)$ values were reported for several early Desmoinesian sandstones collected from cuttings in the Anadarko Basins and from outcrops on the Oklahoma Cherokee Platform. Based on these new detrital zircon data, and comparisons made with detrital zircon data from Paleozoic sandstones and coeval middle Pennsylvanian sandstone units across the North American Craton, several key conclusions are proposed:

1. Early Desmoinesian sandstones in the Midcontinent region can be divided into at least two classification groups based on detrital zircon U-Pb age signatures and detrital framework modes: Type 1 sandstones, which consist of the Taft Sandstone along the western flank of the Ozark Dome, and Type 2 sandstones, which include the Bartlesville (Bluejacket) and Red Fork sandstone on the Cherokee Platform and the Lower Red Fork sandstone in the Anadarko basin.
2. Type 1 sandstones are classified as quartzarenites that are interpreted to reflect regional-scale fluvial systems that recycled sedimentary strata and acquired detritus shed from basement exposed on regional topographic highs. Quartzarenites along the western flank of the Ozark Dome are interpreted to be principally sourced from recycled late Mississippian strata with possible minor contributions from

previously exposed Yavapai-Mazatzal basement in regions around the St. Francois Mountains in southeast Missouri.

3. Type 2 sandstones are classified as sublitharenite – litharenite, with significant fractions of metamorphic rock fragments. Detrital zircon signatures are interpreted to reflect sources of sediments in the Northern Appalachians (southeast New England) and sediment transport to the southern Midcontinent by southwest flowing transcontinental fluvial dispersal system.
4. Detrital zircon age signatures and sedimentologic characteristic support linkage between Appalachian fed fluvial systems in the Forest City and Illinois basins.
5. New data provide additional constraints on the interpretation for multiple dispersal paths for sediment derived from the central and southern Appalachians during the Middle Pennsylvanian. Westward flowing fluvial systems from the central and southern Appalachians either did not move across the central Laurentian craton during the Middle Pennsylvanian, or were impeded by the Ozark Uplift.
6. The large population of Yavapai-Mazatzal grains in the Taft sandstone and their relative absence in the Type 2 sandstones suggest the Nemaha ridge is not the primary source of metamorphic fragments in the early Desmoinesian sandstones. New detrital zircon data support the idea that metamorphic fragment population could be partially linked to the exhumation of peri-Gondwana terranes presently exposed from Newfoundland to southeast New England.

7. The time-equivalent Taft and Red Fork sandstones are interpreted to be compositionally and depositionally distinct and are not correlated stratigraphically.

REFERENCES

- Algeo, T. J., Heckel, P. H., 2008, The late Pennsylvanian midcontinent sea of North America: a review, *Palaeogeography, Palaeoclimatology, Palaeoecology*, Vol. 268, pg. 205-221
- Anderson, C.J., 1992, Distribution of submarine fan facies of the Upper Red Fork interval in the Anadarko Basin, Western Oklahoma: Unpublished M.S. thesis, Oklahoma State University, 230 p.
- Andrews, R., 1997, The Red Fork Play, Oklahoma Geological Survey Special Publication, v. 97, no. 1, p 13-21
- Balke, S. C., 1984, The petrology, diagenesis, stratigraphy, deposition environments, and clay mineralogy of the Red Fork Sandstone in North-Central Oklahoma: Unpublished M.S. thesis, Oklahoma State University, 117 p.
- Becker, T.P., Thomas, W.A., Samson, S.D., and Gehrels, G.E., 2005, Detrital zircon evidence of Laurentian crustal dominance in the lower Pennsylvanian deposits of the Alleghanian clastic wedge in eastern North America: *Sedimentary Geology*, V. 182, p. 59–86, doi:10.1016/j.sedgeo.2005.07.014
- Belousova, E., Griffin, W. L., O'Reilly, S. Y., Fisher, N. L., 2002, Igneous zircon: trace element composition as an indicator of source rock type. *Contrib. Mineral. Petrol.* V. 143, no. 5, p. 602–622.
- Botev, Z. I., Grotowski, J. F., Kroese, D. P., 2010, Kernel density estimation via diffusion. *Ann. Stat.* v. 38, no. 5, p. 2916–2957.
- Bradley, D.C. & O'Sullivan, P., 2016, Detrital zircon geochronology of pre-and syn-collisional strata, Acadian orogen, Maine Appalachians. *Basin Research*

- Bickford, M. E., Harrower, K. L., Hoppe, W. J., Nelson, B. K., Nusbaum, R. L., Thomas, J. J., 1981, Rb-Sr and U-Pb geochronology and distribution of rock types in the Precambrian basement of Missouri and Kansas, Geological Society of America Bulletin, Part I, v. 92, p. 323-341
- Bickford, M.E., McLelland, J.M., Mueller, P.A., Kamenov, G.D., and Needle, M., 2010, Hafnium isotopic compositions of zircon from Adirondack AMCG Suites: Implications for the petrogenesis of anorthosites, gabbros, and granitic members of the suites: Canadian Mineralogist, v. 48, p. 751–761, doi:10.3749/canmin.48.2.751
- Cecil, C.B., 2003, The concept of autocyclic and allocyclic controls on sedimentation and stratigraphy, emphasizing the climatic variable: SEPM Special Publication 77, p. 13-20.
- Chapman, A.D., Laskowski, A.K., 2019, Detrital zircon U-Pb data reveal a Mississippian sediment dispersal network originating in the Appalachian orogen, traversing North America along its southern shelf, and reaching as far as the southwest United States. Lithosphere; 11 (4): 581–587. doi:
- Cole, D., Myrow, P., Fike, D.A., Hakim, A., and Gehrels, 2015, Uppermost Devonian (Famennian) to Lower Mississippian events of the western U.S.: Stratigraphy, sedimentology, chemostratigraphy, and detrital zircon geochronology. Palaeogeography, Palaeoclimatology, Palaeoecology. v. 427, p. 1-19.
- Dickinson, R.W., Beard, L.S., Brakenridge, C.R., Erjavec, J.I., Ferguson, R.C., Inman, K.F., Knepp, R.A., Lindberg, F.A., Ryberg, P.T., 1983, Provenance of North American Phanerozoic sandstones in relation to tectonic setting, Geological Society of America Bulletin, v. 94, p. 222-235
- Dyman, Thaddeus. S., 1989, Quantitative petrographic analysis of Desmoinesian sandstones from Oklahoma, Oklahoma Geological Survey, Circular 90: 162-175
- Fyffe, L.R., Barr, S.M., Johnson, S.C., McLeod, M.J., McNicoll, V.J., Valverde-Vaquero, P., van Staal, C.R., and White, C.E., 2009, Detrital zircon ages from Neoproterozoic and early Paleozoic conglomerate and sandstone units of New Brunswick and coastal Maine: Implications for the tectonic evolution of Ganderia: Atlantic Geology, v. 45, p 110–144, doi:10.4138/atlgeol.2009.006
- Folk, R. L., 1968, Petrology of Sedimentary Rocks: Hemphills Bookstore, Austin, Texas, 170 p.
- Gehrels, G.E., Valencia, V., and Ruiz, J., 2008, Enhanced precision, accuracy, efficiency, and spatial resolution of U-Pb ages by laser ablation-multicollector-inductively coupled plasma-mass spectrometry: Geochemistry Geophysics Geosystems, v. 9, Q03017, doi:10.1029/2007GC001805

- Gehrels G.E. Blakey R. Karlstrom K.E. Timmons J.M. Dickinson B. Pecha M., 2011, Detrital zircon U-Pb geochronology of Paleozoic strata in the Grand Canyon, Arizona: *Lithosphere*, v. 3, p. 183–200, doi:10.1130/L121.1.
- Gehrels, G.E., and Pecha, M.E., 2014, Detrital zircon U-Pb geochronology and Hf isotope geochemistry of Paleozoic and Triassic passive margin strata of western North America: *Geosphere*, v. 10, p. 49–65, doi:10.1130/GES00889.1.
- Goode, J.W., Vervoort, J.D., 2006, Origin of Mesoproterozoic A-type granites in Laurentia: Hf isotope evidence, *Earth and Planetary Science Letters*, v. 243, p. 711-731
- Hanson, R.E., Puckett, R.E., Keller, G.R., Brueseke, M.E., Bulen, C.L., Mertzman, S.A., Finegan, S.A., McCleery, D.A., 2013, Intraplate magmatism related to opening of the southern Iapetus Ocean: Cambrian Wichita igneous province in the Southern Oklahoma rift zone, *Lithos*, v. 174, p. 57-70
- Henderson, B.J., Collins, W.J., Murphy, J.B., Gutierrez-Alonso, G., and Hand, M., 2015, Gondwanan basement terranes of the Variscan–Appalachian orogen: Baltican, Saharan and West African hafnium isotopic fingerprints in Avalonia, Iberia and the Armorican terranes: *Tectonophysics*, v. 681, p. 278–304, doi:10.1016/j.tecto.2015.11.020
- Heran, W.D., Green, G.N., Stoesser, D.B., 2003, A digital geologic map database for the state of Oklahoma, USGS Publication Warehouse, v.1, no.1, doi: 10.3133/ofr03247
- Hiess, J., Condon, D.J., McLean, N., and Noble, S.R., 2012, 238U/235U systematics in terrestrial uranium-bearing minerals: *Science*, v. 335, p. 1610–1614, doi:10.1126/science.1215507
- Horstwood, M.S.A., Kosler, J., Gehrels, G., Jackson, S., McLean, N., Paton, C., Pearson, N.J., Sircombe, K., Sylvester, P., Vermeesch, P., Bowring, J., Condon, D.J., and Schoene, B., 2016, Community-derived standards for LA-ICP-MS U-Th-Pb geochronology—Uncertainty propagation, age interpretation and data reporting: *Geostandards and Geoanalytical Research*, doi:10.1111/j.1751-908X.2016.00379.x
- Jensen, M., 2016, Critical evaluation of middle and late Pennsylvanian cyclic sedimentation and stratigraphic architecture in the southern Anadarko basin, Oklahoma: Unpublished M.S. thesis, Oklahoma State University
- Johnson, C., 1984, Depositional environments, reservoir trends, and diagenesis of the Red Fork sandstones in portions of Elaine, Caddo, and Custer Counties, Oklahoma: Unpublished M.S. thesis, Oklahoma State University, 109 p.

- Johnson, K. S., 2008, Geologic History of Oklahoma, Oklahoma Geological Survey, Educational Publication no. 9, p. 3-5
- Jordan, L., 1957, Subsurface Stratigraphic Names of Oklahoma: Oklahoma Geological Survey Guidebook, v. 1, 220 p.
- Kissock, J.k., Finzel, E.S., Malone, D.H., Craddock, J.P., 2017, Lower–Middle Pennsylvanian strata in the North American midcontinent record the interplay between erosional unroofing of the Appalachians and eustatic sea-level rise. *Geosphere* ; 14 (1): 141–161.
- Konstantinou, A., Wirth, K.R., Vervoort, J.D., Malone, D.H., Davidson, C., and Craddock, J.P., 2014, Provenance of quartz arenites of the early Paleozoic midcontinent region, USA: *The Journal of Geology*, v. 122, p. 201–216, doi:10.1086/675327
- Kuykendall, N. D., 1985, The petrography, diagenesis, and depositional setting of the Glen (Bartlesville) sandstone, William Berryhill unit, Glen Pool Field, Creek County, Oklahoma: Unpublished M.S. thesis, Oklahoma State University, 366 p.
- Loan, M.L., 2011. New Constraints on the Age and Deposition of the Metasedimentary Rocks in the Nashoba terrane, SE New England: Unpublished M.S. Thesis, Boston College, Chestnut Hill, MA, USA, 125 pp.
- Ludwig, K.R., 2003. Isoplot 3.00 –A Geochronological Toolkit for Microsoft Excel, in Berkeley. Geochronology Center Special Publication No. 4, Berkeley, CA.
- Mason, E.P., 1982, The petrology, diagenesis and depositional environment of the Bartlesville Sandstone in the Cushing Oil Field, Creek County, Oklahoma: Unpublished M.S. thesis, Oklahoma State University, 141 p.
- McGuire, P.R., 2017, U-Pb detrital zircon signatures of the Ouachita orogenic belt: Unpublished M.S. thesis, Texas Christian University, 43 p.
- Moore, G.E., 1979, Pennsylvanian paleogeography of the southern Midcontinent, in Hyne, N.J., ed., Pennsylvanian sandstones of the mid-continent: Tulsa Geological Society Special Publication 1, p. 2-12.
- Mueller, P.A., Kamenov, G.D., Heatherington, A.L., and Richards, J., 2008, Crustal evolution in the southern Appalachian orogen: Evidence from Hf Isotopes in detrital zircons: *The Journal of Geology*, v. 116, p. 414–422, doi:10.1086/589311
- Northcutt, R., Andrews, R., 1997, The Bartlesville Play, Oklahoma Geological Survey Special Publication, v. 97, no. 6, p. 13-25

- Perry, W.J., Jr., 1988, Tectonic evolution of the Anadarko basin, U.S. Geological Survey Bulletin 1866-A, p. A1-A16
- Pickell, J.M., 2012, Detrital zircon geochronology of Middle Ordovician siliciclastic sediment on the southern Laurentian shelf: Unpublished M.S. thesis, College Station, Texas A&M University, 120 p.
- Puckette, J.O., 1990, Depositional setting, facies, and petrology, of Cabaniss (Upper “Cherokee”) Group in Beckham, Dewey, Custer, Ellis, Roger Mills, and Washita Counties, Oklahoma: Unpublished M.S. thesis, Oklahoma State University, 144 p.
- Rascoe, B., Adler, F. J., 1983, Permo-Carboniferous hydrocarbon accumulations, Mid-Continent, U.S.A., AAPG Bulletin, v. 67, p. 979-1001
- Rivers, T., Culshaw, N., Hynes, A., Indares, A., Jamieson, R., and Martignole, J., 2012, The Grenville orogen—A post-LITHOPROBE perspective, in Percival, J.A., Cook, F.A., and Clowes, R.M., eds., Tectonic Styles in Canada: The LITHOPROBE Perspective: Geological Association of Canada Special Paper 49, p. 97–236.
- Robertson, K. S., 1983, Stratigraphy, depositional environments, petrology, diagenesis, and hydrocarbon maturation related to the Red Fork Sandstone in North-Central Oklahoma: Unpublished M.S. thesis, Oklahoma State University, 130 p.
- Ross, C. A., and Ross, J. R. P., 1987, Late Paleozoic sea levels and depositional sequences, in A. Ross and D. Haman eds., Timing and depositional history of eustatic sequences: Constraints on seismic stratigraphy: Cushman Foundation for Foraminiferal Research, Special Publication no. 24, p. 137-139.
- Saylor, J. E., and Sundell, K. E., 2016, Quantifying comparison of large detrital geochronology data sets, *Geosphere* v.12, no. 1, p. 203-220.
- Saylor, J. E., Jordan, J. C., Sundell, K. E., Wang, X., Wang, S., and Deng, T., 2017, Topographic growth of the Jishi Shan and its impact on basin and hydrology evolution, NE Tibetan Plateau, *Basin Research* v. 30, no. 3, p. 544-563.
- Siddoway, C.S. and Gehrels, G.E., 2014, Basement-hosted sandstone injectites of Colorado: A vestige of the Neoproterozoic revealed through detrital zircon provenance analysis. *Lithosphere*, v. 6, p. 403-408.
- Sloss, L.L., 1988, Tectonic evolution of the craton in Phanerozoic time, in Sloss, L.L., ed., *Sedimentary Cover—North American Craton: U.S.:* Boulder, Colorado, Geological Society of America, *The Geology of North America*, v. D-2, p. 25–51.

- Stacey, J.S., and Kramers, J.D., 1975, Approximation of terrestrial lead isotope evolution by a two-stage model: *Earth and Planetary Science Letters*, v. 26, p. 207–221, doi:10.1016/0012-821X(75)90088-6.
- Steiger, R.H., and Jager, E., 1977, Subcommission on geochronology: Convention on the use of decay constants in geo- and cosmochronology: *Earth and Planetary Science Letters*, v. 36, p. 359–362, doi:10.1016/0012-821X(77)90060-7.
- Sundell, K. E., and Saylor, J. E., 2017, Unmixing detrital geochronology age distributions, *Geochemistry, Geophysics, Geosystems* v. 18, no. 8, p. 2872-2886.
- Sundell, K. E., Saylor, J. E., Pecha, M., 2019, Sediment provenance and recycling of detrital zircons from Cenozoic Altiplano strata in southern Peru and implications for the crustal evolution of west-central South America, *Book: Andean Tectonics, Journal of South American Earth Sciences*.
- Tate, W.L., 1985, The depositional environment, petrology, diagenesis, and petroleum geology of the Red Fork Sandstone in Central Oklahoma: Unpublished M.S. thesis, Oklahoma State University, 185 p.
- Thomas, W. A., 2011, Detrital-zircon Geochronology and Sedimentary Provenance, *Lithosphere*, v. 3, no. 4, p. 304-308.
- Thomas, W.A., Tucker, R.D., Astini, R.A., Denison, R.E., 2012, Ages of pre-rift basement and synrift rocks along the conjugate rift and transform margins of the Argentine Precordillera and Laurentia, *Geosphere*, v. 8, no. 6, p. 1366-1383, doi:10.1130/GES00800.1
- Thomas, W.A., Gehrels, G.E., and Romero, M.C., 2016, Detrital zircons from crystalline rocks along the Southern Oklahoma fault system, Wichita and Arbuckle Mountains, USA: *Geosphere*, v. 12, no. 4, p. 1224–1234, doi:10.1130/GES01316.1.
- Thomas, W.A., Gehrels, G.E., Greb, S.F., Nadon, G.C., Satkoski, A.M., and Romero, M.C., 2017, Detrital zircons and sediment dispersal in the Appalachian foreland: *Geosphere*, v. 13, no. 6, p. 2206–2230, doi:10.1130/GES01525.1.
- Udayashankar, K.V., 1985, Depositional environment, petrology, and diagenesis of Red Fork Sandstone in Central Dewey County, Oklahoma: Unpublished M.S. thesis, Oklahoma State University, 169 p.
- Vermeesch, P., 2004. How many grains are needed for a provenance study? *Earth Planet. Sci. Lett.* 224, p. 351- 441.

- Vermeesch, P., 2013, Multi-sample comparison of detrital age distributions. *Chem. Geol.*, v. 341, p. 140–146.
- Vervoort, J. D., Patchett, P. J., 1996, Behavior of hafnium and neodymium isotopes in the crust: Constraints from Precambrian crustally derived granites. *Geochim. Cosmochim. Acta*, v. 60, no. 19, p. 3717–3733.
- Vervoort, J. D., Blichert-Toft, J., 1999, Evolution of the depleted mantle: Hf isotope evidence from juvenile rocks through time. *Geochim. Cosmochim. Acta*, v. 63, no. 3–4, p. 533–556.
- Vervoort, J. D., Patchett, P. J., Blichert-Toft, J., Albarède, F., 1999, Relationships between Lu–Hf and Sm–Nd isotopic systems in the global sedimentary system. *Earth Planet. Sci. Lett.*, v. 168, no. 1, p. 79–99.
- Visher, G. S., Saitta, B.S., and Phares, R. S., 1971, Pennsylvanian Delta Patterns and Petroleum Occurrences in Eastern Oklahoma: *Amer. Assoc. Petrol. Geol. Bull.*, Vol. 55, p. 1206 - 1230.
- Wang, W., & Bidgoli, T. S., 2019, Detrital zircon geochronologic constraints on patterns and drivers of continental-scale sediment dispersal in the Late Mississippian. *Geochemistry, Geophysics, Geosystems*, v. 20, p. 5522–5543. <https://doi.org/10.1029/2019GC008469>
- Weirich, T. E., 1953, Shelf principle of oil origin, migration, and accumulation: *AAPG Bulletin*, v. 37, p. 2027-2045
- West, D.P. Jr., Yates, M.G., Gerbi, C., and Barnard, N.Q., 2008, Metamorphosed Ordovician Fe- and Mn-rich rocks in south-central Maine: From peri-Gondwanan deposition through Acadian metamorphism. *Am. Min.* 93:270-282.
- Willner, A.P., Barr, S.M., Gerdes, A., Massonne, H.-J., and White, C.E., 2013, Origin and evolution of Avalonia: Evidence from U–Pb and Lu–Hf isotopes in zircon from the Mira terrane, Canada, and the Stavelot–Venn Massif, Belgium: *Journal of the Geological Society*, V. 170, p. 769–784, doi:10.1144/jgs2012-152
- Willner, A.P., Gerdes, A., Massonne, H.-J., van Staal, C.R., and Zagorevski, A., 2014, Crustal evolution of the northeast Laurentian margin and the peri-Gondwanan microcontinent Ganderia prior to and during closure of the Iapetus Ocean: Detrital zircon U–Pb and Hf isotope evidence from Newfoundland: *Geoscience Canada*, V. 41, p. 345–364, doi:10.12789/geocanj.2014.41.046.
- Whitmeyer, S. J., & Karlstrom, K. E., 2007, Tectonic model for the Proterozoic growth of North America. *Geosphere*, v. 3, no. 4, p. 220–259, <https://doi.org/10.1130/GES00055.1>

Xie, X., Cains, W., Manger, W.L., 2016, U–Pb detrital zircon evidence of transcontinental sediment dispersal: provenance of Late Mississippian Wedington Sandstone member, NW Arkansas, *International Geology Review*, v. 58, p. 1951-1966.

APPENDICES

APPENDIX A: ZIRCON IMAGES

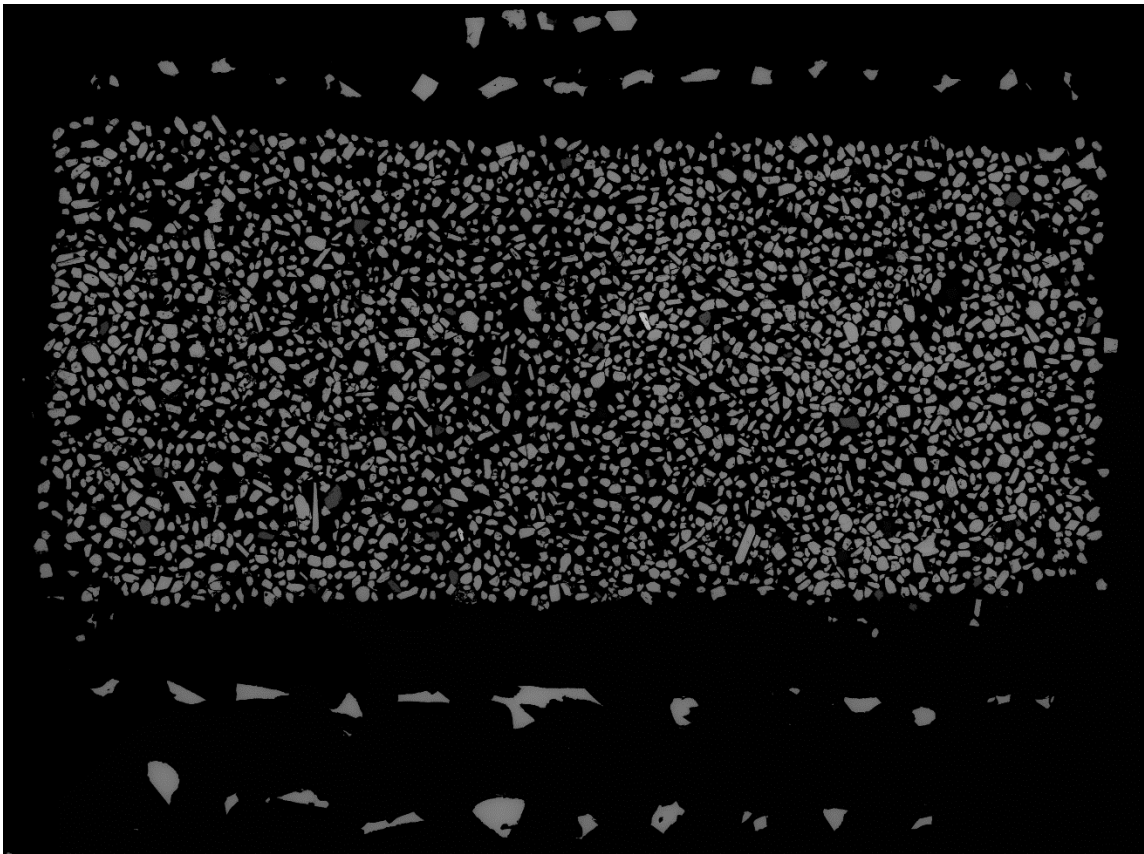


Figure 19. BSE image of mounted zircons from subsample BV 1.

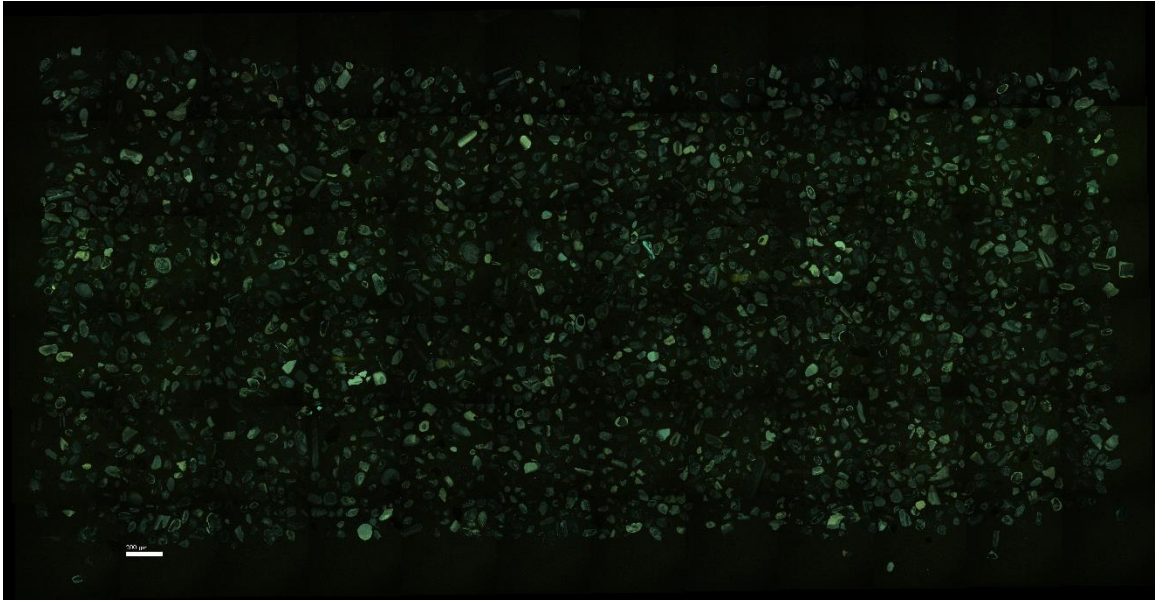


Figure 20. CL image of mounted zircons from subsample BV 1.

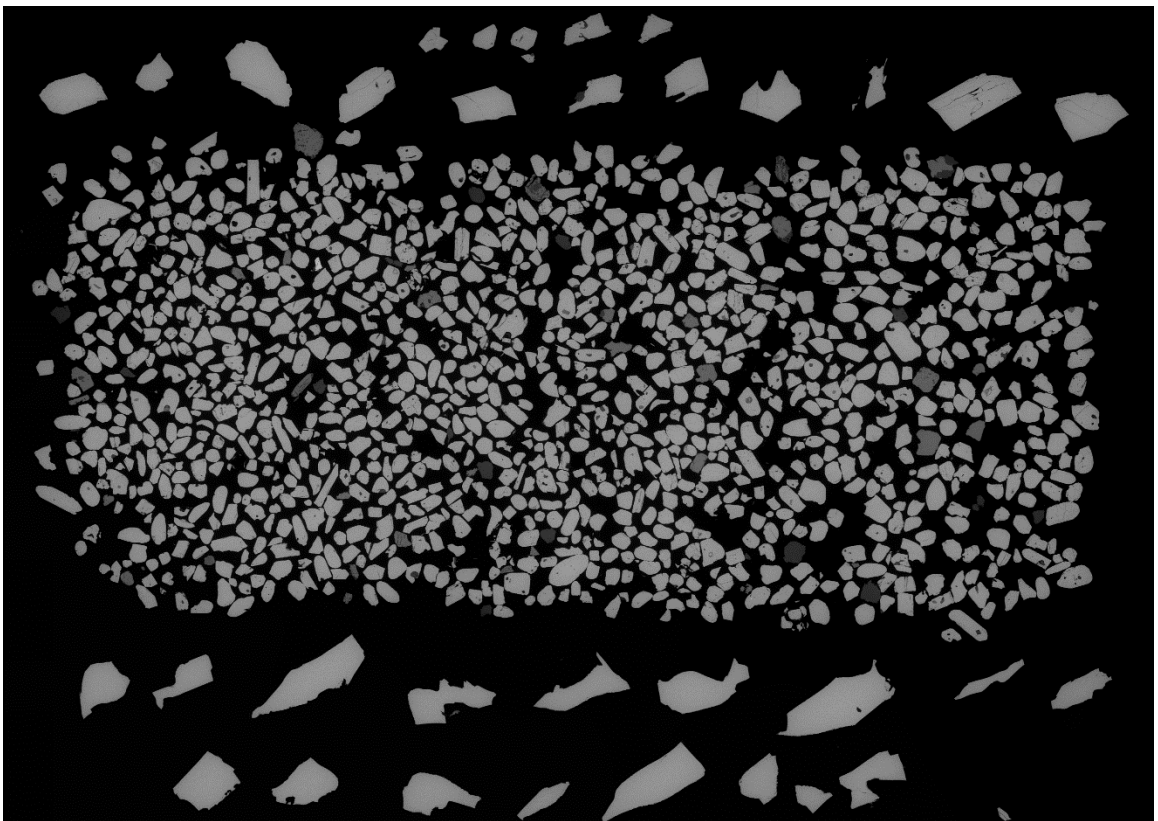


Figure 21. BSE image of mounted zircons from subsample BV 2.

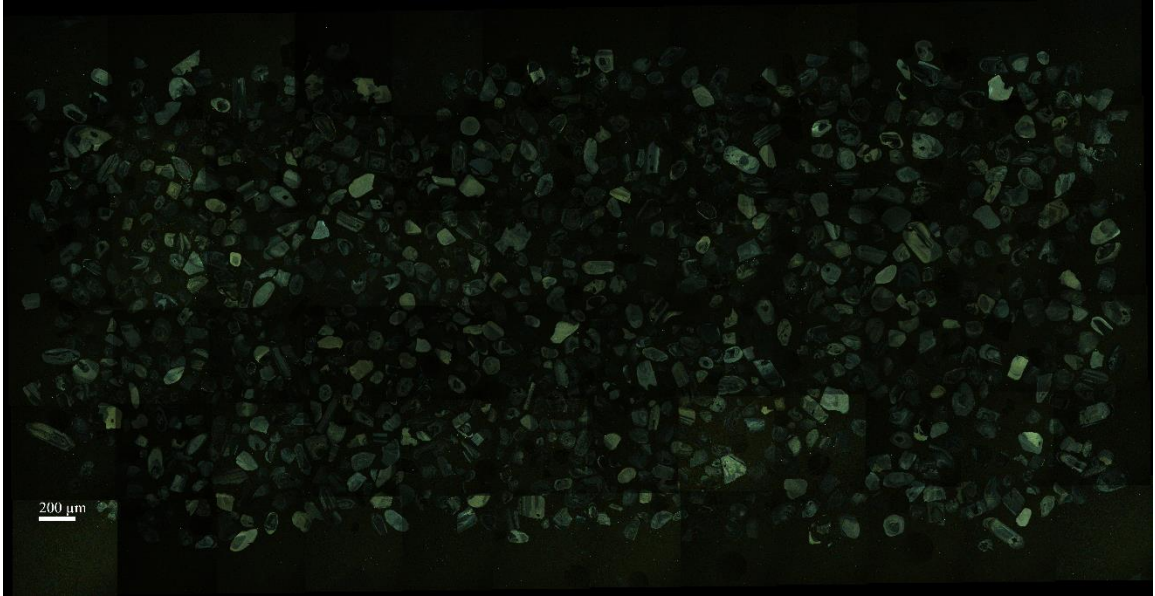


Figure 22. CL image of mounted zircons from subsample BV 2.

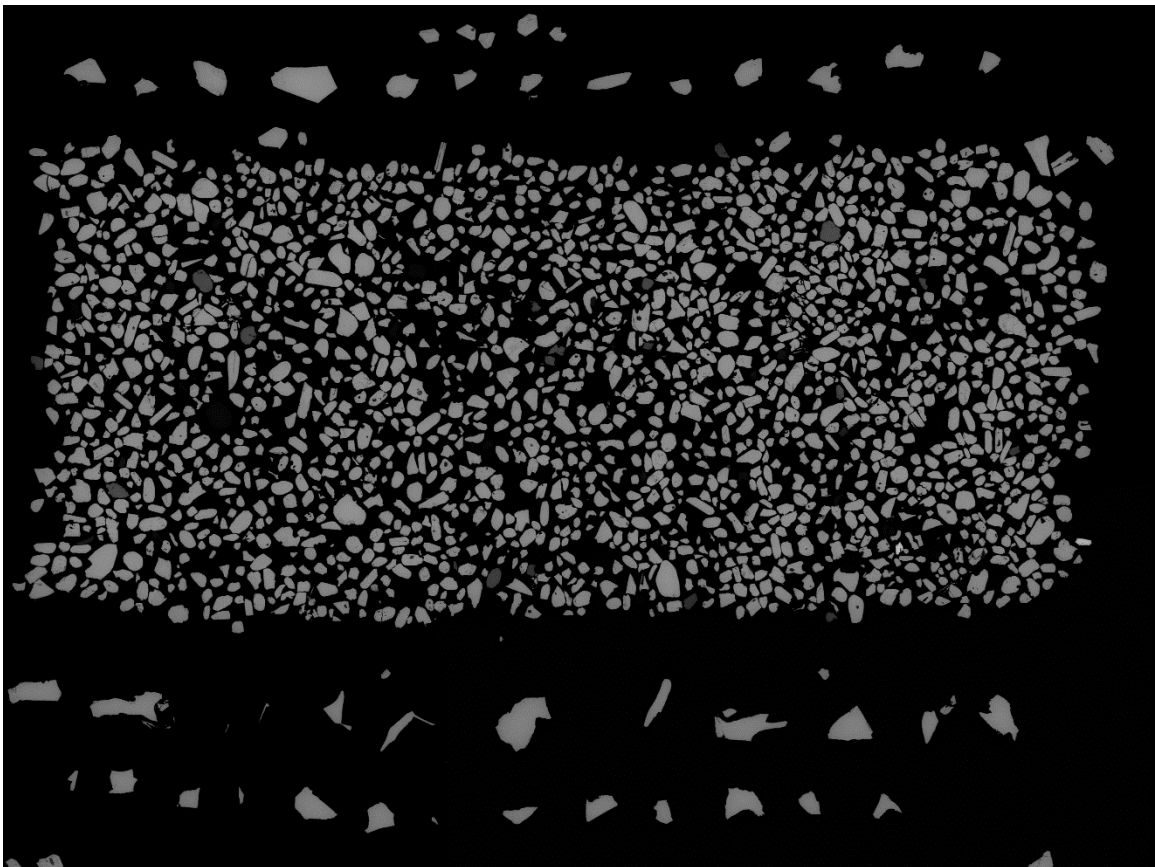


Figure 23. BSE image of mounted zircons from subsample BV 3.

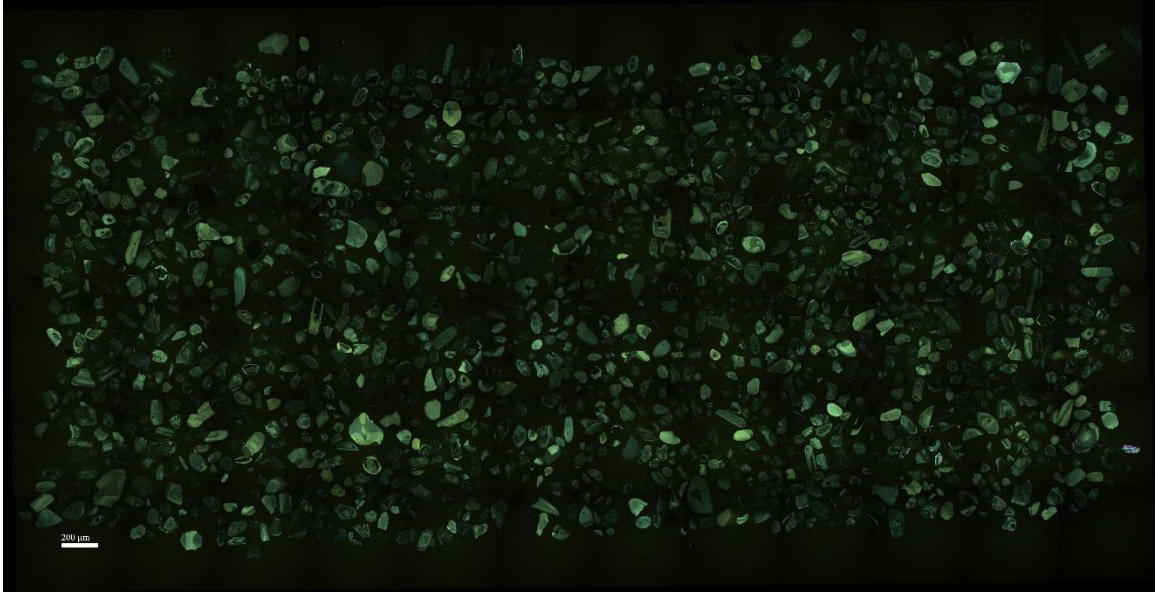


Figure 24. CL image of mounted zircons from subsample BV 3.

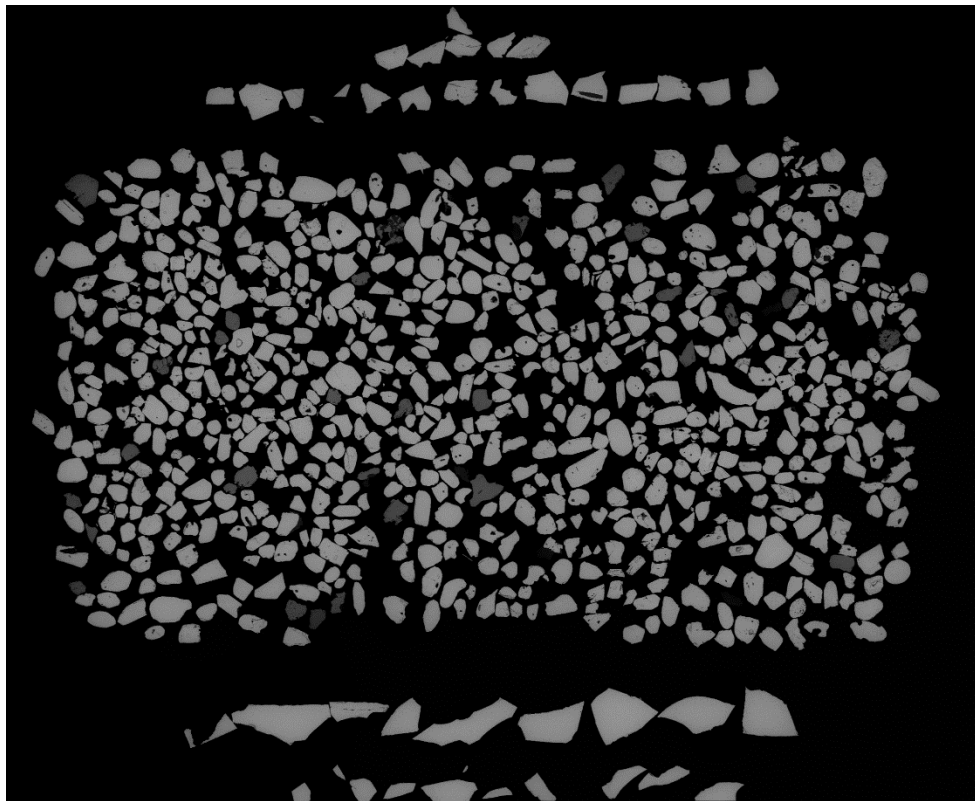


Figure 25. BSE image of mounted zircons from subsample BV 4.

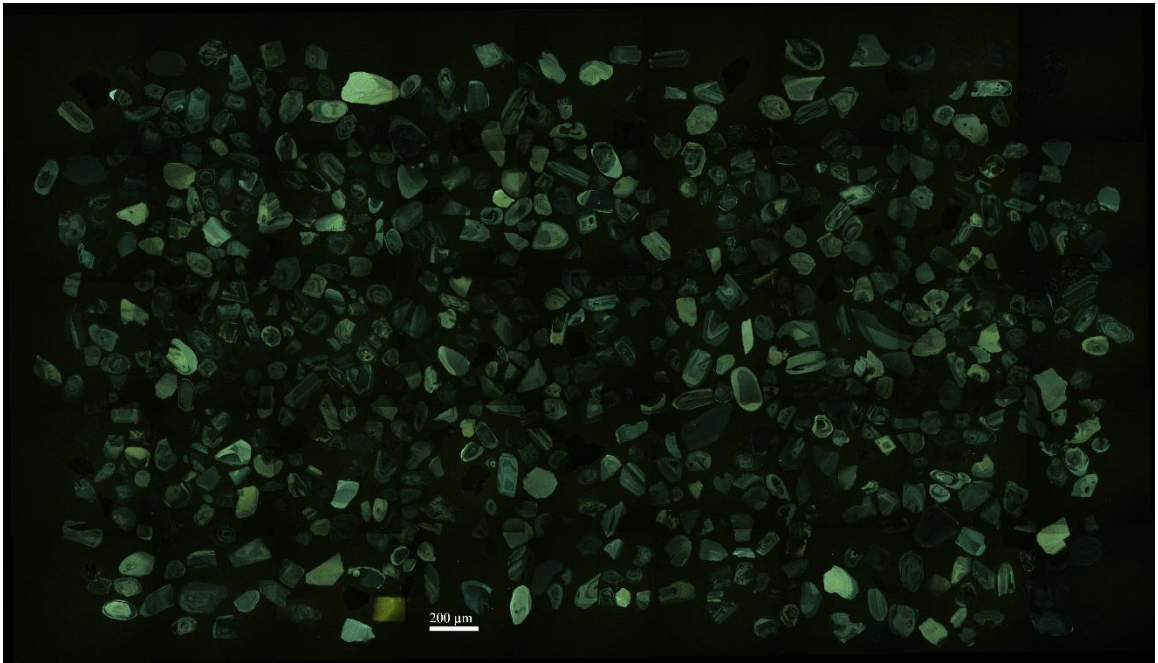


Figure 26. CL image of mounted zircons from subsample BV 4.

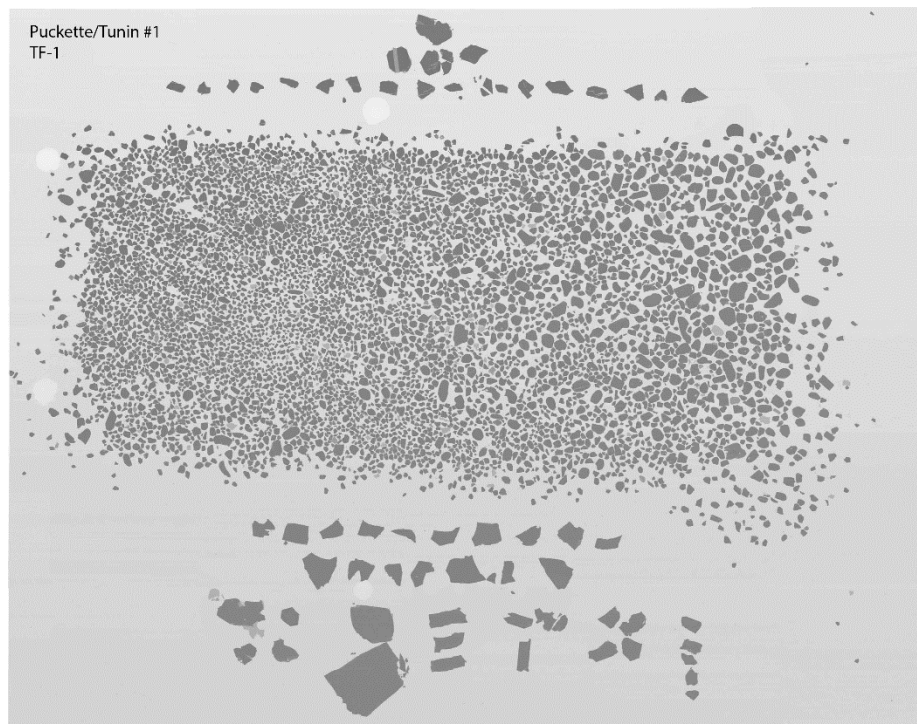


Figure 27. BSE image of mounted zircons from sample Tf-1.

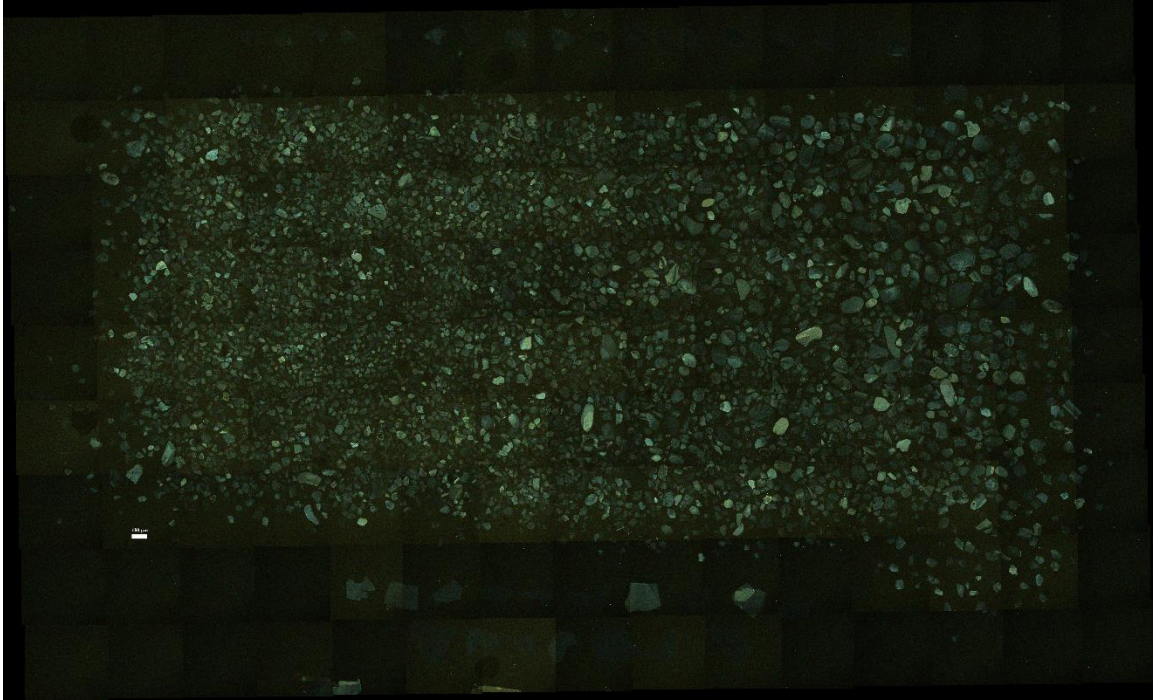


Figure 28. CL image of mounted zircons from sample Tf-1.

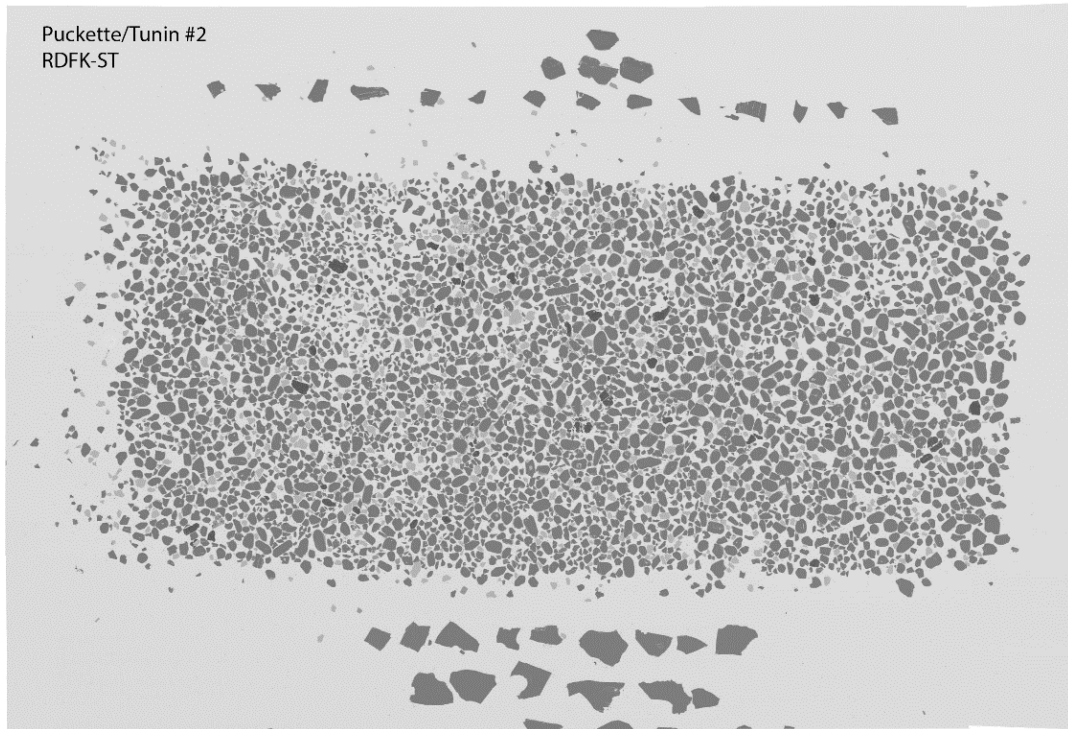


Figure 29. BSE image of mounted zircons from sample RDFK-ST.

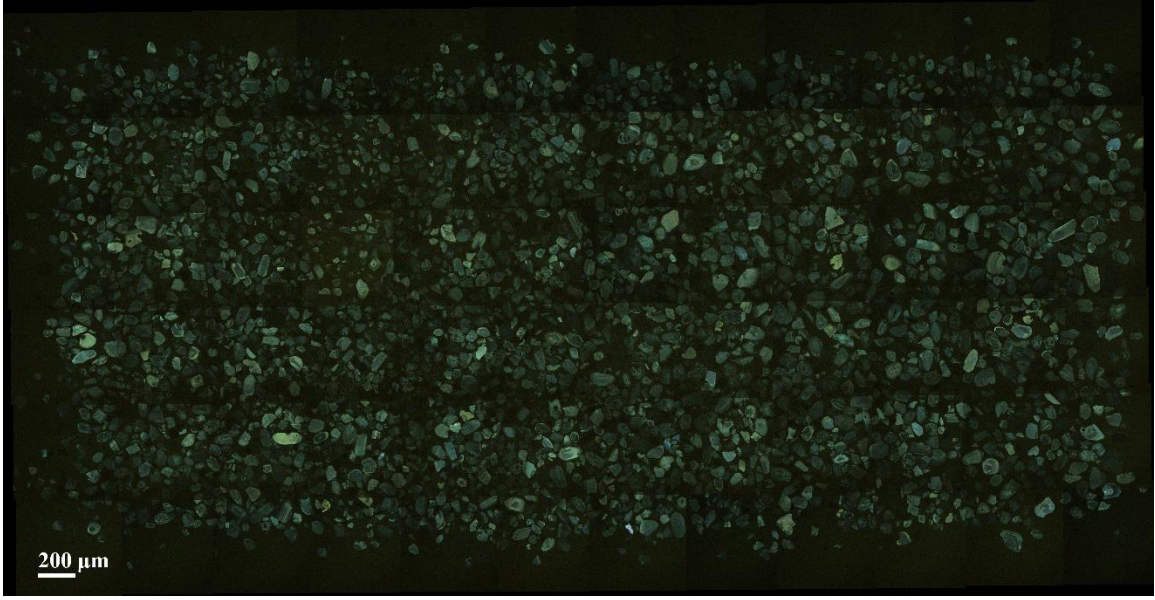


Figure 30. CL image of mounted zircons from sample RDFK-ST.

APPENDIX B: DATA TABLES

Age-Pick (TF-1)				
MIN AGE	MAX AGE	# GRAINS	PEAK AGE	# GRAINS
419	431	3	425	4
460	472	2	467	3
544	564	4	553	4
566	586	4	577	4
603	659	11	610	4
887	1215	66	626	5
1292	1312	0	650	3
1314	1364	5	892	4
1368	1471	10	941	8
1612	1739	70	1003	14
1742	1750	0	1043	17
1768	1810	4	1088	20
1822	1826	0	1344	5
1898	1917	0	1384	4
2081	2112	4	1445	6
2569	2596	3	1680	56
			1793	4
			2099	4
			2583	3

Table 2. Age-pick calculations for sample TF-1.

Age-Pick (RDFK-ST)				
MIN AGE	MAX AGE	# GRAINS	PEAK AGE	# GRAINS
360	367	2	363	3
390	396	2	390	3
399	402	0	418	9
404	431	12	440	3
436	446	3	468	3
467	476	2	549	20
522	567	26	610	30
577	664	54	638	9
865	873	0	939	4
905	1176	33	1032	12
1181	1185	0	1083	12
1203	1208	0	1145	5
1211	1237	2	1233	3
1243	1259	0	1296	5
1270	1322	4	1496	3
1411	1429	1	1877	5
1474	1518	3	1974	4
1614	1629	0	2044	3
1744	1747	0	2092	6
1853	1901	4	2713	4

Table 3. Age-pick calculations for sample RDFK-ST.

Age-Pick (BV1-4)				
MIN AGE	MAX AGE	# GRAINS	PEAK AGE	# GRAINS
318	324	3	323	3
327	339	3	334	3
355	475	60	365	6
515	699	137	377	8
748	772	3	416	23
778	788	1	430	12
877	1419	142	453	3
1423	1432	0	468	3
1446	1471	2	545	21
1479	1533	6	600	32
1580	1677	17	616	44
1707	1712	0	652	13
1722	1821	13	699	3
1853	1924	6	760	3
1936	2161	29	909	8
2662	2681	1	1002	28
2685	2689	0	1067	27
			1098	35
			1134	32
			1187	14
			1207	16
			1236	15
			1320	8
			1373	9
			1462	3
			1514	6
			1633	14
			1741	6
			1783	8
			1891	7
			1938	3
			1978	6
			2016	4
			2096	9
			2124	8
			2149	3

Table 4. Age-pick calculations for composite sample BV 1-4.

U-Pb-εHf(t)					
BV 1-4		TF-1		RDFK-ST	
U-Pb Age	εHf(t)	U-Pb Age	εHf(t)	U-Pb Age	εHf(t)
600	-4.4	376	1.9	542	-2.3
608	-6.3	386	1.8	547	-1.9
629	9.7	425	0.2	550	4.0
549	-4.7	431	-7.1	550	-1.6
558	-2.3	464	11.3	556	-1.6
407	-1.2	552	0.8	599	4.9
423	-3.9	609	2.7	600	-7.8
413	-2.7	612	9.5	601	-10.8
423	-1.4	625	3.5	602	-0.8
417	-3.1	647	5.9	606	-8.2
1084	-0.4	1000	3.4	608	3.7
1087	3.3	1002	0.7	608	10.2
1063	4.0	1005	6.2	608	10.2
1124	0.5	1036	4.2	614	9.9
1223	5.1	1042	-3.5	614	-18.3
418	1.5	1371	5.8	1022	1.4
363	0.2	1417	6.1	1045	-0.9
339	6.8	1429	3.2	1078	3.7
383	0.6	1445	3.4	1086	0.7
420	-0.8	1651	7.7	1152	3.6
531	2.4	1651	8.5	411	2.2
594	6.2	1654	9.5	416	1.5
651	3.5	1662	4.0	417	-1.4
546	-2.0	1665	6.8	420	-6.0
629	-10.6	1671	7.0	422	-4.9
1063	8.7	1675	6.7	530	-1.0
1126	5.7	1678	6.0	530	7.1
993	0.8	1703	6.7	536	-11.7
1080	3.8	1707	7.3	536	-1.4

Table 5. U-Pb-εHf(t) date table for all samples analyzed in this study.

1160	5.3	1715	8.5	537	-5.3
419	-1.6				
379	-1.3				
367	0.1				
402	-1.6				
412	-3.1				
624	-4.4				
598	-0.7				
545	-1.5				
644	3.1				
610	-0.3				
1083	0.3				
1157	3.0				
1005	1.4				
1149	3.2				
1131	0.6				
365	-3.3				
372	-0.1				
390	0.8				
433	-0.8				
438	-8.6				
542	2.9				
604	-8.3				
613	10.5				
589	2.3				
636	3.4				
999	2.4				
1100	1.8				
1051	1.2				
1007	1.4				
1051	1.9				

Table 5. Continued.

APPENDIX C: PETROGRAPHIC IMAGES

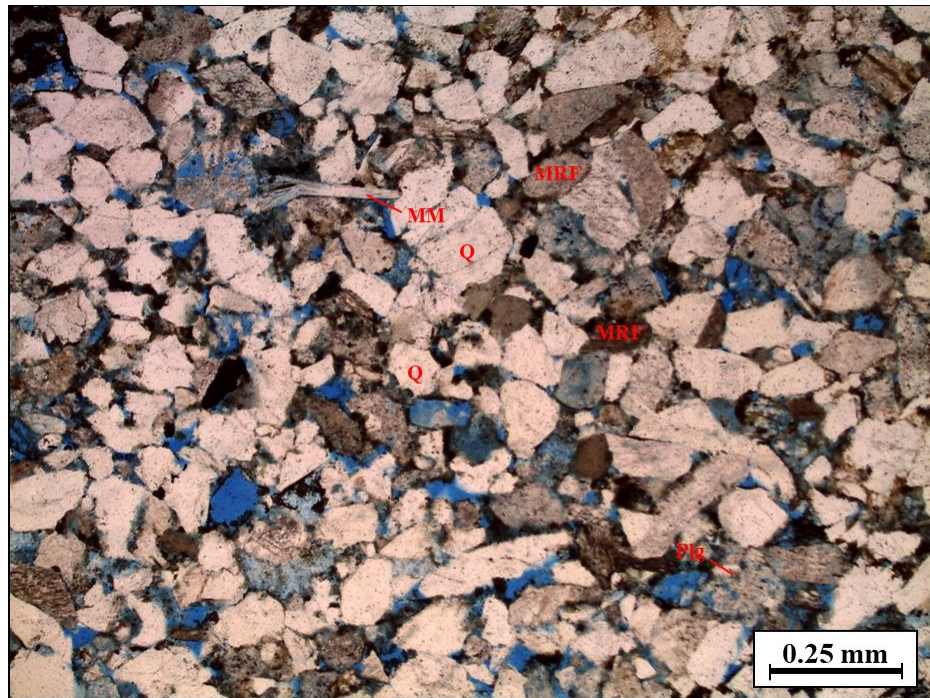


Figure 31. Photomicrograph from the Bluejacket outcrop sample in plain polarized light (ppl). Quartz (Q), plagioclase feldspar (Plg), muscovite Mica (MM), metamorphic rock fragment (MRF).

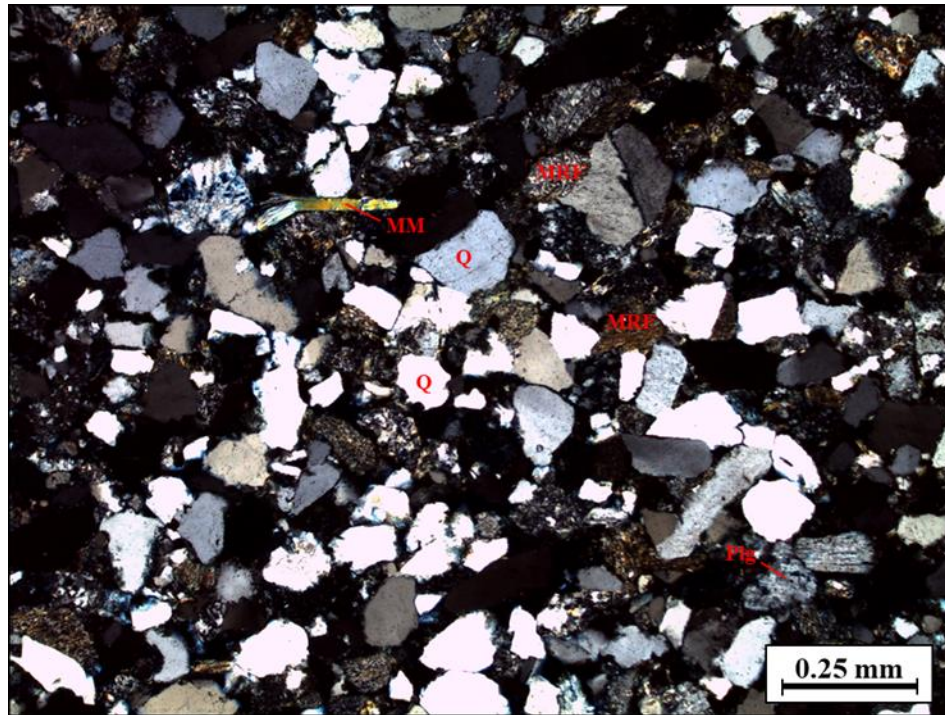


Figure 32. Photomicrograph from **Figure 31** in cross polarized light (cpl).

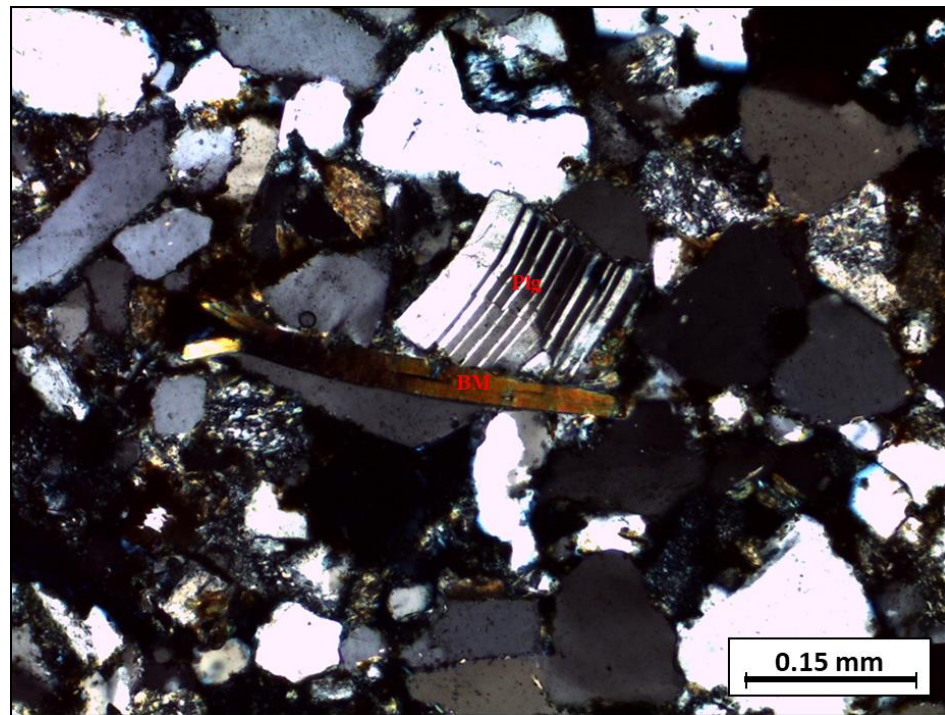


Figure 33. Bluejacket outcrop photomicrographic (cpl). Biotite mica (BM), plagioclase feldspar (plg).

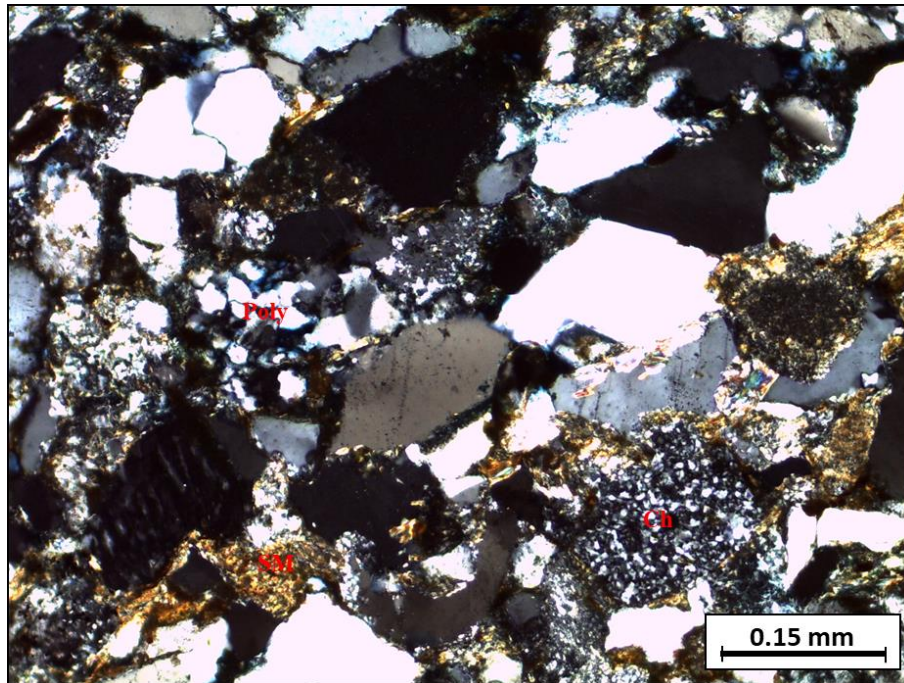


Figure 34. Bluejacket outcrop photomicrographic (cpl). Chert (ch), polycrystalline quartz (Poly), Schistose metamorphic rock fragment (SM).

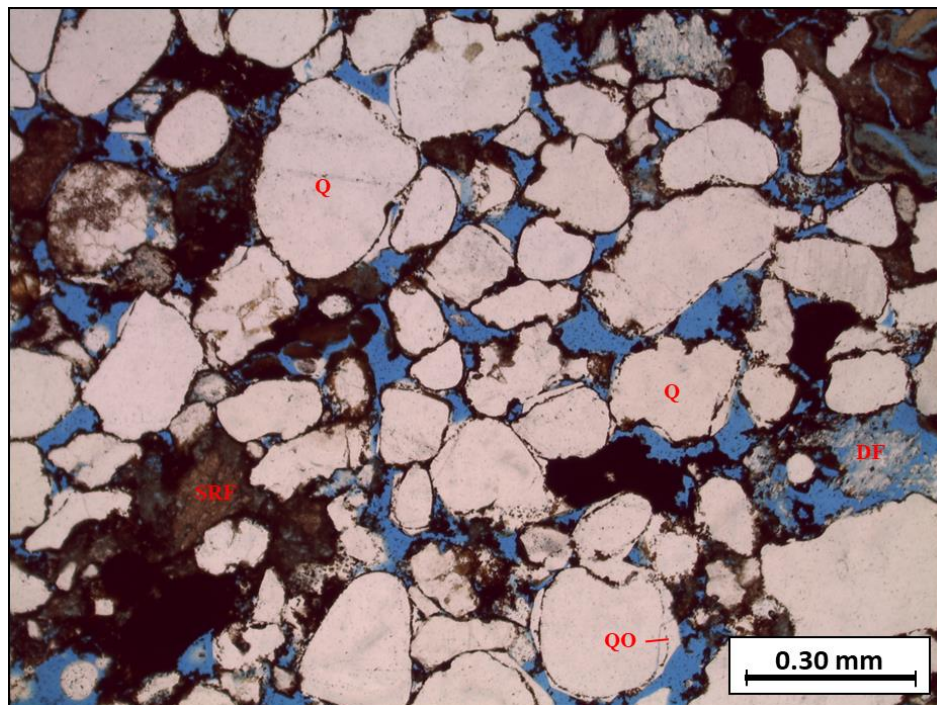


Figure 35. Photomicrograph from the Taft outcrop sample (ppl). Quartz (Q), dissolution feldspar (DF), sedimentary rock fragment (SRF), quartz overgrowth (QO).

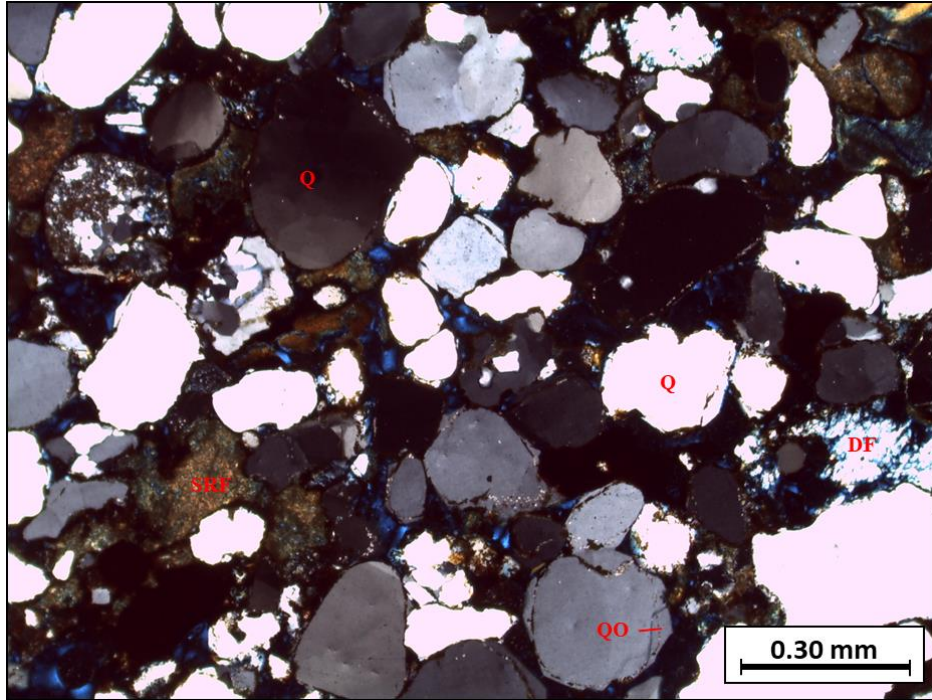


Figure 36. Photomicrograph from **Figure 35** in cross polarized light.

VITA

Zachery T. Tunin

Candidate for the Degree of

Master of Science

Thesis: DETRITAL ZIRCON GEOCHRONOLOGY AND PROVENANCE ANALYSIS OF THE DESMOINESIAN (MIDDLE PENNSYLVANIAN) BARTLESVILLE AND RED FORK SANDSTONES, CHEROKEE PLATFORM AND ANADARKO BASIN, OKLAHOMA

Major Field: GEOLOGY

Biographical:

Education:

Completed the requirements for the Master of Science in Geology at Oklahoma State University, Stillwater, Oklahoma in December, 2020.

Completed the requirements for the Bachelor of Science in Geology at Oklahoma State University, Stillwater, Oklahoma in 2018.

Experience:

Geoscience Intern – ExxonMobil Corp., Spring, Texas, Summer 2020

Graduate Research Assistant, Boone Pickens School of Geology, Stillwater, Oklahoma, August 2018 to May 2020

Geology Intern – Continental Resources., Oklahoma City, Oklahoma, Summer 2019

Geology Intern – Continental Resources., Oklahoma City, Oklahoma, Summer 2018

Petro Pro – Oklahoma Energy Resource Board, Oklahoma City, Oklahoma, March 2016 – Present

Professional Memberships:

Geological Society of America (GSA)

American Association of Petroleum Geologist (AAPG)